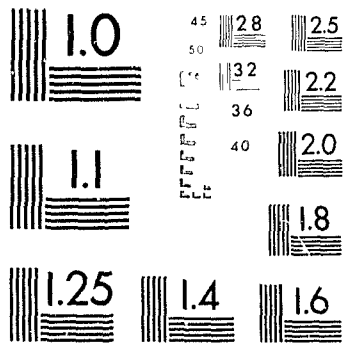


# 1

PM-1 3½"x4" PHOTOGRAPHIC MICROCOPY TARGET  
NBS 1010a ANSI/ISO #2 EQUIVALENT



PRECISION<sup>SM</sup> RESOLUTION TARGETS



National Library  
of Canada

Bibliothèque nationale  
du Canada

Acquisitions and  
Bibliographic Services Branch

Direction des acquisitions et  
des services bibliographiques

395 Wellington Street  
Ottawa, Ontario  
K1A 0N4

395, rue Wellington  
Ottawa (Ontario)  
K1A 0N4

*Your file* *Votre référence*

*Our file* *Notre référence*

## NOTICE

## AVIS

The quality of this microform is heavily dependent upon the quality of the original thesis submitted for microfilming. Every effort has been made to ensure the highest quality of reproduction possible.

La qualité de cette microforme dépend grandement de la qualité de la thèse soumise au microfilmage. Nous avons tout fait pour assurer une qualité supérieure de reproduction.

If pages are missing, contact the university which granted the degree.

S'il manque des pages, veuillez communiquer avec l'université qui a conféré le grade.

Some pages may have indistinct print especially if the original pages were typed with a poor typewriter ribbon or if the university sent us an inferior photocopy.

La qualité d'impression de certaines pages peut laisser à désirer, surtout si les pages originales ont été dactylographiées à l'aide d'un ruban usé ou si l'université nous a fait parvenir une photocopie de qualité inférieure.

Reproduction in full or in part of this microform is governed by the Canadian Copyright Act, R.S.C. 1970, c. C-30, and subsequent amendments.

La reproduction, même partielle, de cette microforme est soumise à la Loi canadienne sur le droit d'auteur, SRC 1970, c. C-30, et ses amendements subséquents.

NEW PRODUCTION IN THE TROPICAL PACIFIC  
REGION

By  
Maria Angélica Peña Aguilar

SUBMITTED IN PARTIAL FULFILLMENT OF THE  
REQUIREMENTS FOR THE DEGREE OF  
DOCTOR OF PHILOSOPHY  
AT  
DALHOUSIE UNIVERSITY  
HALIFAX, NOVA SCOTIA  
JULY 1994

© Copyright by Maria Angélica Peña Aguilar, 1994



National Library  
of Canada

Bibliothèque nationale  
du Canada

Acquisitions and  
Bibliographic Services Branch

Direction des acquisitions et  
des services bibliographiques

395 Wellington Street  
Ottawa, Ontario  
K1A 0N4

395, rue Wellington  
Ottawa (Ontario)  
K1A 0N4

*Your file* *Votre référence*

*Our file* *Notre référence*

THE AUTHOR HAS GRANTED AN  
IRREVOCABLE NON-EXCLUSIVE  
LICENCE ALLOWING THE NATIONAL  
LIBRARY OF CANADA TO  
REPRODUCE, LOAN, DISTRIBUTE OR  
SELL COPIES OF HIS/HER THESIS BY  
ANY MEANS AND IN ANY FORM OR  
FORMAT, MAKING THIS THESIS  
AVAILABLE TO INTERESTED  
PERSONS.

L'AUTEUR A ACCORDE UNE LICENCE  
IRREVOCABLE ET NON EXCLUSIVE  
PERMETTANT A LA BIBLIOTHEQUE  
NATIONALE DU CANADA DE  
REPRODUIRE, PRETER, DISTRIBUER  
OU VENDRE DES COPIES DE SA  
THESE DE QUELQUE MANIERE ET  
SOUS QUELQUE FORME QUE CE SOIT  
POUR METTRE DES EXEMPLAIRES DE  
CETTE THESE A LA DISPOSITION DES  
PERSONNE INTERESSEES.

THE AUTHOR RETAINS OWNERSHIP  
OF THE COPYRIGHT IN HIS/HER  
THESIS. NEITHER THE THESIS NOR  
SUBSTANTIAL EXTRACTS FROM IT  
MAY BE PRINTED OR OTHERWISE  
REPRODUCED WITHOUT HIS/HER  
PERMISSION.

L'AUTEUR CONSERVE LA PROPRIETE  
DU DROIT D'AUTEUR QUI PROTEGE  
SA THESE. NI LA THESE NI DES  
EXTRAITS SUBSTANTIELS DE CELLE-  
CI NE DOIVENT ETRE IMPRIMES OU  
AUTREMENT REPRODUITS SANS SON  
AUTORISATION.

ISBN 0-612-05151-X

Canada

Name Maria Angeles Peña Aguilar

Dissertation Abstracts International is arranged by broad, general subject categories. Please select the one subject which most nearly describes the content of your dissertation. Enter the corresponding four-digit code in the spaces provided.

new production in the tropical Pacific region

0416

U·M·I

SUBJECT TERM

SUBJECT CODE

Subject Categories

**THE HUMANITIES AND SOCIAL SCIENCES**

**COMMUNICATIONS AND THE ARTS**

Arabic literature 0729  
 Art History 0377  
 Cinema 0900  
 Dance 0308  
 Fine Arts 0357  
 Information Science 0723  
 Journalism 0391  
 Library Science 0399  
 Mass Communications 0708  
 Music 0413  
 Speech Communication 0459  
 Theater 0465

**EDUCATION**

General 0515  
 Administration 0514  
 Adult and Continuing 0513  
 Agricultural 0517  
 Art 0273  
 Bilingual and Multicultural 0282  
 Business 0688  
 Community College 0275  
 Curriculum and Instruction 0727  
 Early Childhood 0518  
 Elementary 0524  
 Finance 0277  
 Guidance and Counseling 0519  
 Health 0680  
 Higher 0745  
 History of 0520  
 Home Economics 0278  
 Industrial 0521  
 Language and Literature 0279  
 Mathematics 0280  
 Music 0522  
 Philosophy of 0998  
 Physical 0523

Psychology 0525  
 Reading 0535  
 Religious 0527  
 Sciences 0714  
 Secondary 0533  
 Social Sciences 0534  
 Sociology 0340  
 Special 0529  
 Teacher Training 0530  
 Technology 0710  
 Tests and Measurements 0288  
 Vocational 0747

**LANGUAGE, LITERATURE AND LINGUISTICS**

Language 0679  
 General 0289  
 Ancient 0290  
 Linguistics 0291  
 Modern  
 Literature 0401  
 General 0294  
 Classical 0295  
 Comparative 0297  
 Medieval 0298  
 Modern 0316  
 African 0591  
 American 0305  
 Asian 0352  
 Canadian (English) 0355  
 Canadian (French) 0593  
 English 0311  
 Germanic 0312  
 Latin American 0315  
 Middle Eastern 0313  
 Romance 0314  
 Slavic and East European

**PHILOSOPHY, RELIGION AND THEOLOGY**

Philosophy 0422  
 Religion 0318  
 General 0321  
 Biblical Studies 0319  
 Clergy 0320  
 History of 0322  
 Philosophy of 0469  
 Theology

**SOCIAL SCIENCES**

American Studies 0323  
 Anthropology 0324  
 Archaeology 0326  
 Cultural 0327  
 Physical  
 Business Administration 0310  
 General 0272  
 Accounting 0770  
 Banking 0454  
 Management 0338  
 Marketing 0385  
 Canadian Studies  
 Economics 0501  
 General 0503  
 Agricultural 0505  
 Commerce Business 0508  
 Finance 0509  
 History 0510  
 Labor 0511  
 Theory 0358  
 Folklore 0366  
 Geography 0351  
 Gerontology  
 History 0578  
 General

Ancient 0579  
 Medieval 0581  
 Modern 0582  
 Black 0328  
 African 0331  
 Asia, Australia and Oceania 0332  
 Canadian 0334  
 European 0335  
 Latin American 0336  
 Middle Eastern 0333  
 United States 0337  
 History of Science 0585  
 Law 0398  
 Political Science 0615  
 General  
 International Law and Relations 0616  
 Public Administration 0617  
 Recreation 0814  
 Social Work 0452  
 Sociology 0620  
 General  
 Criminology and Penology 0627  
 Demography 0938  
 Ethnic and Racial Studies 0631  
 Individual and Family Studies 0628  
 Industrial and Labor Relations 0629  
 Public and Social Welfare 0630  
 Social Structure and Development 0700  
 Theory and Methods 0344  
 Transportation 0709  
 Urban and Regional Planning 0999  
 Women's Studies 0453

**THE SCIENCES AND ENGINEERING**

**BIOLOGICAL SCIENCES**

Agriculture 0473  
 General 0285  
 Agronomy  
 Animal Culture and Nutrition 0475  
 Animal Pathology 0476  
 Food Science and Technology 0359  
 Forestry and Wildlife 0478  
 Plant Culture 0479  
 Plant Pathology 0480  
 Plant Physiology 0817  
 Range Management 0777  
 Wood Technology 0746  
 Biology 0306  
 General 0287  
 Anatomy 0308  
 Biochemistry 0309  
 Botany 0309  
 Cell 0379  
 Ecology 0329  
 Entomology 0353  
 Genetics 0369  
 Immunology 0793  
 Microbiology 0410  
 Molecular 0307  
 Neurosciences 0317  
 Oncology 0416  
 Physiology 0433  
 Radiation 0821  
 Veterinary Science 0778  
 Zoology 0472  
 Biophysics 0786  
 General 0760  
 Medical

Geodesy 0370  
 Geology 0372  
 Geophysics 0373  
 Hydrology 0388  
 Mineralogy 0411  
 Paleobotany 0345  
 Paleocology 0426  
 Paleontology 0418  
 Paleozoology 0985  
 Polynology 0427  
 Physical Geography 0368  
 Physical Oceanography 0415

**HEALTH AND ENVIRONMENTAL SCIENCES**

Environmental Sciences 0758  
 Health Sciences 0566  
 General 0300  
 Audiology 0992  
 Chemotherapy 0567  
 Dentistry 0350  
 Education 0769  
 Hospital Management 0758  
 Human Development 0982  
 Immunology 0564  
 Medicine and Surgery 0347  
 Mental Health 0569  
 Nursing 0570  
 Nutrition 0380  
 Obstetrics and Gynecology  
 Occupational Health and Therapy 0354  
 Ophthalmology 0381  
 Pathology 0571  
 Pharmacology 0419  
 Pharmacy 0572  
 Physical Therapy 0382  
 Public Health 0573  
 Radiology 0574  
 Recreation 0575

Speech Pathology 0460  
 Toxicology 0383  
 Home Economics 0386

**PHYSICAL SCIENCES**

Pure Sciences  
 Chemistry 0485  
 General 0749  
 Agricultural 0426  
 Analytical 0487  
 Biochemistry 0488  
 Inorganic 0738  
 Nuclear 0490  
 Organic 0491  
 Pharmaceutical 0494  
 Physical 0495  
 Polymer 0754  
 Radiation 0405  
 Mathematics 0605  
 Physics 0986  
 General  
 Acoustics  
 Astronomy and Astrophysics 0606  
 Atmospheric Science 0608  
 Atomic 0748  
 Electronics and Electricity 0607  
 Elementary Particles and High Energy 0798  
 Fluid and Plasma 0759  
 Molecular 0609  
 Nuclear 0610  
 Optics 0752  
 Radiation 0756  
 Solid State 0611  
 Statistics 0463  
 Applied Sciences  
 Applied Mechanics 0346  
 Computer Science 0984

Engineering 0537  
 General 0538  
 Aerospace 0539  
 Agricultural 0540  
 Automotive 0541  
 Biomedical 0542  
 Chemical 0543  
 Civil 0544  
 Electronics and Electrical 0348  
 Heat and Thermodynamics 0545  
 Hydraulic 0546  
 Industrial 0547  
 Marine 0794  
 Materials Science 0548  
 Mechanical 0743  
 Metallurgy 0551  
 Mining 0552  
 Nuclear 0549  
 Packaging 0765  
 Petroleum 0554  
 Sanitary and Municipal System Science 0790  
 Geotechnology 0428  
 Operations Research 0796  
 Plastics Technology 0795  
 Textile Technology 0994

**PSYCHOLOGY**

General 0621  
 Behavioral 0384  
 Clinical 0622  
 Developmental 0620  
 Experimental 0623  
 Industrial 0624  
 Personality 0625  
 Physiological 0989  
 Psychobiology 0349  
 Psychometrics 0632  
 Social 0451



DALHOUSIE UNIVERSITY

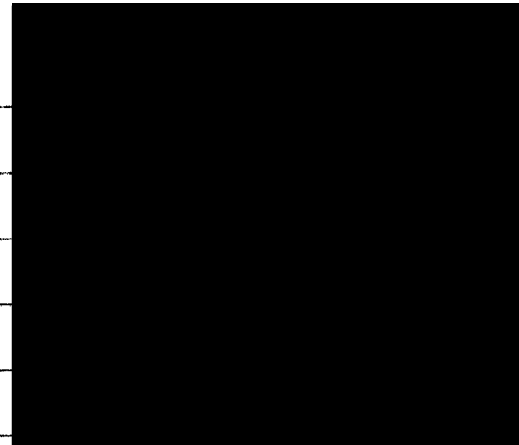
FACULTY OF GRADUATE STUDIES

The undersigned hereby certify that they have read and recommend to the Faculty of Graduate Studies for acceptance a thesis entitled "New Production in the Tropical Pacific Region"

by Maria Angelica Pena-Aguilar  
in partial fulfillment of the requirements for the degree of  
Doctor of Philosophy.

Dated June 27, 1994

External Examiner  
Research Supervisor  
Examining Committee



DALHOUSIE UNIVERSITY

Date: July 1994

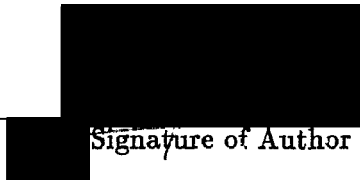
Author: Maria Angélica Peña Aguilar

Title: New Production in the Tropical Pacific Region

Department: Department of Oceanography

Degree: Ph.D. Convocation: October Year: 1994

Permission is herewith granted to Dalhousie University to circulate and to have copied for non-commercial purposes, at its discretion, the above title upon the request of individuals or institutions.



Signature of Author

THE AUTHOR RESERVES OTHER PUBLICATION RIGHTS, AND NEITHER THE THESIS NOR EXTENSIVE EXTRACTS FROM IT MAY BE PRINTED OR OTHERWISE REPRODUCED WITHOUT THE AUTHOR'S WRITTEN PERMISSION.

THE AUTHOR ATTESTS THAT PERMISSION HAS BEEN OBTAINED FOR THE USE OF ANY COPYRIGHTED MATERIAL APPEARING IN THIS THESIS (OTHER THAN BRIEF EXCERPTS REQUIRING ONLY PROPER ACKNOWLEDGEMENT IN SCHOLARLY WRITING) AND THAT ALL SUCH USE IS CLEARLY ACKNOWLEDGED.

*A mis padres*



# Contents

<b>List of Tables</b>	vii
<b>List of Figures</b>	ix
<b>Abstract</b>	xiv
<b>List of symbols</b>	
<b>Acknowledgments</b>	xvii
<b>1 Introduction</b>	<b>1</b>
<b>2 New production in the central equatorial Pacific</b>	<b>7</b>
2.1 Introduction . . . . .	7
2.2 Methods . . . . .	9
2.3 Results . . . . .	12
2.4 Discussion . . . . .	18
<b>3 New production in the warm waters of the tropical Pacific Ocean</b>	<b>29</b>
3.1 Introduction . . . . .	29
3.2 Approach . . . . .	31
3.2.1 Fluxes of heat . . . . .	32
3.2.2 Fluxes of nitrate . . . . .	33
3.2.3 Nitrate-Temperature relationship . . . . .	34

3.3	Data . . . . .	35
3.4	Results . . . . .	39
3.4.1	Temperature and nitrate distribution . . . . .	39
3.4.2	Nitrate-temperature relationship . . . . .	44
3.4.3	Nitrate fluxes . . . . .	46
3.5	Discussion . . . . .	50
3.5.1	Potential sources of error . . . . .	51
3.5.2	Comparison with other new production estimates . . . . .	55
3.5.3	New production and the relationship to net air-sea exchange of carbon . . . . .	57
3.6	Conclusion . . . . .	57
<b>4</b>	<b>The effect of fluctuations in the input of nitrate on phytoplankton biomass and new production</b>	<b>59</b>
4.1	Introduction . . . . .	59
4.2	Model Description . . . . .	62
4.3	Steady-state solution . . . . .	70
4.4	Variability in the input of nitrate . . . . .	81
4.5	Discussion . . . . .	93
4.5.1	The role of predation on surface nitrate concentration . . . . .	93
4.5.2	Control of phytoplankton biomass in oligotrophic ocean . . . . .	96
4.5.3	Role of variations in the nitrate input on new production . . . . .	98
4.5.4	Control of $f$ -ratio . . . . .	98
<b>5</b>	<b>Conclusions</b>	<b>101</b>
<b>6</b>	<b>Bibliography</b>	<b>104</b>

# List of Tables

2.1	Location, depth of the euphotic zone ( $Z_{eu}$ ) and surface nutrient (nitrate and silicate) concentrations at each station occupied. . . . .	10
2.2	Chl <i>a</i> , primary productivity ( $\text{mmol C m}^{-2} \text{d}^{-1}$ ), and nitrogen uptake ( $\text{mmol N m}^{-2} \text{d}^{-1}$ ) integrated over the euphotic zone. Ammonium uptake rates were calculated based on the expected range of substrate concentration ( $0.01$ to $0.15 \text{ mmol m}^{-3}$ at the equatorial region and $0.01$ to $0.12 \text{ mmol m}^{-3}$ at the other regions). Means and coefficients of variation ( $CV = \text{standard deviation} / \text{mean}$ and expressed as percentage) computed for each region (see text for regional designation). . . . .	15
2.3	Comparison of nutrient concentration ( $\text{mmol m}^{-3}$ ), chl <i>a</i> ( $\text{mg m}^{-2}$ ) and hourly rates of primary productivity ( $\text{mg C m}^{-2} \text{h}^{-1}$ ) and nitrogen uptake ( $\text{mmol N m}^{-2} \text{h}^{-1}$ ) integrated over the euphotic zone in the equatorial Pacific region. Mean values (standard deviation). . . . .	24
3.1	The net surface heat flux, mean turbulent nitrate transport and total surface area enclosed by the $26^\circ\text{C}$ isotherm in the tropical Pacific and the corresponding mean new production using the Redfield ratio of C/N of 6.6 (at/at). . . . .	48
3.2	The mean advective nitrate balance of the region enclosed by the $26^\circ\text{C}$ isotherm in the tropical Pacific and the corresponding mean new production using the Redfield ratio of C/N of 6.6 (at/at). . . . .	49
4.1	Model variables and parameters . . . . .	64

4.2	Zooplankton parameters used in simulation with $w=1$ ( $\text{m d}^{-1}$ ) and the steady-state values of the model variables. . . . .	83
4.3	Zooplankton parameters used in simulation with $w=0.25$ ( $\text{m d}^{-1}$ ) and the steady-state values of the model variables. . . . .	84
4.4	Matrix of correlation between the variation of ammonia ( $A$ ), nitrate ( $N$ ), phytoplankton ( $P$ ), zooplankton ( $Z$ ), new production ( $P\gamma_N$ ) and regenerated production ( $P\gamma_A$ ) for different nitrate input, all simulations combined. . . . .	90

# List of Figures

2.1	Vertical sections of temperature, nitrate, chl <i>a</i> , PON, and nitrate uptake along the cruise track. Longitudinal variations between stations were ignored. Negative latitudes are south. . . . .	13
2.2	Vertical profiles of nitrate uptake and nitrate uptake normalized to chl <i>a</i> in A) southern, B) equatorial and C) northern regions. Values represent the mean rates and their standard errors. . . . .	17
2.3	Relationship between nitrate concentration and the chl <i>a</i> -normalized uptake rate, all data combined ( $r^2 = 0.6$ ; $n=64$ ). . . . .	19
2.4	Relationship between chl <i>a</i> concentration and nitrate uptake, all data combined ( $n=64$ ). . . . .	20
2.5	Chl <i>a</i> -normalized nitrate uptake plotted against light level at all stations along the transect. . . . .	21
3.1	Location of the stations used in this analysis. Filled circles = NODC (3,845 stns.); triangles = Ocean Atlas (454 stns.); and open circles = Fiedler and colleagues (574 stns.). . . . .	36
3.2	Yearly and monthly distribution of the National Oceanographic Data Center (NODC) data. . . . .	37
3.3	(a) Surface distribution of temperature ( $^{\circ}\text{C}$ ) in the tropical Pacific region and (b) its five degree squares standard deviation. . . . .	40
3.4	(a) Surface distribution of nitrate concentration ( $\mu\text{M}$ ) in the tropical Pacific region and (b) its five degree squares standard deviation. . . . .	41

3.5	(a) The depth of the 26°C isotherm subsurface boundary (m) and (b) its five degree squares standard deviation. . . . .	42
3.6	(a) Nitrate concentration ( $\mu\text{M}$ ) at the depth of the 26°C isotherm and (b) its five degree squares standard deviation. . . . .	43
3.7	Scatter plot of temperature ( $^{\circ}\text{C}$ ) vs nitrate concentration ( $\mu\text{M}$ ) in the upper 250 m of the region enclosed by the 26°C isotherm ( $n=48,100$ ). The same relationship is shown for the surface values in the insert ( $n=4,870$ ). . . . .	45
3.8	(a) The slope of the temperature-nitrate relationship ( $\mu\text{M } ^{\circ}\text{C}^{-1}$ ) at the base of the 26°C and (b) the standard deviation of the slope at every 5° square in the region enclosed by the 26°C isotherm. . . . .	47
4.1	Diagrammatic representation of the simple plankton model. . . . .	63
4.2	Combinations of nitrate and ammonium ( $N$ and $A$ ; $\mu\text{M}$ ), relative to their respective half-saturation constants ( $k_N$ and $k_A$ ; $\mu\text{M}$ ), for which growth is nitrogen- saturated ( $\gamma_A + \gamma_N = 1$ ). Solutions are presented for different values of the ammonia inhibition term ( $\Psi$ ; $\mu\text{M}$ ) times the half-saturation constant of ammonium uptake ( $k_A$ ), calculated from equations 4.5 (a; $\gamma_1$ ) and 4.6 (b; $\gamma_2$ ). The space to the right of each line represents nutrient concentration exceeding saturation. In these formulations, growth rates greater than $\mu_m$ are predicted. . . . .	67
4.3	Contours of predicted $f$ -ratios as a function of nitrate ( $N$ ) and ammonia ( $A$ ) concentrations ( $\mu\text{M}$ ) relative to their respective half-saturation constant ( $k_N$ and $k_A$ ; $\mu\text{M}$ ): a) $\gamma_1$ ; equation 4.5, b) $\gamma_2$ ; equation 4.6, and c) $\gamma_3$ ; equation 4.7. The values of $\gamma_1$ and $\gamma_2$ were estimated using a fixed value of $\Psi = 1.5 \mu\text{M}^{-1}$ . When $N/k_N$ is $>2$ , the $f$ -ratio in a) and b) is mostly dependent on $A/k_A$ , whereas in c) the $f$ -ratio is directly proportional to the ratio of $N/k_N$ to $A/k_A$ . . . . .	68

4.4	Zooplankton grazing rate as a function of phytoplankton biomass. a) $\lambda_1$ , s-shaped grazing formulation [ <i>Hollings</i> , 1965], b) $\lambda_2$ , Ivlev formulation [ <i>Ivlev</i> , 1955], and c) $\lambda_3$ , Mayzaud and Poulet formulation [ <i>Mayzaud and Poulet</i> , 1978]. . . . .	71
4.5	The ratio of zooplankton biomass ( $\mu\text{M}$ ) to phytoplankton biomass ( $\mu\text{M}$ ) at steady-state as a function of the phytoplankton specific growth rate ( $\text{d}^{-1}$ ) relative to the zooplankton specific growth rate ( $\text{d}^{-1}$ ) for different values of the zooplankton assimilation efficiency ( $\beta$ ) and the ratio of phytoplankton specific mortality rate to phytoplankton specific growth rate ( $m/\mu_m(\gamma_N + \gamma_A)$ ; dimensionless). Efficiency in assimilation and growth translates into greater accumulation of zooplankton. . . . .	73
4.6	Non-dimensional steady-state solution of phytoplankton biomass ( $P$ ; $\mu\text{M}$ ) relative to the half-saturation concentration of grazing ( $k_g$ ; $\mu\text{M}$ ) as a function of the ratio of zooplankton maximum specific grazing rate ( $G_m$ ; $\text{d}^{-1}$ ) to zooplankton specific mortality rate ( $d$ ; $\text{d}^{-1}$ ). Solutions are presented for different grazing formulations: a) $\lambda_1$ ; equation 4.15, b) $\lambda_2$ ; equation 4.16, and c) $\lambda_3$ ; equation 4.17. . . . .	74
4.7	Non-dimensionalized representation of the isolines of normalized nitrate uptake ( $\gamma_N$ ) as a function of the ratio of nitrate concentration in the mixed layer ( $N$ ; $\mu\text{M}$ ) to that below this layer ( $N_z$ ; $\mu\text{M}$ ) and the ratio of phytoplankton growth rate ( $P\mu_m$ ; $\mu\text{M d}^{-1}$ ) to nitrate input ( $F(t)N_z$ ; $\mu\text{M d}^{-1}$ ). . . . .	77
4.8	Contours of normalized nitrate uptake ( $\gamma_N$ ) at steady-state as a function of the dimensionless ratio of $k_g\mu_m$ to nitrate transport ( $FN_z$ ) and the ratio of zooplankton maximum specific grazing rate ( $G_m$ ; $\text{d}^{-1}$ ) to zooplankton specific mortality rate ( $d$ ; $\text{d}^{-1}$ ) for a fixed value of $\beta = 0.4$ , computed for different levels of residual nitrate: a) all nitrate is consumed; $N/N_z=0$ , b) 70% of the nitrate input is consumed; $N/N_z=0.3$ , and c) 50% is consumed; $N/N_z=0.5$ . . . . .	79

4.9	<i>f</i> -ratios at steady-state as a function of zooplankton excretion rate ( <i>b</i> ), regeneration efficiency of dead zooplankton ( <i>c</i> ) and zooplankton assimilation efficiency ( $\beta$ ) for a fixed value of the regeneration efficiency of dead phytoplankton $a = 0.5$ and the ratio of phytoplankton specific mortality rate to phytoplankton specific growth rate $m/\mu_m(\gamma_N + \gamma_A) = 0.1$ (dimensionless). . . . .	80
4.10	Model output of nitrate, phytoplankton and zooplankton concentrations for a simulation with a high amplitude ( $w = 1 \text{ m d}^{-1}$ ) of nitrate inputs of: a) 4 days periods, and b) 14 days. Parameters values correspond to simulation IV ( $Z/P \sim 1$ and $P/k_g \sim 1$ ) and are shown in Table 4.2. . . . .	85
4.11	Model output of nitrate, phytoplankton and zooplankton concentrations for a simulation with a low amplitude ( $w = 0.25 \text{ m d}^{-1}$ ) of nitrate inputs of: a) 4 days periods, and b) 14 days. Parameters values correspond to simulation XII ( $Z/P \sim 1$ and $P/k_g > 1$ ) and are shown in Table 4.3. . . . .	86
4.12	Amplitude of variations in the concentration of phytoplankton (circles; $10^{-1} \mu\text{M}$ ), zooplankton (squares; $10^{-1} \mu\text{M}$ ), and nitrate (diamonds; $\mu\text{M}$ ) at different frequencies of the nitrate fluctuations for simulations with high input of nitrate ( $w = 1 \text{ m d}^{-1}$ ). Parameter values used in each simulation are given in Table 4.2. . . . .	88
4.13	Time delay between the maximum input of nitrate to the mixed layer and maximum concentration of phytoplankton (circles), zooplankton (squares) and nitrate (diamonds) in simulations where a significant variation in concentrations was obtained. Results are presented for different frequencies of the nitrate fluctuations for simulations with a high input of nitrate ( $w = 1 \text{ m d}^{-1}$ ). Parameters values as in Fig 4.10.	89



4.14 Amplitude of variations in the concentration of phytoplankton (circles), zooplankton (squares) and, nitrate (diamonds) at different frequencies of the nitrate fluctuations for simulations with low input of nitrate ( $w=0.25 \text{ m d}^{-1}$ ). See Table 4.3 for values of the parameters used in each simulation. . . . . 91

## Abstract

The amount of carbon exported from the surface layers of the world's oceans is strongly influenced by processes at low latitudes; it has been estimated that the export flux of carbon, or "new" production, in the equatorial Pacific could account for a significant proportion (25 to 50 %) of the global total. In this study, rates of new production were estimated from discrete measurements of nitrate uptake along a transect across the equatorial Pacific region at 135°W, and from an analysis of nitrate and heat balance in the warm waters of the tropical Pacific.

Results from direct measurements of N (nitrate and ammonia) uptake and primary productivity showed higher rates of total and new production near the equator which coincided with higher concentrations of chlorophyll and nitrate. Despite significant variations in nitrate concentration, variability of phytoplankton biomass and production was low along the transect. Although nitrate was abundant at the equator, regenerated N was the major source of inorganic N used by phytoplankton.

The average depth-integrated new production rate in the warm waters of the tropical Pacific was computed through a horizontal and vertical nitrate balance. The net turbulent flux of nitrate into the region was computed using the climatological net surface heat flux and the nitrate-temperature relationship. The net advective nitrate transport into the region was estimated using the mean nitrate distribution obtained from historical data and previous results from a general circulation model of the tropical Pacific. The rate of new production resulting from vertical turbulent nitrate fluxes ( $24 \text{ mg C m}^{-2} \text{ d}^{-1}$ ) is similar in magnitude as that due to advective transport ( $20 \text{ mg C m}^{-2} \text{ d}^{-1}$ ).

A simple biological model of the mixed layer was used to study the effects of fluctuations in the input of nitrate on phytoplankton biomass and new production. The steady-state solutions of the model were analyzed to determine the influence of parameter values on model output and simulations were carried out varying the frequency and magnitude of the nitrate input. When phytoplankton was growing at its maximum capacity or when biomass was limited by grazing, phytoplankton biomass did not respond to variations in the nitrate input, even when the nitrate input to the euphotic zone was high. From the frequency response, it was found that periods equal to or less than 4 days did not influence phytoplankton biomass and new production. On longer time scales, the magnitude of the biomass increase depended inversely on the frequency.

This thesis supports the suggestion that nitrate utilization or new production in the equatorial Pacific is controlled by zooplankton grazing. Alternatively, it has been suggested that the availability of iron could be limiting phytoplankton growth and nutrient utilization in this region. Results from the model indicate that iron limitation of phytoplankton growth alone is not sufficient to explain the maintenance of low chlorophyll and high nitrate concentrations.

## List of symbols

$c_p$	Specific heat of seawater	$\text{J kg}^{-1} \text{ } ^\circ\text{C}^{-1}$
$\rho$	water density	$\text{kg m}^{-3}$
$E$	irradiance vector	$\text{J m}^{-2} \text{ s}^{-1}$
$T$	temperature	$^\circ\text{C}$
$T'$	temperature fluctuations	$^\circ\text{C}$
$U$	velocity	$\text{m s}^{-1}$
$U'$	velocity fluctuations	$\text{m s}^{-1}$
$N$	nitrate concentration	$\mu\text{M}$
$N'$	fluctuations in the nitrate concentration	$\mu\text{M}$
$Q_o$	net surface heat flux	$\text{W m}^{-2}$
$A_S$	surface area	$\text{m}^2$
$A_T$	surface of constant mean temperature	$\text{m}^2$
$W$	vertical velocity	$\text{m s}^{-1}$
$P_n$	new production rate	$\text{mmol N m}^{-3} \text{ s}^{-1}$
$P_N$	depth integrated new production	$\text{mmol N m}^{-2} \text{ s}^{-1}$
$z_T$	depth of subsurface isothermal boundary	$\text{m}$
$P$	phytoplankton biomass	$\mu\text{M}$
$Z$	Zooplankton biomass	$\mu\text{M}$
$A$	Ammonia concentration	$\mu\text{M}$
$\mu_m$	Phytoplankton maximum specific growth rate	$\text{d}^{-1}$
$\gamma_N$	Normalized nitrate uptake	
$\gamma_A$	Normalized ammonia uptake	

$\lambda$	Specific zooplankton grazing rate	$\text{d}^{-1}$
$m$	Phytoplankton specific mortality rate	$\text{d}^{-1}$
$F$	Net water transport	$\text{d}^{-1}$
$\beta$	Zooplankton assimilation efficiency	
$d$	Zooplankton specific mortality rate	$\text{d}^{-1}$
$a$	Regeneration efficiency of dead phytoplankton	
$b$	Regeneration efficiency of zooplankton unassimilated food	
$c$	Regeneration efficiency of dead zooplankton	
$N_z$	Nitrate concentration below the mixed layer	$\mu\text{M}$
$k_N$	Half-saturation constant for nitrate uptake	$\mu\text{M}$
$k_A$	Half-saturation constant for ammonia uptake	$\mu\text{M}$
$\Psi$	Ammonia inhibition parameter	$\mu\text{M}^{-1}$
$G_m$	Maximum specific ingestion rate	$\text{d}^{-1}$
$k_g$	Half-saturation constant of ingestion rate	$\mu\text{M}$
$F_0$	Minimum water transport	$\text{d}^{-1}$
$w$	vertical velocity	$\text{m d}^{-1}$
$H$	Mixed layer depth	$\text{m}$
$t$	Time	$\text{d}$
$\omega$	Frequency	$\text{d}^{-1}$

# Acknowledgements

I would like to thank all the members of my committee for their advice, help and encouragement. It has been a pleasure to interact with them. I will be always grateful to my supervisor Marlon Lewis for his support and for allowing me the freedom to explore my ideas even when they differed from his. I thank Glen Harrison for being always willing to spend many hours discussing concepts and boosting my enthusiasm. He was always there to help and discuss my doubts from the small practical ones to the existential. I thank John Cullen for sharing his stimulating ideas and suggestions, and for pushing me to think ever harder, even when I thought I couldn't. I thank Dan Kelley for his willingness to respond quickly with good advice. Thank you. I have learned so much from all of you.

My sincere thanks also go to all the people in the 2nd floor D-lab, past and present, for their friendship, help and support that made these years enjoyable. I thank my friends and family for their love, patience and support.

# Chapter 1

## Introduction

Primary production is composed of two fractions: new production, which is based on nutrients imported to the euphotic zone (traditionally defined from the surface to the depth of the 1% light intensity), and regenerated production which is fueled by nutrients recycled within the euphotic zone through community metabolism [*Dugdale and Goering, 1967*]. The main source of nutrients for new production is the upwelling and diffusion of nutrients from deep water into the euphotic zone. This input of nitrate occurs on scales that range from a small, more or less continuous molecular flux through the nutricline to larger episodic fluxes associated with destabilization of the mixed layer, as in the case of upwelling or storm-induced deepening of the mixed layer [*Klein and Coste, 1984; Eppley and Renger, 1988; Jenkins, 1988*]. New production can be further subdivided into organic matter which accumulates in the euphotic zone, and that which is exported from the euphotic zone. In the steady-state condition, new production is equivalent to the downward flux of organic matter to the ocean interior on an appropriately large scale [*Eppley and Peterson, 1979*].

Throughout most of the ocean, phytoplankton production is limited by the availability of light or nutrients. Natural phytoplankton populations are exposed to variability in the nitrate concentration over many space and time scales. Often, such perturbations result from physical events that cause an increase in the biological productivity by up to several orders of magnitude [*Yoder et al., 1983; Hoffman and*

*Ambler, 1988*]. For example, enhanced primary production and chlorophyll concentrations are found in upwelling regions where nitrate is brought to the euphotic zone. Upwelling of nutrient-rich water mainly occurs in coastal areas associated with eastern boundary currents and in oceanic regions associated with current divergences as along the equator and in the Southern Ocean. The upwelling of nutrients to the upper layer is slower along the equatorial Pacific divergences than in coastal upwelling regions [*Brady and Bryden, 1987; Halpern et al., 1989*]. However, due to its quasi-stationary nature and the large area of ocean represented, it has been estimated that if all the nitrate upwelled in the equatorial Pacific region from  $90^{\circ}$  to  $180^{\circ}$ W and from  $5^{\circ}$ N and  $5^{\circ}$ S were used by phytoplankton cells, this region could contribute a large proportion (18-56%) of global new production [*Chavez and Barber, 1987*]. However, only a fraction of the nitrate upwelled is used by phytoplankton cells in this region [*Carr, 1991; Fiedler et al., 1991*]. The unused nitrate is advected laterally to the euphotic zone of adjacent regions where it is either utilized by phytoplankton cells or lost through downwelling.

The equatorial Pacific region is characterized by strong surface and subsurface currents and considerable spatial variability [*Wyrski, 1981; Philander et al., 1987; Moum et al., 1989*]. In the western equatorial Pacific, the thermocline and nutricline are deeper than in the eastern and central regions and upwelled water comes from above the thermocline (and nutricline). Further east, the upwelled water comes from the nutrient-rich water below the shallow pycnocline. This leads to a greater biological productivity in the eastern equatorial Pacific than in the west. Results from physical oceanographic experiments in the equatorial Pacific indicate that the current system is dominated by systematic seasonal variation (instead of eddy dynamics), and that both the interannual variability and the seasonal variability at a specific location can be very large [*Wyrski, 1974; McPhaden and Taft, 1988; Philander, 1989*]. This temporal variability is often as large as the variability along large latitudinal distances. Similarly, the productivity of the equatorial Pacific is very strongly affected by interannual events like El Niño. Studies of both surface productivity and fluxes

to the sediments suggest that the interannual variability associated with these events far exceeds the seasonal variability [*Chavez and Barber, 1985; Dymond and Collier, 1988*].

In the eastern and central equatorial Pacific, surface nutrients (nitrate and phosphate) are not depleted and chlorophyll concentration and primary production are lower than they might be if all the nitrate was utilized [*Thomas, 1979*]. This has been referred to as a high nutrient-low chlorophyll (HNLC) condition [*Minas et al., 1986*]. Results from the few studies of phytoplankton N utilization to date in the eastern and central equatorial Pacific region suggest that, although the input of nitrate is enough to provide all the nitrogen required for phytoplankton production, most of the production is fueled by nitrogen recycled within the euphotic zone (i.e. is regenerated production). For example, in the eastern equatorial Pacific, an *f*-ratio (i.e. the rate of new production relative to the total production; *Eppley and Peterson, 1979*) of 0.1 to 0.3 has been determined by both the  $^{15}\text{N}$  uptake and the carbon/nitrogen flux approaches [*Murray et al., 1989*]. New production rates estimated from box models of nitrate balances in the eastern tropical Pacific are also about 35% of the total production determined by  $^{14}\text{C}$  uptake [*Fiedler et al., 1991*]. In the central equatorial Pacific an *f*-ratio of 0.17 has been measured by  $^{15}\text{N}$  uptake [*Dugdale et al., 1992*]. The general conclusion is that upwelling of nutrients is a necessary but clearly not a sufficient condition for high new and total production and phytoplankton biomass in marine systems.

There are several possible explanations for the high nutrient and low phytoplankton biomass in the equatorial Pacific, but grazing control [e.g. *Walsh, 1976; Banse, 1991; Cullen et al., 1992*] and iron limitation [*Martin et al., 1989; Barber and Chavez, 1991*] have received the most attention. Iron limitation of phytoplankton growth is hypothesized to play a dual role by limiting nutrient utilization and by influencing plankton species composition [*Price et al., 1991*]. However, even if the specific growth rate of phytoplankton is less than optimal, without losses such as grazing by zooplankton, sinking and advection, the phytoplankton stock would still accumulate



and deplete the available nutrients. Since phytoplankton biomass is dominated by cells smaller than  $10\ \mu\text{m}$  [Chavez, 1989; Peña *et al.*, 1990] which sink very slowly (i.e.  $<0.15\ \text{m d}^{-1}$ ; Bienfang and Harrison, 1984), and physical transport of chlorophyll removes around 1% of the integrated chlorophyll concentration [Carr, 1991], the main loss term of the phytoplankton biomass in this region seems to be herbivorous grazing. Similarly, Frost and Franzen [1994] used a simple chemostat model to show that grazing control is essential to reproduce the present conditions of high nutrients, low phytoplankton biomass, and phytoplankton specific growth rate observed in the equatorial upwelling zone. Before the dominance of small phytoplankton cells in the ocean was widely recognized, Walsh [1976] suggested that herbivory was the process responsible for the equatorial HNLC condition. He suggested that grazing control results from the lack of physical variability on time scales of days to weeks which facilitates a close coupling between the growth of phytoplankton cells and zooplankton grazing [see also Parsons and Lalli, 1988].

A change in the species composition of phytoplankton favoring large phytoplankton cells (i.e. mainly diatoms) has been observed in many iron-enriched incubation experiments [Martin *et al.*, 1989; Hudson and Morel, 1990; Martin *et al.*, 1991; Buma *et al.*, 1991; Coale, 1991]. Thus, low iron levels might favor the growth of small phytoplankton cells in the open ocean, which might be more efficiently grazed by zooplankton. This result has led to the suggestion [Cullen, 1991; Martin *et al.*, 1991; Morel *et al.*, 1991] that enrichment with iron could substantially change the food-web structure towards a system with larger phytoplankton cells and higher rates of new production [Michaels and Silver, 1988]. However, even if the growth rate of large phytoplankton cells increased, iron fertilization might not have the expected effect due to the overriding effects of grazing pressure. Recently, iron was added to the surface waters of the equatorial Pacific Ocean south of the Galapagos Islands. From the preliminary results, it appears that phytoplankton growth was indeed stimulated upon iron enrichment [Wells, 1994]. However, the magnitude of the ecosystem response was smaller than predicted from the experiments carried out in bottles, and

the decrease in nitrate concentration was small. Also, in contrast to previous bottle experiments, the main increase in phytoplankton growth appeared to be that of picoplankton (cells of  $< 2 \mu m$  in size) rather than large diatoms [Wells, 1994].

In this thesis, the main objectives are:

1. to evaluate existing measurements of new production in the equatorial Pacific,
2. to provide and compare a new estimation of new production rates based on alternative methods, and
3. to investigate the mechanisms that control this rate.

Chapter 2 deals with a field study where discrete direct measurements of new production ( $^{15}\text{NO}_3^-$  uptake) and total production ( $^{14}\text{C}$  uptake) were made along a transect across the equatorial Pacific region at  $135^\circ\text{W}$  from  $15^\circ\text{S}$  to  $15^\circ\text{N}$ . These measurements permit a comparison of the horizontal and vertical distribution of new production rates and  $f$ -ratios over a region with a marked horizontal gradient of nitrate concentrations.

In Chapter 3, a method is presented to estimate the annual mean depth-integrated rate of new production over the warm waters of the tropical Pacific region from a calculation of horizontal and vertical nitrate balances. While previous estimations of new production based on this approach have only considered the flux of nitrate due to upwelling, here the transport of nitrate due to turbulent fluxes is also included. The net turbulent flux of nitrate into the region was computed in terms of the climatological net surface heat flux and the subsurface nitrate-temperature relationship. The net advective transport of nitrate was estimated using the mean nitrate distribution obtained from the analysis of historical data and from previous results of a general circulation model of the tropical Pacific.

Results from a simple biological model of the mixed layer are presented in Chapter 4 to explore the effects of fluctuations in the input of nitrate on phytoplankton biomass and new production rates. Simulations were carried out varying the frequency and

magnitude of the nitrate input. The influence of parameter values on model output is examined and discussed.

Finally, a summary of the principal results from previous chapters and the general conclusions of this thesis are given.

## Chapter 2

# New production in the central equatorial Pacific

### 2.1 Introduction

In much of the ocean, phytoplankton production seems to be constrained by the availability of nitrogen in the euphotic zone. Nitrogen for phytoplankton utilization comes from two sources: nitrogen regenerated (mostly ammonium) in the euphotic zone through food web metabolism, and nitrogen from outside the euphotic zone (mostly nitrate) supplied mainly by vertical fluxes. Primary production has been distinguished as regenerated or new production according to which of these sources of nitrogen is being used by phytoplankton [*Dugdale and Goering, 1967*]. In specific regions of the world ocean (i.e. equatorial Pacific, Northeast Pacific, Southern Ocean), phytoplankton production and biomass are much lower than would be expected from the observed high concentrations of plant nutrients found in the surface layer. This anomalous condition has been called high nutrient-low chlorophyll (HNLC) situation [*Minas et al., 1986*].

In the equatorial Pacific, surface concentrations of plant nutrients are elevated due to quasi-stationary upwelling associated with equatorial divergence [*Cromwell, 1953; Knauss, 1963; Wyrki, 1981*]. It has been estimated that complete utilization

of the nitrate upwelled in this region by phytoplankton cells could account for a significant proportion (18 to 56%) of the global new production [*Chavez and Barber, 1987*] and, hence, a comparable downward flux of organic matter to the ocean interior [*Eppley and Peterson, 1979*]. Few studies of nitrogen utilization by phytoplankton have been done in the equatorial Pacific. Recently, results from  $^{15}\text{N}$  uptake studies have shown an average  $f$ -ratio (nitrate uptake/total-N uptake; as defined by *Eppley and Peterson, 1979*) of 0.17 in the equatorial Pacific region at  $150^\circ\text{W}$  [*Dugdale et al., 1992*] and similar low values ( $f$ -ratios 0.1-0.3) in the eastern equatorial Pacific [*Murray et al., 1989*]. These studies showed that, although nitrate was the dominant form of nitrogen in the environment, most of the production was fuelled by regenerated forms of nitrogen. In contrast, *Eppley and Renger* [1992] using time course measurements of nitrate concentrations observed nitrate removal from the medium at rates far in excess of those determined by  $^{15}\text{N}$ -nitrate incorporation and, when converted to carbon (using a 6.6 C/N molar ratio), were equivalent to the total primary production in the equatorial Pacific at  $150^\circ\text{W}$ , implying an  $f$ -ratio  $\sim 1.0$ .

It has recently been suggested [*Wilkerson and Dugdale, 1992*] that phytoplankton in the equatorial Pacific upwelling region are not able to effectively utilize the available nitrate because initial concentrations are below some 'physiological threshold' necessary to induce maximal nitrate uptake rates as often observed in coastal upwelling regions [e.g. *MacIsaac et al., 1985*; *Wilkerson and Dugdale, 1987*]. On the other hand, *Murray et al.* [1989] suggested that ammonium concentration may be controlling nitrate utilization since a small relative increase in  $\text{NH}_4^+$  appeared to result in a dramatic reduction in the  $f$ -ratio. *Wheeler and Kokkinakis* [1990] have offered a similar explanation for persistence of residual  $\text{NO}_3^-$  in the northeast Pacific surface waters. *Martin et al.* [1989], taking a different approach, have suggested that the availability of iron in the equatorial Pacific region is inadequate to support productivity rates expected based on the high nitrate concentrations. In this regard also, *Price et al.* [1991] have recently shown a clear link between Fe availability and nitrate-based production. Several other studies in the equatorial upwelling region

[Walsh, 1976; Thomas, 1979; Murray *et al.*, 1989; Peña *et al.*, 1990; Cullen *et al.*, 1992] have suggested that grazing controls phytoplankton biomass and productivity. The relatively stable nature of these systems seems to have favored a close coupling between rates of phytoplankton growth and zooplankton grazing and excretion.

In this study, measurements of  $^{15}\text{N}$ -labelled nitrogen incorporation into particulate matter and primary productivity along a transect across the equatorial Pacific at  $135^\circ\text{W}$ , has led to the conclusion that the 'anomalous low' new production (nitrate uptake) in this region may result from grazing and concomitant  $\text{NH}_4^+$  production and utilization by the phytoplankton.

## 2.2 Methods

Samples were collected aboard the R.V. *Wecoma* (cruise W8803-B) on a transect across the equatorial Pacific region within a few degrees of  $135^\circ\text{W}$  longitude from ca  $15^\circ\text{S}$  to  $15^\circ\text{N}$  in April, 1988. At thirteen stations along this transect (see Table 2.1), water samples were collected in the euphotic zone (between 0 and 120 m) using twelve 5-liter Niskin bottles mounted on a rosette sampling system equipped with a CTD. The Niskin bottles had been retrofitted with silicon O-ring and silicon tubing as the closing mechanism [Price *et al.*, 1986].

Samples for nutrients (nitrate and silicate) concentration were taken from 12 fixed depths at each station (between 0 and 200 m) and determined by the method described by *Strickland and Parsons* [1972] with an autoanalyser. Light penetration and the euphotic depth conventionally defined as the 1% light intensity was determined by Secchi disk lowering (1% light level = 3 times the Secchi depth).

Uptake rates of nitrate and ammonium were measured by incorporation of  $^{15}\text{N}$  at 4-6 depths. Water samples of 1 or 2L were incubated on deck in polycarbonate bottles which were inoculated with either  $^{15}\text{NH}_4\text{Cl}$  or  $\text{Na}^{15}\text{NO}_3^-$  (99.0 atom %  $^{15}\text{N}$ ) such that added  $^{15}\text{NH}_4^+$  concentrations were  $0.05 \text{ mmol m}^{-3}$  and  $^{15}\text{NO}_3^-$  concentrations were  $0.5 \text{ mmol m}^{-3}$ .  $^{15}\text{NO}_3^-$  enrichments were  $> 10\%$  of ambient concentrations

Table 2.1: Location, depth of the euphotic zone ( $Z_{eu}$ ) and surface nutrient (nitrate and silicate) concentrations at each station occupied.

Station No	Location Latitude	Long.(W)	$Z_{eu}$ (m)	Nitrate ( $\text{mmol m}^{-3}$ )	Silicate ( $\text{mmol m}^{-3}$ )
4	14° 56.4'S	133° 54.6'	120	0	1.2
11	12° 09.4'S	134° 19.5'	105	0.3	1.3
20	5° 58.0'S	134° 59.4'	81	4.7	2.6
34	1° 59.9'S	133° 00.2'	87	4.5	0.6
39	0° 59.9'S	133° 35.5'	69	4.5	0.9
50	0° 30.8'N	133° 18.8'	63	5.3	1.9
55	2° 0.30'N	133° 37.9'	72	5.1	1.1
60	4° 17.2'N	133° 30.5'	75	0.4	0.8
65	5° 45.1'N	135° 00.0'	78	0.9	2.1
73	7° 13.7'N	137° 33.3'	81	0.2	1.8
78	9° 03.4'N	136° 47.5'	81	0.2	1.8
88	11° 05.2'N	136° 26.8'	84	0.1	1.8
96	15° 40.9'N	143° 05.7'	120	0	1.6

in the surface layer except in the nitrate abundant stations (Stns 20 to 60) where they were ~10%. Neutral density screens were used to approximate the light attenuation at the depth from which the samples were drawn. Samples were incubated between dawn and local noon, except at Stn 4 where incubation took place in the afternoon, and lasted for no more than 6 h in order to minimize isotope dilution effects due to  $\text{NH}_4^+$  recycling [Glibert *et al.*, 1982a] and to overcome the possible bias introduced by initial 'surge' uptake [Dugdale and Wilkerson, 1986]. The uptake rates of ammonium were not corrected for isotope dilution, since it has been shown that the error should be relatively small in open ocean waters [Kanda *et al.*, 1987]. At the end of the incubation period, samples were filtered onto precombusted Whatman GF/F glass fiber filters, which were then frozen and transported back to the lab. After oven-drying the filters, the  $^{15}\text{N}$ -enrichment of the particulate matter was determined using the micro-Dumas combustion technique and analysis by emission spectrometry [Fiedler and Proksch, 1975; Harrison, 1983]. Uptake rates are reported as  $\text{mmol N m}^{-3} \text{ h}^{-1}$  computed by multiplying the specific uptake rates,  $V$  ( $\text{h}^{-1}$ ), times the particulate organic nitrogen (PON) concentration of the sample determined at the beginning of the incubation [Dugdale and Goering, 1967]. The uptake rates of ammonium were calculated based on the expected range of substrate concentrations, since ammonium levels were not directly measured in this study. The values chosen were  $0.01 \text{ mmol m}^{-3}$ , corresponding to the lower concentration range observed in open ocean waters [Brzezinski, 1988], and the values ( $0.12$  and  $0.15 \text{ mmol m}^{-3}$ ) found by Dugdale *et al.* [1992] along a transect similar to ours across the equatorial Pacific region at  $150^\circ\text{W}$ ; the two values represent average concentrations outside and within the equatorial zone, respectively. Integrated daily nitrogen uptake rates were computed by multiplying hourly rates by 24 [Harrison *et al.*, 1992].

Primary productivity was determined in duplicate at four depths (between 0 and 120 m) by measuring the uptake of  $^{14}\text{C}$ -bicarbonate in samples incubated in 125 ml pyrex bottles. As with  $^{15}\text{N}$  uptake experiments, samples were incubated in simulated *in situ* incubators over 6 h. Incubations were ended by filtering the sample through a



Whatman GF/F filter and rinsing with 0.01N HCl. Correction for abiotic uptake was made with one 'time-zero' control bottle from each depth. Total added radioactivity in each sample was determined by adding 50 ml of water from the incubation bottle to a scintillation vial containing 10 ml of scintillation cocktail.  $^{14}\text{C}$  activity was determined by scintillation spectrometry and carbon uptake estimated by the method of *Steemann Nielsen* [1952]. To estimate daily primary production, integrated hourly primary production rates were multiplied by 12 to estimate photoperiod production and the values in turn were reduced by 15% to approximate dark respiration losses [*Steemann Nielsen and Hansen*, 1959].

Chl *a* concentrations, corrected for phaeopigment, were measured fluorometrically [*Holm-Hansen et al.*, 1965] at 6 depths. Duplicate water samples (100 ml) were filtered through Whatman GF/F filters and then extracted with 90% acetone in the dark at  $-20^{\circ}\text{C}$  for 24h. The fluorescence was measured with a Turner Design fluorometer previously calibrated against pure chl *a* (Sigma). For total PON, duplicate 1 liter samples were passed through combusted GF/F filters and stored at  $-20^{\circ}\text{C}$ ; they were later dried at  $60^{\circ}\text{C}$  and analyzed with a Perkin Elmer elemental analyzer (model 2400) calibrated with a cyclohexanone standard.

## 2.3 Results

Vertical sections of temperature, nitrate, chl *a*, PON and nitrate uptake rates are shown in Fig. 2.1. The latitudinal distribution of surface temperature and nitrate showed a marked horizontal gradient, with a decrease in temperatures and an increase in nitrate concentration around the equator, indicating upwelling at the equatorial divergence. Nitrate concentrations in the upper layer were  $>4 \text{ mmol m}^{-3}$  between  $6^{\circ}\text{S}$  and  $3^{\circ}\text{N}$  and decreased poleward; low temperature values ( $< 26^{\circ}\text{C}$ ) were in a narrower band ( $\sim 3^{\circ}\text{S}$  to  $3^{\circ}\text{N}$ ). Vertically, nitrate concentrations increased with depth north of  $6^{\circ}\text{S}$ , but to the south no vertical gradient in the upper 120 m (euphotic zone; see Table 2.1) was found. In contrast to the marked gradient of nitrate concentrations,

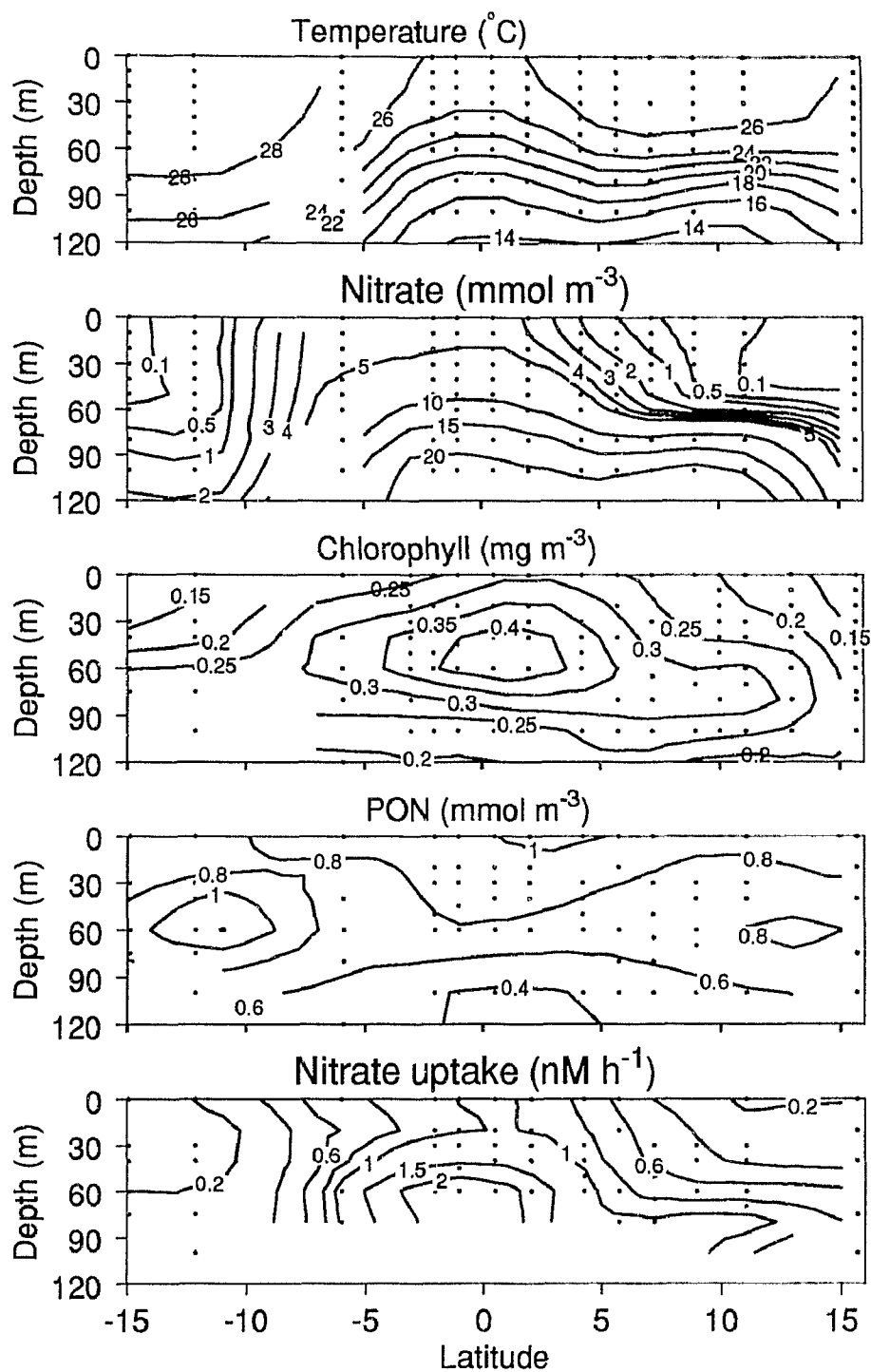


Figure 2.1: Vertical sections of temperature, nitrate, chl *a*, PON, and nitrate uptake along the cruise track. Longitudinal variations between stations were ignored. Negative latitudes are south.

chl *a* concentrations were low and relatively constant along the transect. Higher concentrations ( $0.5 \text{ mg m}^{-3}$ ) were found at subsurface depths near the equator and lower values ( $<0.2 \text{ mg m}^{-3}$ ) towards the south. Along the transect, PON concentrations showed a different pattern from that of chl *a*; its highest values ( $>1 \text{ mmol m}^{-3}$ ) were found in the surface layer near the equator and at subsurface depths around  $12^\circ\text{S}$ . These differing distributions of chl *a* and PON suggested, as previously reported [Peña *et al.*, 1991], that non-phytoplanktonic particles were abundant along this transect. In general, the uptake rates of  $\text{NO}_3^-$  showed a similar distribution to that of  $\text{NO}_3^-$  concentrations. Uptake rates in the upper layer were higher in the equatorial region (maximum  $1.6 \text{ mmol N m}^{-3} \text{ h}^{-1}$  at  $2^\circ\text{N}$ ) and tended to increase with depth where nitrate concentrations also increased. Whereas surface layer  $\text{NO}_3^-$  concentrations varied by greater than 50-fold along the transect, the uptake rates of nitrate were less variable ( $\sim 10$ -fold).

Along the transect, nitrate and silicate concentrations showed a different pattern (Table 2.1). Surface nitrate concentrations ranged from undetectable ( $<0.05 \text{ mmol m}^{-3}$ ) to  $5.3 \text{ mmol m}^{-3}$ , whereas surface silicate concentrations were always detectable and less variable (range  $0.6$  to  $2.6 \text{ mmol m}^{-3}$ ). Stations were subdivided into three groups according to nitrate concentration [Peña *et al.*, 1990]: (1) stations south of the equator where nitrate was low ( $<0.3 \text{ mmol m}^{-3}$ ) or undetectable throughout the euphotic zone (Stns 4 and 11), (2) stations in the equatorial region where nitrate was abundant ( $>4 \text{ mmol m}^{-3}$ ) in the euphotic zone (Stns 20 to 55) and, (3) stations north of the equator where nitrate concentrations were intermediate between the other groups (undetectable to  $<1 \text{ mmol m}^{-3}$ ) in the upper layer but where a strong nitracline existed near the bottom of the euphotic zone (Stns 60 to 96).

The integrated values of chl *a*, primary production and nitrogen uptake over the euphotic zone for each station and region are summarized in Table 2.2. The highest rate of  $\text{NO}_3^-$  uptake ( $3.48 \text{ mmol N m}^{-2} \text{ d}^{-1}$ ) was found at  $1^\circ\text{S}$ , coinciding with the highest chl *a* concentration ( $27.4 \text{ mg m}^{-2}$ ) and primary productivity ( $86.1 \text{ mmol C m}^{-2} \text{ d}^{-1}$ ). Despite the relatively constant concentrations of chl *a* along the transect

Table 2.2: Chl *a*, primary productivity ( $\text{mmol C m}^{-2} \text{d}^{-1}$ ), and nitrogen uptake ( $\text{mmol N m}^{-2} \text{d}^{-1}$ ) integrated over the euphotic zone. Ammonium uptake rates were calculated based on the expected range of substrate concentration ( $0.01$  to  $0.15 \text{ mmol m}^{-3}$  at the equatorial region and  $0.01$  to  $0.12 \text{ mmol m}^{-3}$  at the other regions). Means and coefficients of variation (CV=standard deviation divided by mean and expressed as percentage) computed for each region (see text for regional designation).

Station No	Chl <i>a</i> ( $\text{mg m}^{-2}$ )	Primary productivity	$\text{NO}_3^-$ uptake	$\text{NH}_4^+$ uptake	f-ratio <sup>a</sup>
<i>South of the equator</i>					
4	18.7	38.4	0.75	2.80-22.83	0.13
11	22.4	47.4	0.38	1.63-14.12	0.05
Mean	20.6	42.9	0.56	2.22-18.47	0.09
C.V.	9.0	10.5	32.5	26.5-23.6	44.4
<i>Equatorial region</i>					
20	22.1	32.2	1.15	1.22-12.99	0.24
34	24.3	20.8	2.64	0.53- 5.64	0.84
39	27.4	86.1	3.48	0.34- 3.63	0.27
50	27.9	83.8	2.64	1.95-20.83	0.21
55	24.5	47.8	2.64	1.41-14.93	0.37
Mean	25.2	54.2	2.51	1.09-11.60	0.39
C.V.	8.5	49.1	30.0	54.0-54.1	60.4
<i>North of the Equator</i>					
60	26.3	69.2	1.10	1.43-12.40	0.11
65	24.4	33.7	1.27	1.79-15.44	0.25
73	25.1	37.3	1.39	5.18-44.89	0.24
78	19.2	16.7	0.70	2.23-19.37	0.28
88	25.8	34.1	1.20	2.96-25.59	0.23
96	15.1	32.2	0.91	5.94-51.47	0.19
Mean	22.6	37.3	1.10	3.26-28.19	0.22
C.V.	18.3	42.3	21.1	52.5-52.6	25.2

$$^a\text{f-ratio} = (\text{NO}_3^- \text{ uptake} \times 6.6) / \text{primary productivity}$$

(range 15.1 to 27.9 mg m<sup>-2</sup>), however, integrated primary production and new production varied 5-fold (range 16.7 to 86.1 mmol C m<sup>-2</sup> d<sup>-1</sup>) and 9-fold (range 0.38 to 3.48 mmol N m<sup>-2</sup> d<sup>-1</sup>), respectively. Regionally, the highest mean integrated values of chl *a*, primary production, and NO<sub>3</sub><sup>-</sup> uptake were observed in the equatorial region. South of the equator, integrated chl *a* and primary production were similar to those north of the equator, but nitrate uptake rates were significantly lower. Estimates of ammonium uptake rates ranged from 0.34 to 51.47 mmol N m<sup>-2</sup> d<sup>-1</sup> and, except by the stations between 2°S and 2°N, exceeded nitrate uptake regardless of the assumed ambient NH<sub>4</sub><sup>+</sup> concentration (Table 2.2). If NH<sub>4</sub><sup>+</sup> levels observed during the 150°W study of *Dugdale et al.* [1992] were typical also for 135°W, then NH<sub>4</sub><sup>+</sup> uptake averaged from 82% to 96% of the total (NO<sub>3</sub><sup>-</sup> plus NH<sub>4</sub><sup>+</sup>) uptake, the lower value representing the equatorial region.

*F*-ratios (Table 2.2) were calculated as the ratio of integrated nitrate uptake (converted to C using a 6.6 C/N molar ratio) and integrated primary production measured as <sup>14</sup>C uptake and not by the conventional method of *Eppley and Peterson* [1979], i.e. nitrate uptake / Total-N uptake, since accurate estimates of NH<sub>4</sub><sup>+</sup> uptake could not be made. *F*-ratios calculated in this manner were lower than 0.4 along the transect. The only exception occurred at 2°S (stn 34) where a high *f*-ratio (0.85) was observed, resulting from low primary production rather than high new production. Among the three regions, the average *f*-ratio north of the equator (0.22) and south of the equator (0.09) were 2 to 4 times lower than that in the equatorial region (0.39).

The mean vertical profile of nitrate uptake and the rate normalized to chl *a* in the three regions is shown in Fig. 2.2. Absolute NO<sub>3</sub><sup>-</sup> uptake rates were higher in the equatorial region than the other regions at all depths sampled. In this region, higher uptake rates were found at subsurface depths (maximum 2.7 mmol N m<sup>-3</sup> h<sup>-1</sup> at 60 m) compared with the upper 40 m (avg. 1.1 mmol N m<sup>-3</sup> h<sup>-1</sup>). A subsurface increase in NO<sub>3</sub><sup>-</sup> uptake approximately 3 times the mean value of the upper 60 m (1.3 mmol N m<sup>-3</sup> h<sup>-1</sup> at 80 m compared with 0.43) was also observed north of the equator. South of the equator, where a nutricline was absent in the euphotic zone,

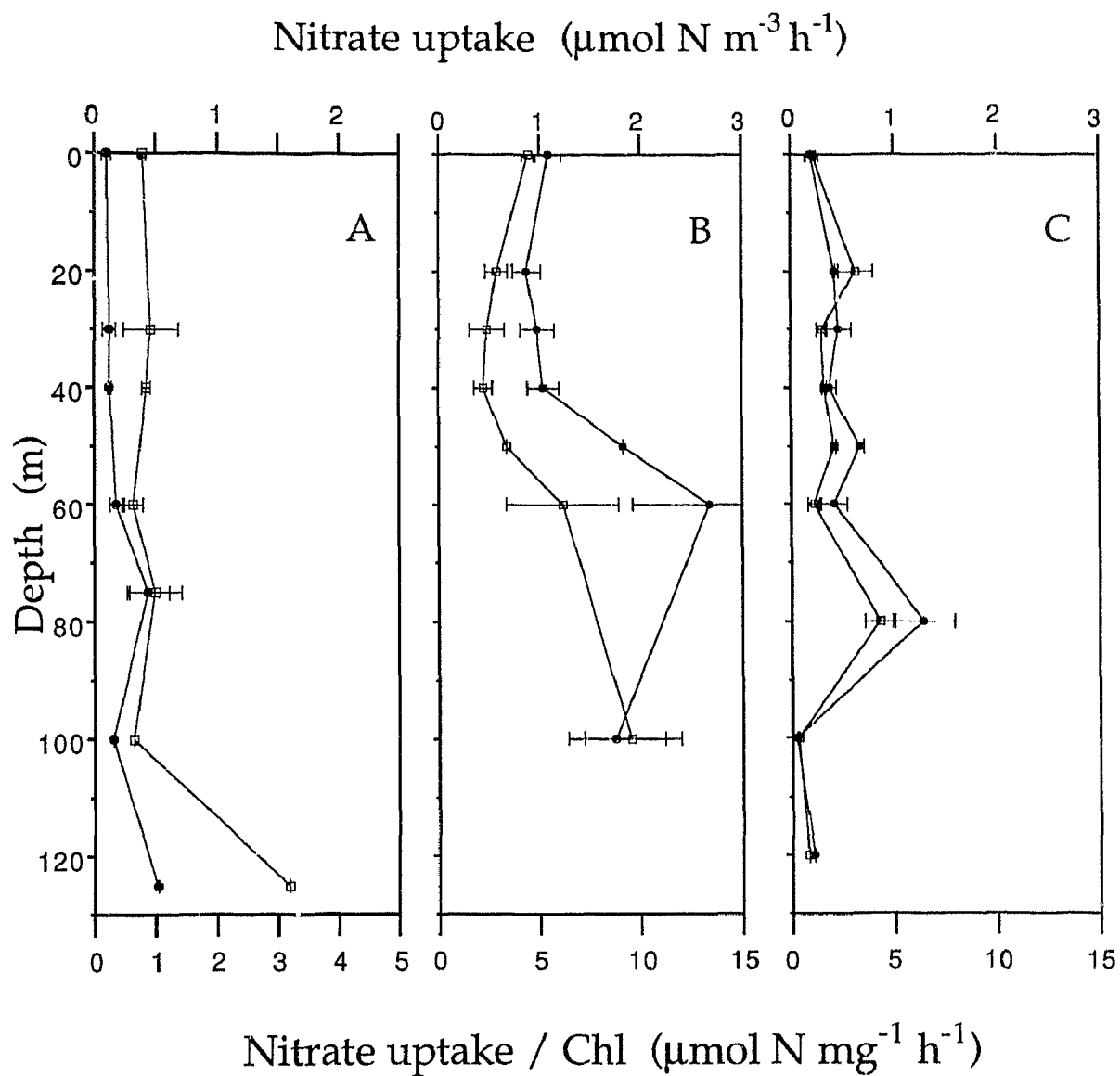


Figure 2.2: Vertical profiles of nitrate uptake and nitrate uptake normalized to chl *a* in A) southern, B) equatorial and C) northern regions. Values represent the mean rates and their standard errors.

the values were low (range 0.1 to 0.52 mmol N m<sup>-3</sup> h<sup>-1</sup>) and remained relatively constant with depth. Chl *a*-normalized uptake rates showed a similar vertical pattern in each region; highest values were observed at subsurface depths rather than in the upper layer. In the equatorial region, the highest normalized uptake rate was at 100 m.

Considering all data, a significant positive correlation ( $r^2=0.6$ ) was found between the chl *a*-normalized NO<sub>3</sub><sup>-</sup> uptake rates and the ambient nitrate concentration (Fig. 2.3). A similar relationship was found between absolute NO<sub>3</sub><sup>-</sup> uptake and chl *a* concentration (Fig. 2.4).

The influence of light intensity on normalized nitrate was examined by comparing the different light levels experiments (Fig. 2.5). Although a high variation in uptake rates was observed at all light levels, a systematic light-dependence of NO<sub>3</sub><sup>-</sup> uptake was not apparent. Nitrate was removed at significant rates even at the 1% level of surface light intensity.

## 2.4 Discussion

Latitudinal distribution along this transect showed the typical increase in nitrate concentration at the equator associated with upwelling at the equatorial divergence [Knauss, 1963; Wyrski, 1981]. Similarly, higher concentrations of chl *a*, primary production and new production rates were found near the equator ( $\sim 1^\circ\text{S}$ ). Despite the marked gradient in surface nitrate concentration among the regions, however, mean integrated new production rates were regionally similar. Only south of the equator were considerably lower values observed.

Since phytoplankton are minor contributors to PON in this region [Peña *et al.*, 1991; Eppley *et al.*, 1992], the rates of nitrate uptake were normalized to chl *a* rather than to PON to facilitate regional intercomparisons. In the equatorial region, the rates of nitrate uptake were similar to those previously found in this region [Dugdale *et al.*, 1992] and in the range of values reported in other high nutrient-low chlorophyll

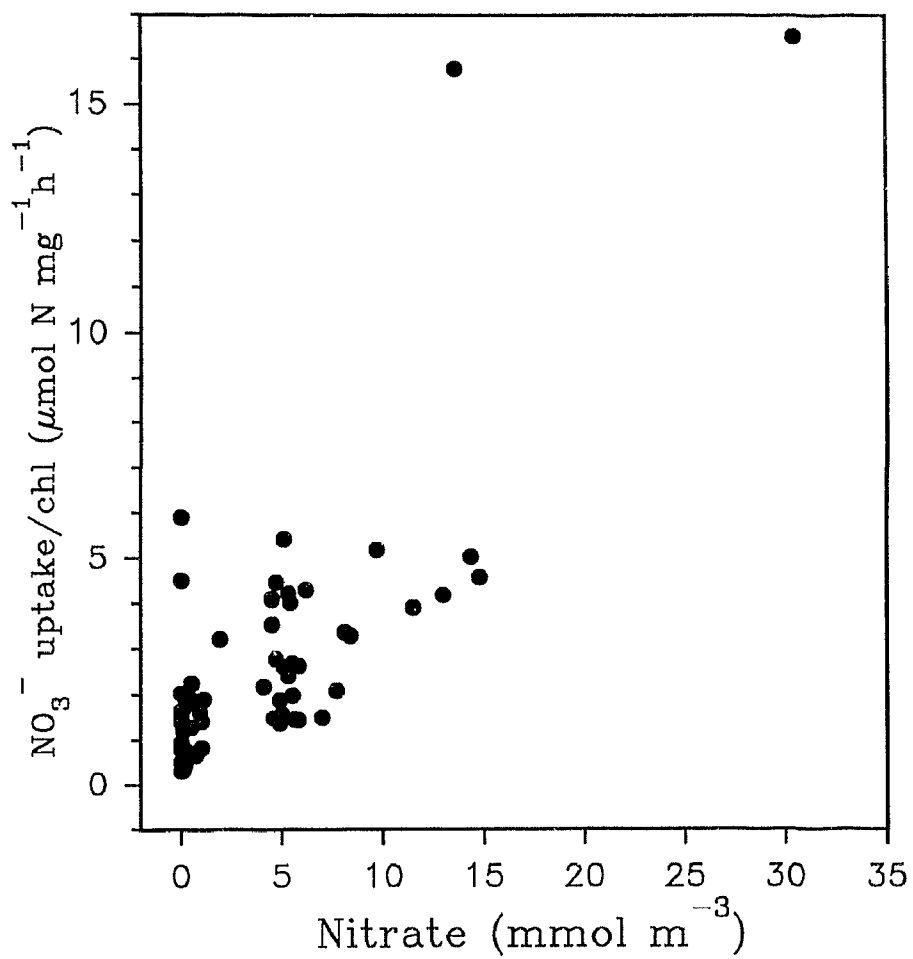


Figure 2.3: Relationship between nitrate concentration and the chl *a*-normalized uptake rate, all data combined ( $r^2 = 0.6$ ;  $n=64$ ).



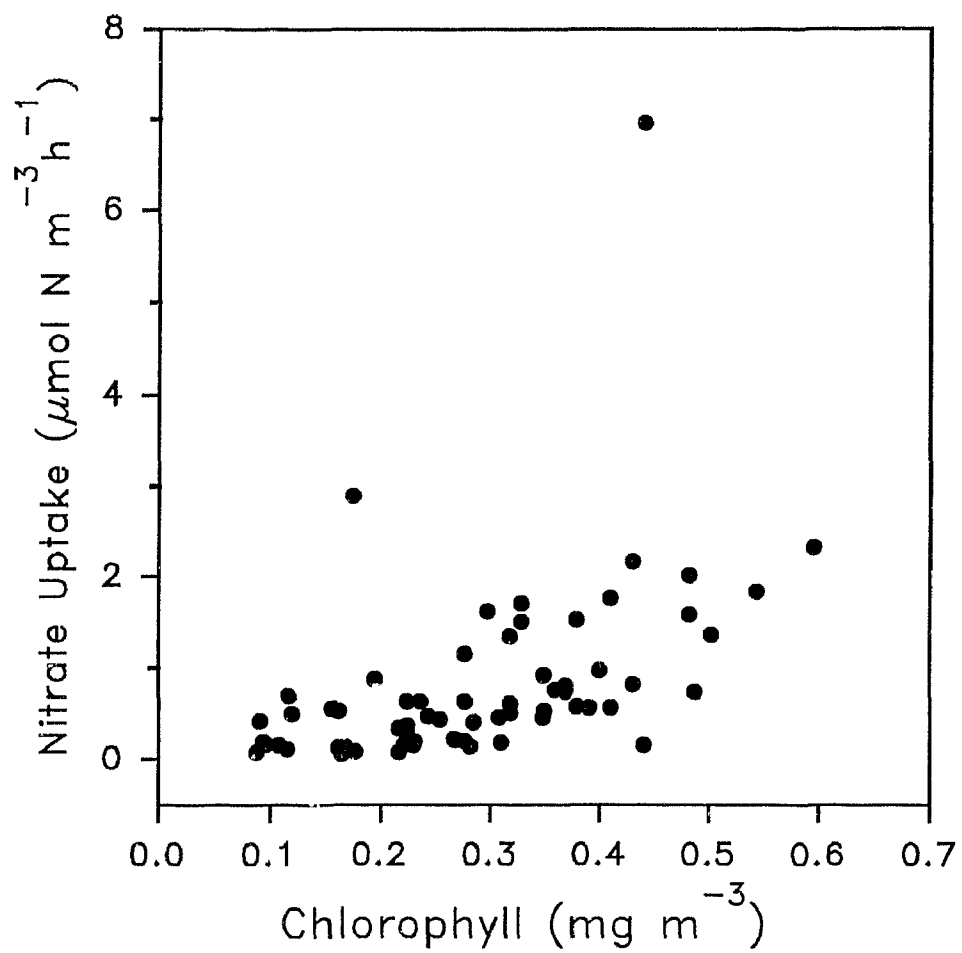


Figure 2.4: Relationship between chl *a* concentration and nitrate uptake, all data combined (n=64).

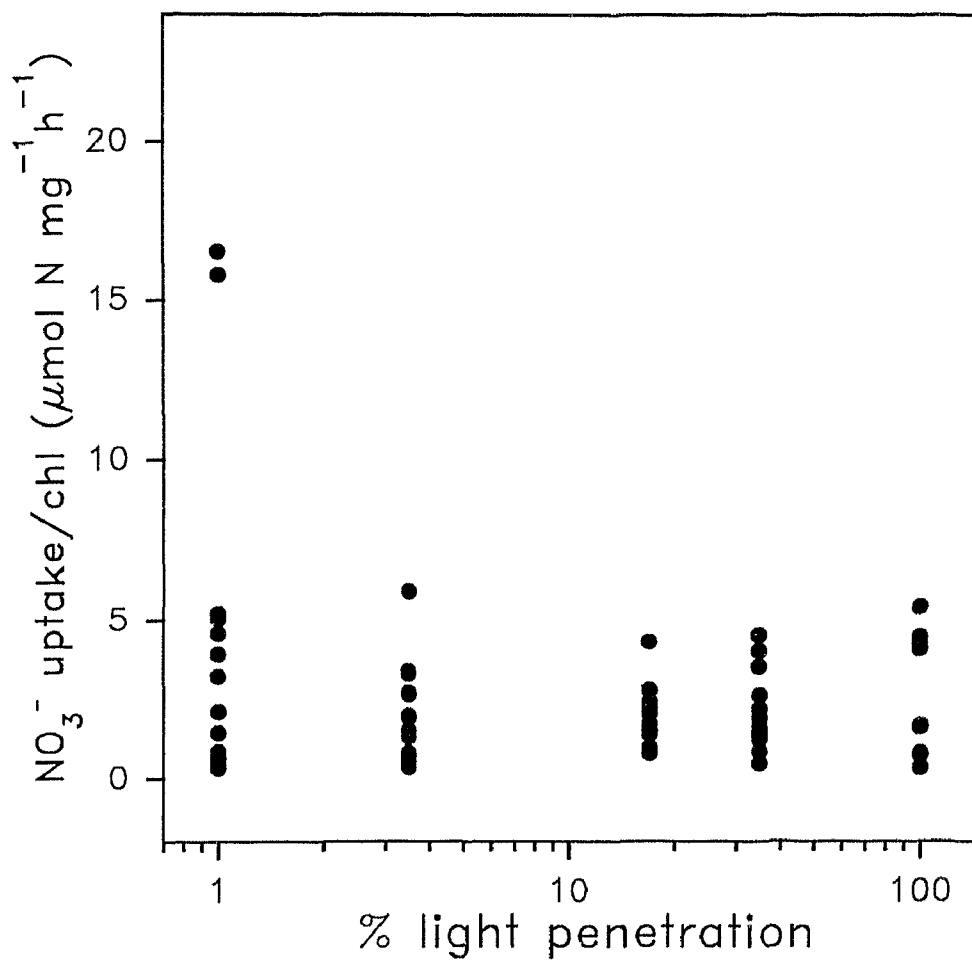


Figure 2.5: Chl *a*-normalized nitrate uptake plotted against light level at all stations along the transect.

environments such as the subarctic Pacific [*Wheeler and Kokkinakis*, 1990] and the Southern Ocean [*Glibert et al.*, 1982b]. The similarity in the nitrogen uptake rates suggests that phytoplankton cells in the equatorial Pacific region were performing in a manner similar to that of cells found in other oceanic environments where surface nitrate concentrations are comparably high.

Studies in coastal upwelling regions [*MacIsaac et al.*, 1985; *Wilkerson and Dugdale*, 1987] have shown that maximum rates of phytoplankton nitrate uptake develop over several generation times (shift-up) due to phytoplankton physiological adaptation. The rate of shift-up appears to be related to irradiance level and the ambient concentration of nitrate at the time of upwelling. In the equatorial Pacific region at 150°W, *Wilkerson and Dugdale* [1992] found little or no shift-up in nitrate uptake. This led them to hypothesize that phytoplankton cells in this region are not able to completely use the nitrate available because nitrate concentrations are lower than that necessary to induce shift-up. On the other hand, it has been shown [*Garside*, 1991] that shift-up may be an artifact of normalizing uptake rates to PON which has a time-dependent phytoplankton nitrogen component. In coastal upwelling systems, for example, the proportion of phytoplankton biomass in the PON increases with time, due in part to the exclusion of grazers during bottle incubations. In the equatorial Pacific region where much smaller phytoplankton cells dominate [*Chavez*, 1989; *Peña et al.*, 1990], the proportion of phytoplankton in the PON may change less since their (smaller) grazers are not as effectively removed from the incubation bottle.

Nitrogen uptake is generally thought to be light-dependent, with the uptake of nitrate being more light sensitive than that of ammonium [e.g. *MacIsaac and Dugdale*, 1972]. Therefore, to estimate daily nitrate uptake rates, hourly rates are often multiplied by 12. Recently, however, several studies have shown significant uptake of nitrate at night [*Glibert et al.*, 1982b; *Cochlan et al.*, 1991; *Harrison et al.*, 1992]. In the central equatorial Pacific, *Eppley and Renger* [1992] found disappearance of nitrate during night-time incubations that were unexpectedly high and equal to or

greater than daytime disappearance. In the present study, the light dependence of nitrate uptake was not investigated explicitly. However, since uptake rates of nitrate were not significantly diminished deep in the euphotic zone compared with the surface, our daily rates of nitrate uptake were obtained assuming constant uptake over 24 h. Daily uptake rates in the equatorial Pacific at 150°W, on the other hand, were estimated assuming a 12 h day for  $\text{NO}_3^-$  and a 18 h day for  $\text{NH}_4^+$  [Dugdale *et al.*, 1992] and in the eastern equatorial Pacific a 12 h and a 24 h day for  $\text{NO}_3^-$  and  $\text{NH}_4^+$ , respectively [Murray *et al.*, 1989]. These computational differences alone could explain the higher values of  $f$ -ratios found in this study compared to those previously reported (see Table 2.3) and point to the importance of diel studies in accurately establishing daily rates.

In this study,  $f$ -ratios were estimated based on nitrate uptake and total production as  $^{14}\text{C}$  uptake instead of the traditional approach based on total nitrogen uptake (usually  $\text{NO}_3^-$  and  $\text{NH}_4^+$ ). In the equatorial Pacific at 150°W, similar values of  $f$ -ratios have been estimated by both methods [Dugdale *et al.*, 1992]. Along our 135°W transect, the calculated  $f$ -ratios were low (Table 2.2) indicating that regenerated nitrogen was the major source of inorganic-N used by phytoplankton. Even in the equatorial region, where nitrate was abundant, the average new production represented less than 40% of the total production. Even though nitrate concentrations were similar within a region,  $f$ -ratios were variable, particularly at the equator (range 0.21 to 0.84). This implies that factors in addition to nitrate concentration are also influencing new production and the  $f$ -ratio. In order to compare our results with those of others working in this area, hourly rates of nitrogen uptake and  $f$ -ratio were computed (Table 2.3). Average nitrate uptake and  $f$ -ratio at the equator were similar to those found at 150°W, but lower than those reported in the eastern equatorial Pacific region (85°W). The opposite trend was observed for the primary production rates. Price *et al.* [1991] found somewhat higher  $f$ -ratios in a more recent study at 140°W.

Table 2.3: Comparison of nutrient concentration ( $\text{mmol m}^{-3}$ ), chl *a* ( $\text{mg m}^{-2}$ ) and hourly rates of primary productivity ( $\text{mg C m}^{-2} \text{h}^{-1}$ ) and nitrogen uptake ( $\text{mmol N m}^{-2} \text{h}^{-1}$ ) integrated over the euphotic zone in the equatorial Pacific region. Mean values (standard deviation).

	~85° W Murray et al. (1989)	135° W present study	150° W Dugdale et al. (1992)
Nitrate	9.4 (1.3)	4.8 (0.3)	5
Ammonium	0.7 (0.5)	n/a	0.2
Chl <i>a</i>	32.0 (2.4)	25.2 (2.1)	n/a
$\text{NO}_3^-$ uptake	0.184 (0.01)	0.105 (0.03)	0.102 (0.03)
$\text{NH}_4^+$ uptake	0.273 (0.04)	0.045-0.483 (0.03-0.29)	0.351 (0.10)
Primary productivity	32.2 (2.1)	54.2 (26.5)	55.7 (4.3)
f-ratio <sup>a</sup>	0.4	0.7-0.18	0.22
f-ratio <sup>b</sup>	0.44	0.15	0.14

<sup>a</sup>f-ratio= $\text{NO}_3^-$  uptake/ $(\text{NO}_3^- + \text{NH}_4^+)$  uptake

<sup>b</sup>f-ratio= $(\text{NO}_3^-$  uptake  $\times$  6.6)/primary productivity

n/a: no data available

Since the  $f$ -ratios were consistently low in the equatorial Pacific region, the implication is that the food web structure is more like that of oligotrophic subtropical regions than coastal upwelling areas [Murray *et al.*, 1989]. This is consistent with observations of phytoplankton standing stock, as measured by chl  $a$ , which remained low despite the production values [Walsh, 1976; Peña *et al.*, 1990; Cullen *et al.*, 1992]; thus, consideration of standing stock and rate of growth alone suggest a tight coupling between phytoplankton cells and grazers. The existence of a regeneration-based system implies a more complex microbial food web leading to macrozooplankton than one based on new nutrients. In the equatorial Pacific at 150°W, Eppley and Renger [1992] found rates of nitrate utilization that exceeded the rates of nitrate incorporation into particulate matter leading them to speculate that the production of dissolved organic matter is significant and that this could be an expression of an active microbial food web. The occurrence of high grazing pressure in the equatorial region will increase the availability of regenerated nitrogen and reduce the absolute consumption of nitrogen by reduction in the phytoplankton biomass.

Because ammonium concentrations were not measured in this study, accurate determination of the rates of regenerated production was not possible. However, there are some comments we can make based on the estimated range of  $\text{NH}_4^+$  uptake rates. First, the ammonium concentration in the equatorial region cannot be as low as that observed in the oligotrophic ocean (Sargasso Sea) if the  $f$ -ratio computed using total  $^{15}\text{N}$  is similar to that estimated using total production as  $^{14}\text{C}$  uptake [Dugdale *et al.*, 1992]. This is consistent with recent measurements of  $\text{NH}_4^+$  concentration in the central equatorial Pacific region where 0.1-0.3  $\text{mmol m}^{-3}$  of ammonium were found [Wilkerson and Dugdale, 1992]. Alternatively, the uptake of other regenerated nitrogen forms (i.e. urea) could be contributing considerably to total nitrogen uptake.

Several laboratory and field studies in marine systems have shown that phytoplankton prefer  $\text{NH}_4^+$  over other forms of nitrogen [Conway, 1977; McCarthy *et al.*, 1977; Syrett, 1981; Glibert *et al.*, 1982b]. The physiological basis for this preference seems to be the greater energetic costs associated with the transport, reduction, and

assimilation of  $\text{NO}_3^-$ . However, *Thompson et al.* [1989] found that any advantage that may be gained due to the lower energetic cost of growth on  $\text{NH}_4^+$  would be restricted to situations involving high photon flux density (and no other limiting substrate). At low photon flux density, there would be no clear advantage, in terms of growth rate, to the use of  $\text{NH}_4^+$  over  $\text{NO}_3^-$ . It has been suggested that the presence of  $\text{NH}_4^+$  may substantially inhibit the uptake of  $\text{NO}_3^-$  by phytoplankton [*McCarthy*, 1981; *Wheeler and Kokkinakis*, 1990]. Although the evidence for ammonium inhibition in the field has been lately questioned [*Dortch*, 1990; *Price et al.*, 1991], the preference for ammonium uptake over other nitrogen forms is still widely accepted.

Most of the research on nitrogen physiology of phytoplankton has focussed on diatoms. There is little information about the physiology of small phytoplankton cells that tend to dominate in open ocean systems, although some studies suggest that this physiology may differ considerably. For example, *Probyn et al.* [1990] found nanoplankton and picoplankton activity continued almost unchanged during the dark while net plankton activity declined markedly. Also, it has been suggested that large diatoms show a preference for growth on  $\text{NO}_3^-$  [*Mulone*, 1980], while  $\text{NH}_4^+$  is preferred by small phytoplankton [e.g. *Nalewajko and Garside*, 1983; *Probyn*, 1985; *Harrison and Wood*, 1988].

In several regions, it has been observed that nitrate uptake rates are higher near the base of the euphotic zone than in the surface layer [*Conway and Whittedge*, 1979; *Nelson and Conway*, 1979; *Priscu*, 1984; *Lewis et al.*, 1986]. This pattern is generally thought to reflect the increase in nitrate availability within the subsurface nutricline region. Nitrate uptake rates in the present study increased with depth at the stations where nitrate concentration increased. This was also evident in the equatorial Pacific region where nitrate was abundant throughout the euphotic zone. Since uptake rates of nitrate generally saturate at lower nitrate concentrations than those observed in the equatorial region [e.g. *MacIsaac and Dugdale*, 1969], the increase in  $\text{NO}_3^-$  uptake must have been influenced by factors other than changes in  $\text{NO}_3^-$  availability. For

example, changes in the interaction between nitrate and ammonium uptake responding to lowering irradiance as discussed previously. In the equatorial Pacific region at 150°W, the concentration of nitrate, as well as its uptake rates, remained uniform throughout the euphotic zone [Dugdale *et al.*, 1992]. Thus, along the equatorial Pacific region vertical variations in nitrate uptake rates appear to follow longitudinal variations in the depth of the nitracline [Barber and Chavez, 1991].

The increase in nitrate uptake with depth observed here was not paralleled by an increase in the carbon uptake. This uncoupling in the vertical has often been observed [e.g. McCarthy and Nevins, 1986] and values integrated over the euphotic zone rather than at particular depths are more relevant when considering biochemical ratios. In the regions investigated in this study where the mixed layer is much shallower than the euphotic zone, the balance between N and C uptake by phytoplankton cells was not evident. It could be argued that the uptake and assimilation of nitrogen is frequently uncoupled, and that a significant fraction of the nitrogen taken up by phytoplankton cells is released as dissolved organic or inorganic nitrogen. This may be particularly true when small cells that presumably have a low capacity to store nutrients are dominant, as in the equatorial region. The availability of DON could, in turn, stimulate ammonium regeneration by heterotrophic bacteria [Kirchman *et al.*, 1989], increasing its availability for phytoplankton utilization. Alternatively, the uptake of nitrate may be due in part to non-photosynthetic organisms as suggested by Eppley and Renger [1992]. In the present study, a clear relationship between chl *a* and  $\text{NO}_3^-$  uptake was not observed, therefore we can not exclude the possibility that heterotrophic  $\text{NO}_3^-$  uptake may have been important.

In most oceanic regions, the availability of nitrogen is thought to limit phytoplankton production [e.g. Dugdale, 1967]. In these nutrient limited systems, nitrate flux to the euphotic zone sets the upper limit on new production such that new production and the *f*-ratio may be derived of ambient  $\text{NO}_3^-$  concentration or primary productivity level [Eppley and Peterson, 1979; Platt and Harrison, 1985; Harrison *et al.*, 1987]. In contrast, in the equatorial Pacific region where nitrate is abundant,



estimates of new production rates based on these relationships significantly overestimate the measured values [Dugdale *et al.*, 1992]. In this region, as in other oceanic regions where nitrate is abundant, the availability of regenerated nitrogen [Glibert *et al.*, 1982b; Wheeler and Kokkinakis, 1990] or the absence of trace metals [Price *et al.*, 1991] ultimately may set the limit on the uptake of nitrate.

Results from this study indicate, as others have, that the most abundant nitrogen form is not necessarily the most important in the nutrition of the phytoplankton. In the equatorial Pacific region, since phytoplankton meet most of their growth requirement for nitrogen from regenerated sources (i.e.  $\text{NH}_4^+$ ), it is not surprising that nitrate concentrations remain high. It is unclear, however, how spatial and temporal variations in  $\text{NO}_3^-$  and  $\text{NH}_4^+$  concentration may affect the rate of new production. Although few studies of nitrogen uptake have been done in the equatorial Pacific region to date, it is clear that more information will be needed on the interactions between the different nitrogen forms and on the importance of other growth substances (e.g. Fe) to phytoplankton nitrogen nutrition before efforts to model new production will progress further.

# Chapter 3

## New production in the warm waters of the tropical Pacific Ocean

### 3.1 Introduction

The equatorial Pacific region is among the most productive oceanic regimes [Betzer *et al.*, 1984; Chavez and Barber, 1987]; and, because of the upwelling of deep nutrient rich water to the euphotic zone throughout the year, may contribute to a significant fraction of the global new production. In the eastern and central equatorial Pacific, the effect of upwelling is evident as a tongue of cold nutrient-rich surface water [Wyrtki, 1981]. In contrast, the thermocline and nutricline are deeper in the western equatorial Pacific than in the eastern and central regions [Craig *et al.*, 1982] so upwelling brings mostly warm, nutrient-poor water from above the thermocline (nutricline) into the upper surface layer. It has been estimated [Chavez and Barber, 1987] that the nitrate upwelled eastward of the dateline in the equatorial Pacific could support a high proportion (18-56%) of the global new production. However, this represents an upper bound estimate for that region since only a fraction of the nitrate upwelled is used by phytoplankton locally. In fact, a significant amount of the nitrate

is transported away from the region [Carr, 1991; Fiedler *et al.*, 1991]. In contrast to the eastern equatorial Pacific, little is known about the contribution to global new production by the warm pools of the western equatorial Pacific. Since in this region nitrate upwelling is less intense, turbulent vertical transport of nitrate should be a relatively more important physical input.

New production is defined as the production of phytoplankton resulting from nitrogen supplied from outside the euphotic zone [Dugdale and Goering, 1967] whereas regenerated production is that production associated with nitrogen regenerated within the euphotic zone. In the open ocean, the main external source of nutrients to the euphotic zone is the upwelling and turbulent transport of nutrients from deep water. New production can be measured by a number of methods such as sediment traps at the bottom of the euphotic zone, the uptake of  $^{15}\text{N}$ -labelled nitrate, or the net flux of nitrate into the euphotic zone. New production also gives a measure of the primary production which can be removed from the surface layer of the ocean without destroying the long term integrity of the pelagic ecosystem [Eppley and Peterson, 1979; Platt *et al.*, 1989]. As such, rates of new production, when averaged over time scales longer than a year, represent the biologically-mediated transport of carbon from the ocean surface layer to the ocean interior. This is not net transport, however. Several studies have shown considerably spatial and temporal variability in the rates of new production even in open ocean regions. Therefore, the way measurements are averaged has a profound effect on the results [Platt and Harrison, 1985].

The ability to evaluate the importance of the tropical Pacific region to global new production and to predict anomalous conditions has been constrained by a lack of synoptic observations in this large and remote area of the ocean. Attempts have been made to estimate new production in coastal upwelling [Dugdale *et al.*, 1989] and frontal regions [Sathyendranath *et al.*, 1991] from satellite observations of sea surface temperature, the observed correlation between nitrate concentration and temperature, and empirical relationships between nitrate concentration and new production. In the North Atlantic, a lower limit to new production has been estimated from

changes in phytoplankton biomass determined from the coastal zone color scanner (CZCS) data and variations in the depth of the nutricline [*Campbell and Aarup, 1992*]. In oceanic regions, as in the western tropical Pacific, where surface nitrate concentrations are generally undetectable by conventional techniques and, where seasonal variations in phytoplankton biomass are small [*Dandonneau, 1992*], the above methods for estimating new production are not applicable.

Here, we combine the new production model presented by *Lewis [1992]* together with results from a general circulation model of the tropical Pacific [*Philander et al., 1987*] and historical temperature and nitrate data to estimate the annual mean rate of new production in the warm waters of the tropical Pacific region. The analysis is constrained by the horizontal and vertical nitrate balance and employs the surface heat flux, a quantity amenable to remote sensing [*Liu, 1988; Liu and Gautier, 1990*], to estimate nitrate fluxes. While other estimations of new production based on nitrate balance [*Chavez and Barber, 1987; Fiedler et al., 1991*] in this region consider only the input of nitrate due to upwelling, the transport of nitrate due to turbulent fluxes, which are difficult to estimate at large scales, are also evaluated.

## 3.2 Approach

In the tropics, large warm pools of near-surface water are enclosed at the margins by continental land masses and at the surface and depth by constant annual mean temperature isopleths [*Niiler and Stevenson, 1982*]. In a steady-state ocean, heat is conserved and new production is balanced by the net input of essential nutrients into the euphotic zone. To estimate the annual mean new production over the warm waters (temperature  $>26^{\circ}\text{C}$ ) of the tropical Pacific Ocean, we base our arguments on the close relationship between the fluxes of heat and nutrients in this region.

### 3.2.1 Fluxes of heat

In the upper layer of the ocean the heat and mass conservation equation may be written as,

$$c_p \rho (\nabla \cdot \overline{UT} + \nabla \cdot \overline{U'T'}) = \nabla \cdot E \quad (3.1)$$

$$\nabla \cdot \overline{U} = 0 \quad (3.2)$$

where  $T$  is temperature ( $^{\circ}\text{C}$ ),  $U$  is the velocity ( $\text{m s}^{-1}$ ),  $c_p$  is the specific heat of seawater ( $\text{J kg}^{-1} \text{ }^{\circ}\text{C}^{-1}$ ),  $\rho$  is the water density ( $\text{kg m}^{-3}$ ) and  $E$  is the irradiance vector ( $\text{J m}^{-2} \text{ s}^{-1}$ ). Overbars indicate mean values and the primed quantities represent departures from the mean conditions.

A simple model of the heat flux in the warm-water pool of tropical regions has been obtained by *Niiler and Stevenson* [1982] by integrating equations (3.1) and (3.2) over a fixed volume of water which is bounded at depth by a 3-dimensional surface of a constant annual mean temperature ( $A_T$ ), the ocean sea surface ( $A_S$ ) and the insulating continental land masses. By virtue of the constant-temperature boundary condition, the advective term vanishes since water which enters the volume is on average of the same temperature as the water which leaves it and hence there is no net flux of heat by mean advection. Therefore, the steady-state solution is a balance between the net surface heat flux into the volume and the turbulent heat transport out of the volume. The turbulent transport that removes heat from the pool can be caused by a variety of processes operating at different time and space scales from seasonal to microstructure. For instance, this includes eddy heat flux due to time-dependent ocean motions on scales of tens to hundreds of kilometers and turbulent diffusion which operates on scales of a few meters to a few millimeters. In the tropical Pacific warm-water pool, *Niiler and Stevenson* [1982] found that most of the heat transport is due to vertical turbulent transport since horizontal turbulent fluxes are relatively very small. Therefore,

$$\int \int_{A_S} Q_o dA = c_p \rho \int \int_{A_T} \overline{W'T'} ds \quad (3.3)$$

where  $Q_o$  is the net surface heat flux ( $\text{W m}^{-2}$ ) which is integrated over the surface area,  $A_S$ ,  $\overline{W'T'}$  is the mean annual vertical turbulent flux of heat which is integrated over the subsurface isotherm of area  $A_T$ , and  $dA$  and  $ds$  refer to the surface and subsurface elements respectively. Equation (3.3) states that the net surface heat flux into a volume of ocean which is bounded by coast and at depth by a constant mean annual temperature surface is transported out of the volume by turbulent vertical mixing only. A term to account for the penetrating irradiance through the subsurface [Lewis *et al.*, 1990] is small given the depth of the chosen isotherm ( $26^\circ\text{C}$ ).

### 3.2.2 Fluxes of nitrate

Similarly, if the mean concentration of nitrate in the upper layer of the ocean is constant, the net physical input of nitrate into this layer must be equivalent to the nitrate consumption which basically represents new production. Then, the nitrate conservation equation in the upper layer of the ocean is,

$$\nabla \cdot \overline{UN} + \nabla \cdot \overline{U'N'} = P_n \quad (3.4)$$

where  $N$  is the nitrate concentration ( $\text{mmol N m}^{-3}$ ) and  $P_n$  is the local new production rate ( $\text{mmol N m}^{-3} \text{ s}^{-1}$ ). We can proceed by integrating equations (3.4) and (3.2) over the same surface ( $A_S$ ) and subsurface boundaries ( $A_T$ ) as above. In this case, since the nitrate concentration is not constant along the isothermal subsurface boundary ( $A_T$ ), a net advective input of nitrate can occur if water which enters the volume has on average a higher concentration of nitrate than that of the water which leaves the volume. Therefore, new production over the whole volume enclosed by the surface ( $A_S$ ) and subsurface ( $A_T$ ) boundaries and the continental land masses is equivalent to the net advective and turbulent input of nitrate,

$$\int \int_{A_S} P_N dA = \int \int_{A_T} \overline{UN} ds + \int \int_{A_T} \overline{U'N'} ds \quad (3.5)$$

where  $P_N (= \int_0^{z_T} P_n dz)$ , where  $z_T$  is the depth of the subsurface isothermal boundary) represents the depth integrated new production ( $\text{mmol N m}^{-2} \text{ s}^{-1}$ ), and  $\overline{UN}$  and  $\overline{U'N'}$  are the annual mean net flux of nitrate due to advective and turbulent transports respectively.

### 3.2.3 Nitrate-Temperature relationship

In the ocean, temperature and nitrate are well correlated [e.g. *Kamykowski and Zentara, 1986*]. We can exploit this empirical observation to combine equations (3.3) and (3.5), neglecting for now horizontal turbulent fluxes of nitrate, and the spatial covariance between heat flux across the isothermal boundary and the slope of the nitrate-temperature relationship in the region, to yield,

$$\int \int_{A_S} P_N dA = \int \int_{A_T} \overline{UN} ds + \frac{d\overline{N}}{dT} \frac{1}{c_p \rho} \int \int_{A_S} Q_o dA \quad (3.6)$$

Here, the annual mean rate of new production is due to advection plus the turbulent input of nitrate expressed as the product of the net surface heat flux and the average slope of the nitrate-temperature relationship at the base of the subsurface boundary ( $A_T$ ). Note that as before, the turbulent transport refers to a variety of space and time scales of motions (seasonal to microstructure) and, thus, is not equivalent to the vertical turbulent diffusion of nitrate alone. The net surface heat flux can be evaluated from climatology or from satellite observations; the nitrate-temperature relationship can be taken from historical data. Similarly, the advective transport of nitrate can be obtained from the mean water transport normal to the subsurface boundary ( $A_T$ ) and the annual mean nitrate concentration along this boundary.

### 3.3 Data

Approximately 4,870 vertical profiles with simultaneous observations of nitrate concentration and temperature from the tropical Pacific between 20°N and 20°S of latitude and 120°E to 80°W of longitude have been used in this analysis (Fig. 3.1). This data set was obtained from three sources: 1) the National Oceanographic Data Center (NODC), 2) the Ocean Atlas [Osborne *et al.*, 1992] and 3) those obtained by Fiedler and colleagues in the eastern equatorial Pacific between August to December of 1986 to 1988 [P.C. Fiedler, pers. comm.; Fiedler *et al.*, 1991]. These data were reformatted, checked for gross errors and merged. Duplicate data, detected by having identical date, location, depth, temperature and nitrate concentration, were eliminated. Most of the stations (about 80%) were obtained from the NODC data set. The NODC data used here were collected mainly between 1967 and 1972 (Fig. 3.2). We have excluded data collected before 1952 to increase the probability that similar analytical methods have been used in the determination of nitrate concentration. Data were available for all months of the year.

Based on the distribution of temperature and nitrate concentration, the 26°C isotherm was chosen as the subsurface boundary ( $A_T$ ) because it encloses most of the tropical Pacific region and nitrate is generally detectable along the bottom of this isothermal boundary. About 3,300 stations were located inside the region enclosed at the surface by the climatological 26°C isotherm. At each of these stations the depth of the 26°C isotherm and the nitrate concentration at that depth were determined. In the region between 5° to 12°S latitude and 125° to 140°E longitude, a few stations had surface temperatures cooler than 26°C and they were excluded from the analysis. Standard deviation statistics for the observed temperature, isotherm depth and nitrate data were calculated for five-degree squares of latitude and longitude. Since discrete vertical profiles were used in this analysis, the slope of the nitrate-temperature relationship at the base of the 26°C isotherm was operationally defined as that obtained using temperatures between 20-27°C. Given the vertical resolution of the data set, it was not possible to use a narrower range of temperature. To estimate



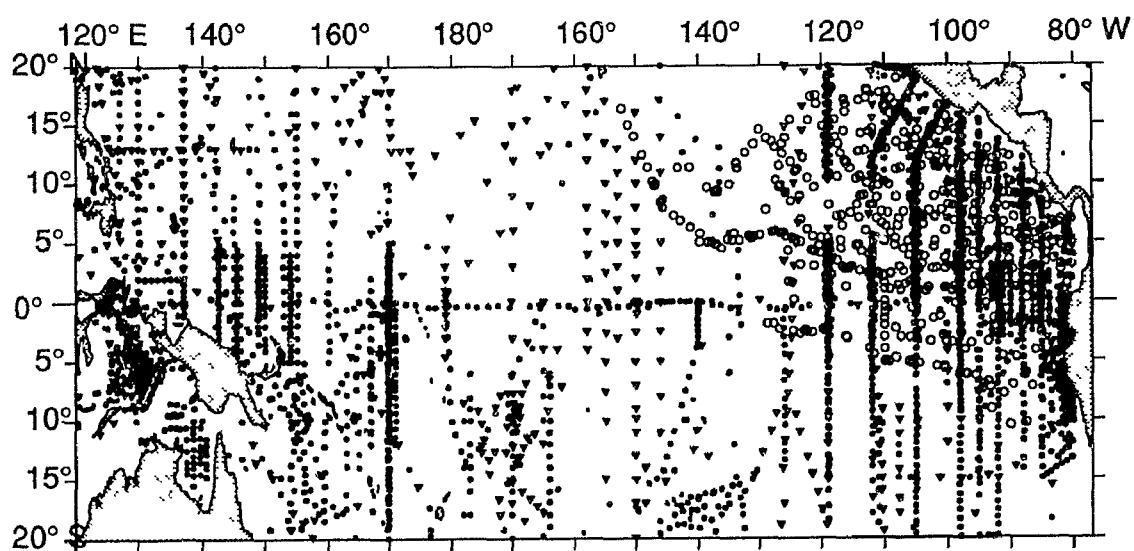


Figure 3.1: Location of the stations used in this analysis. Filled circles = NODC (3,845 stns.); triangles = Ocean Atlas (454 stns.); and open circles = Fiedler and colleagues (574 stns.).

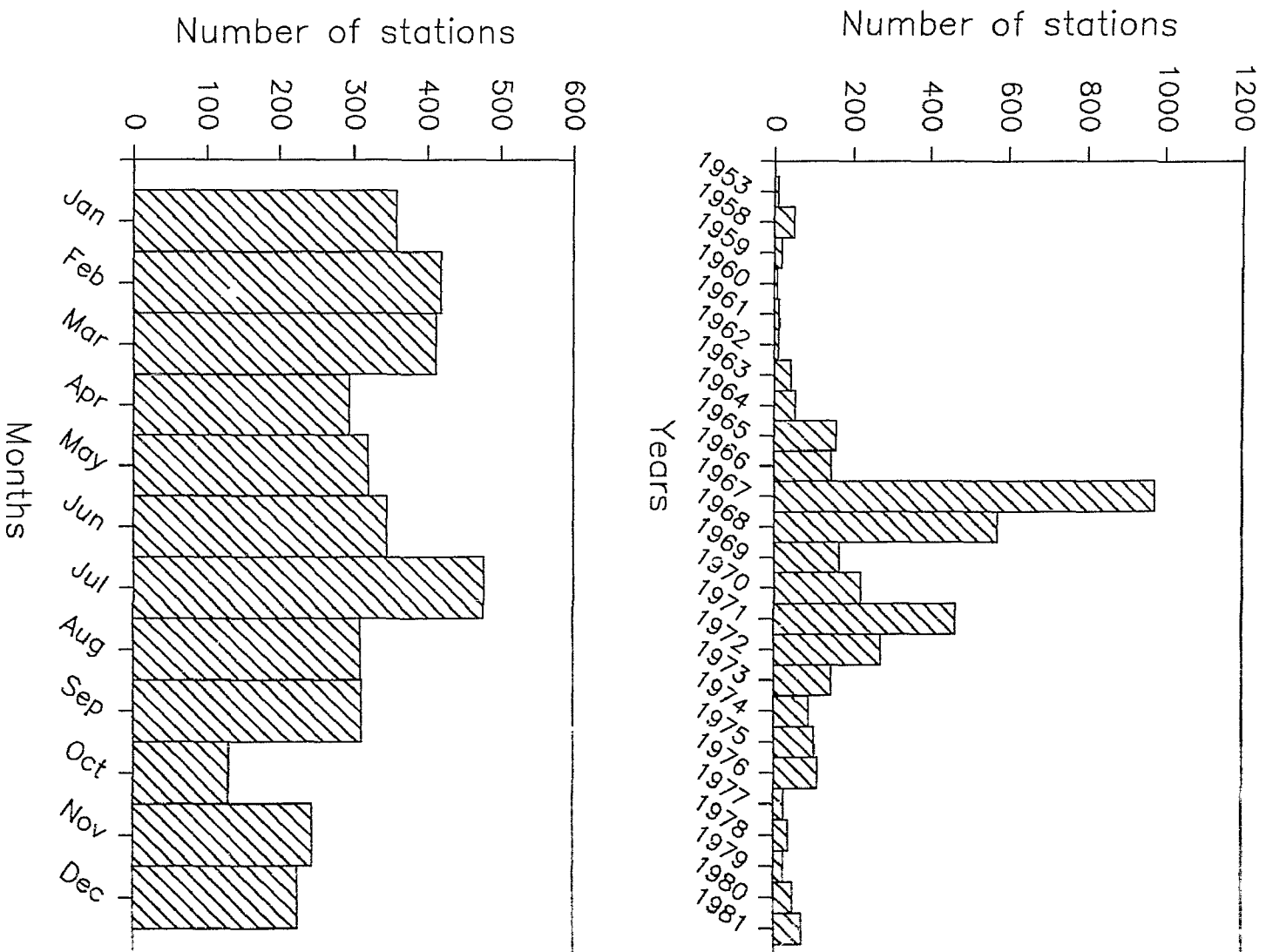


Figure 3.2: Yearly and monthly distribution of the National Oceanographic Data Center (NODC) data.

the mean slope of the region, the surface area enclosed by the 26°C isotherm was divided into 178 boxes of 5 degrees of latitude and longitude. In each of them, the slope was obtained from a linear regression of temperature (independent variable) versus nitrate concentration of the pooled data. Only those five-degree squares containing three or more observations were used in the analysis. The average slope for the entire region, and its 95% confidence intervals, were calculated from the slope values of all the boxes where data was available (164 boxes). Second and third order polynomial regressions between nitrate and temperature were tested and rejected based on a small increment in the correlation coefficient over the linear model.

The advective transport of nitrate into and out of the volume of water which is warmer than 26°C was calculated as the product of the mean nitrate concentration at the subsurface boundary and the mean water transport normal to the boundary. To estimate horizontal nitrate transport at the lateral boundaries, we consider that the warm-water region was bounded on the side by a isothermal well mixed layer of 50 m depth. The concentration of nitrate at the 26°C boundary was obtained from the contoured map of nitrate which was based on the pooled data. The mean water transport across the part of the boundary where nitrate was detectable was calculated by spatial integration of the mean circulation values reported by *Philander et al.* [1987] using the trapezoidal rule. They obtained these values from the third year of simulation of a general circulation model of the tropical Pacific which was forced with monthly averaged climatological winds. The surface area enclosed by the 26°C isotherm and the mean annual net surface heat flux integrated over this area was calculated using three different climatological data sets: *Weare* climatology, which has a 5° by 5° latitude-longitude grid [*Weare et al.*, 1981], *Esbensen and Kushnir* climatology on a 4° latitude by 5° longitude grid [*Esbensen and Kushnir*, 1981], and *Oberhuber* climatology on a 2° by 2° latitude-longitude grid [*Oberhuber*, 1988].

## 3.4 Results

### 3.4.1 Temperature and nitrate distribution

A contour plot of all the sea surface temperature data in the tropical Pacific (Fig. 3.3a) reproduces the main features present in the annual mean climatologies. In the eastern equatorial Pacific, surface temperatures were relatively cool and the gradients were large, indicating upwelling at the equatorial divergence as well as advection from the Peru upwelling region. Farther west, a large pool of water of more than  $28^{\circ}\text{C}$  was found between  $10^{\circ}\text{N}$  and  $15^{\circ}\text{S}$ . The standard deviations of surface temperature (Fig. 3.3b) showed higher values near the coast. A distribution similar to that of temperature was found for the surface nitrate concentrations (Fig. 3.4a), where the highest nitrate concentrations were associated with the coldest surface waters. However, the nitrate-enriched zone was almost symmetrical about the equator, whereas the cold water tongue was less sharply defined to the south. Along the equator, surface nitrate concentrations were  $>4\ \mu\text{M}$  eastward of  $160^{\circ}\text{W}$ . Waters with  $>1\ \mu\text{M}$  extended to about  $170^{\circ}\text{E}$  longitudinally and beyond  $5^{\circ}\text{N}$  and  $\text{S}$  latitudinally. Outside this region, nitrate concentration was generally low ( $<0.5\ \mu\text{M}$ ) or undetectable. The standard deviations of nitrate concentration (Fig. 3.4b) were higher in the eastern side between the equator and  $10^{\circ}\text{S}$  than elsewhere.

In the tropical Pacific, water warmer than  $26^{\circ}\text{C}$  was found beyond  $20^{\circ}\text{N}$  and  $20^{\circ}\text{S}$  westward of  $150^{\circ}\text{W}$  and between  $3^{\circ}$  and  $15^{\circ}\text{N}$  towards the east, coinciding with the North Equatorial Countercurrent. In this region, nitrate was detectable only in the southeastern boundary. Vertically, the  $26^{\circ}\text{C}$  isotherm subsurface boundary was located mainly at depths of 80 to 120 m (Fig. 3.5a) in the western tropical Pacific. Towards the east and away from the equator, the depth of the  $26^{\circ}\text{C}$  isotherm shoaled. The concentration of nitrate at the  $26^{\circ}\text{C}$  isotherm (Fig. 3.6a) was not constant but followed a pattern similar to the isotherm depth. Higher nitrate concentrations ( $>5\ \mu\text{M}$ ) were found near the equator where the isotherm was deeper. Beyond  $15^{\circ}\text{N}$  and  $\text{S}$ , nitrate concentrations were usually undetectable in waters of  $26^{\circ}\text{C}$ . This distribution

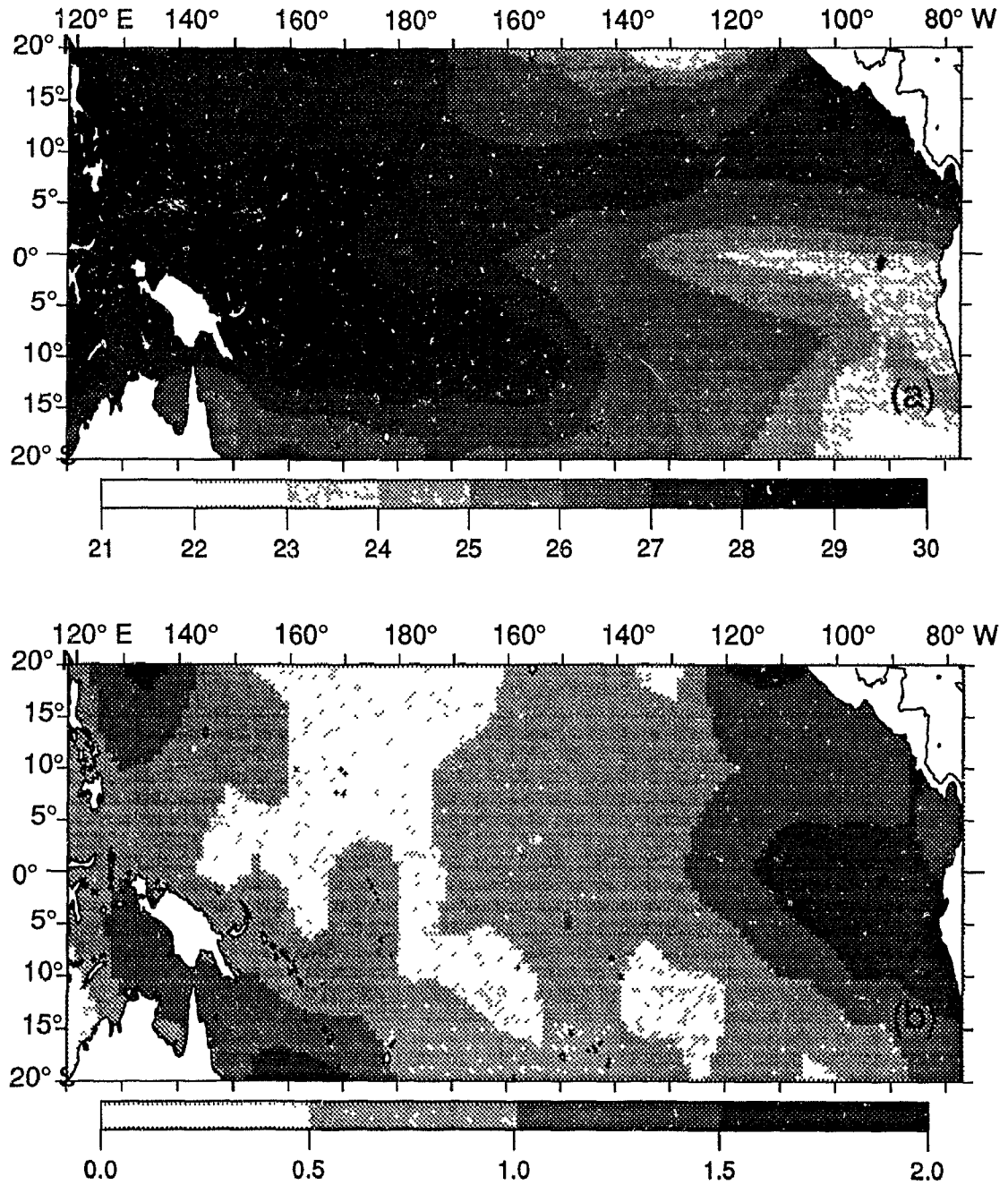


Figure 3.3: (a) Surface distribution of temperature ( $^{\circ}\text{C}$ ) in the tropical Pacific region and (b) its five degree squares standard deviation.

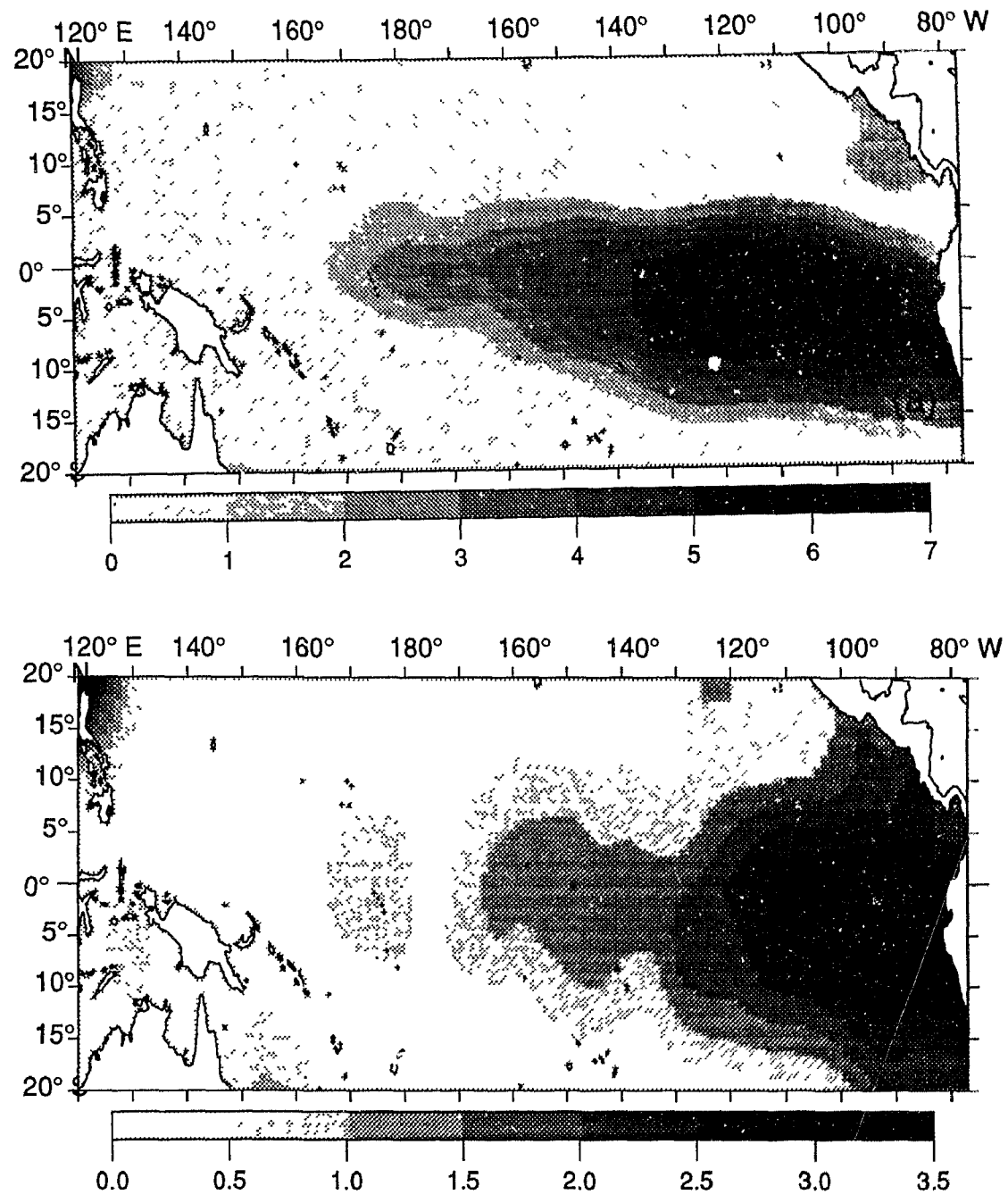


Figure 3.4: (a) Surface distribution of nitrate concentration ( $\mu\text{M}$ ) in the tropical Pacific region and (b) its five degree squares standard deviation.

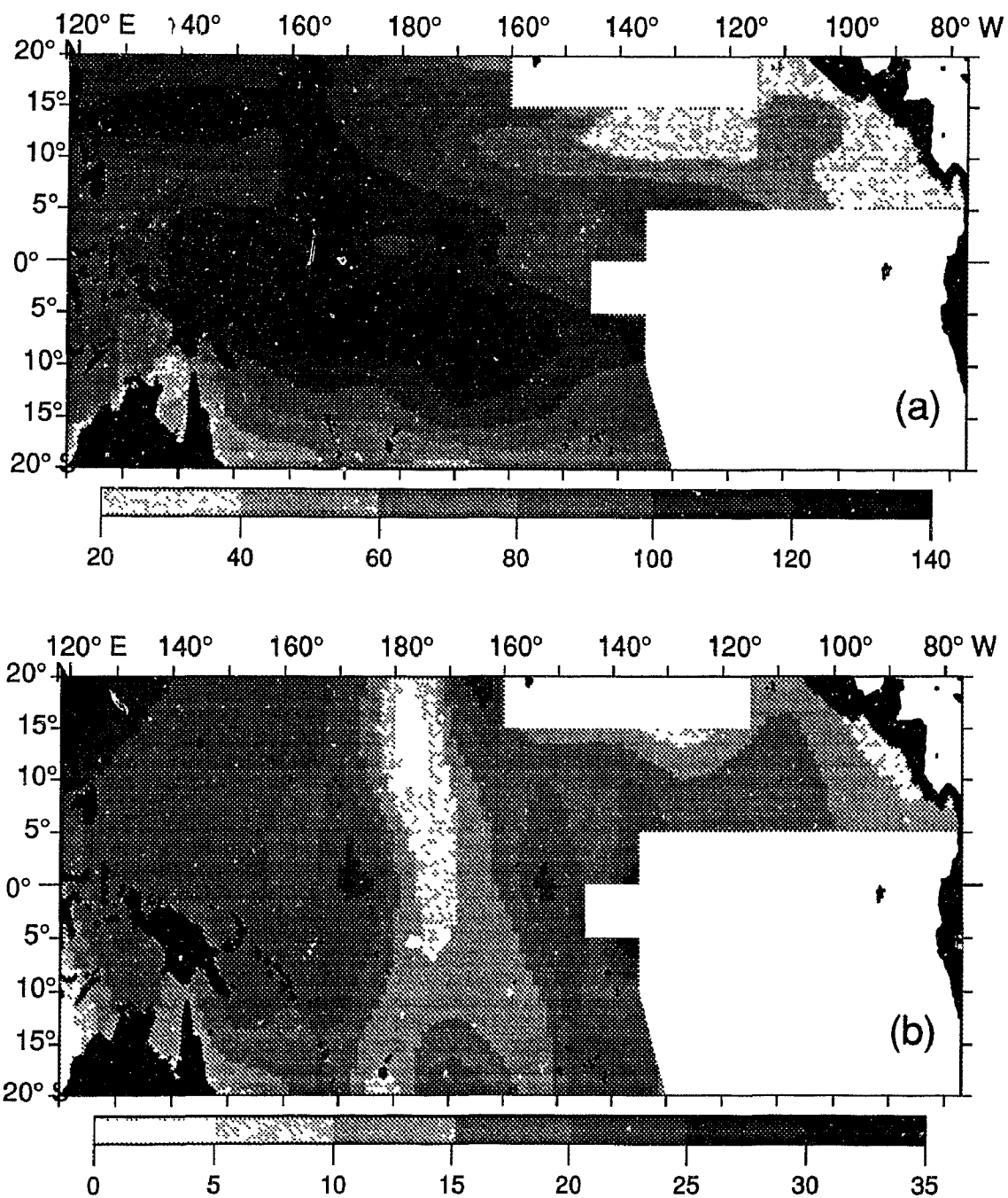


Figure 3.5: (a) The depth of the 26 °C isotherm subsurface boundary (m) and (b) its five degree squares standard deviation.

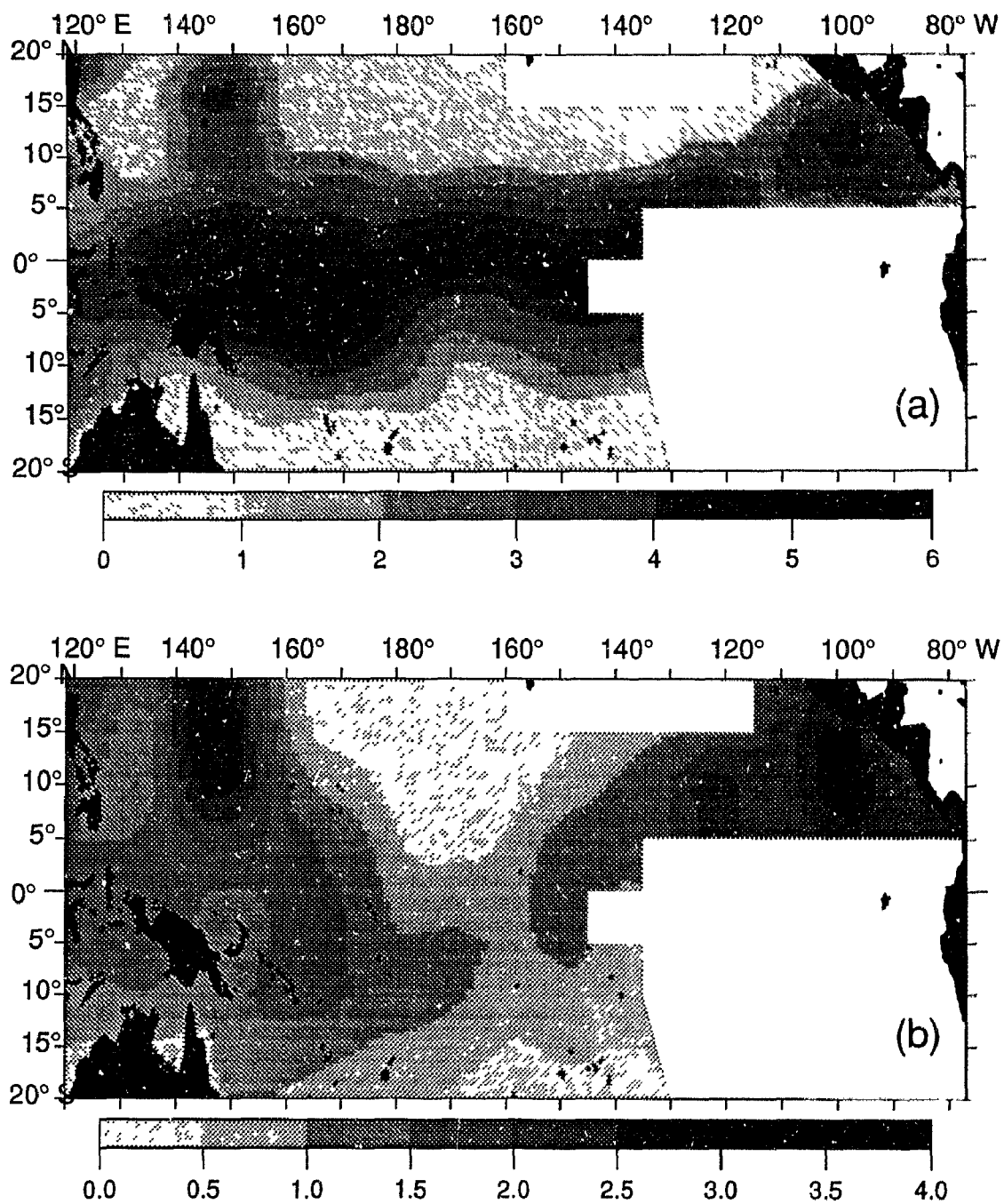


Figure 3.6: (a) Nitrate concentration ( $\mu\text{M}$ ) at the depth of the 26 °C isotherm and (b) its five degree squares standard deviation.



agrees with previous observations along the west coast of North and South America [Zentara and Kamykowski, 1977] where it has been found that a given nutrient concentration occurs at colder temperatures as latitude increases. North of the equator, between 145° and 150°E, a marked gradient of nitrate concentrations was found that was not reflected in the depth of the isotherm. An examination of the data available for this region showed that the depth of the nutricline was sometimes shallower than that of the 26°C isotherm. The variability in the depth (Fig. 3.5b) and in the nitrate concentration (Fig. 3.6b) at the 26°C isotherm was higher on the eastern and western sides than centrally.

### 3.4.2 Nitrate-temperature relationship

A scatter diagram of temperature versus nitrate concentration of all the data available in the upper 250 m of the surface area enclosed by the 26°C boundary is shown in Fig. 3.7. Three different regions can be distinguished in this plot: 1) a region where temperature is low (generally <15°C) but nitrate concentration has a high range (15-36  $\mu\text{M}$ ) of values, 2) an intermediate zone where the gradient of temperature is high (15-26°C) and changes in temperature and nitrate are well correlated, and 3) a warm (>26°C) upper layer where nitrate concentration is undetectable, or, when it is present, the slope of the temperature-nitrate relationship is lower than that of the intermediate region. When only surface data were considered (Fig. 3.7 insert), temperature and nitrate were poorly correlated, indicating that surface temperature is not a good predictor of surface nitrate concentration in this region. Studies of the relationship between temperature and nitrate concentration in the upper layer of the ocean [Kamykowski, 1987; Minas and Minas, 1992] have shown that seasonal and spatial variations in the slope are related to the rate of nitrate uptake by phytoplankton. Below this upper layer, the value depends on the balance between bacterial denitrification and nitrate regeneration from decomposing organic matter as well as physical transport processes [Zentara and Kamykowski, 1977].

The slope of the nitrate-temperature relationship at the base of the 26°C isotherm

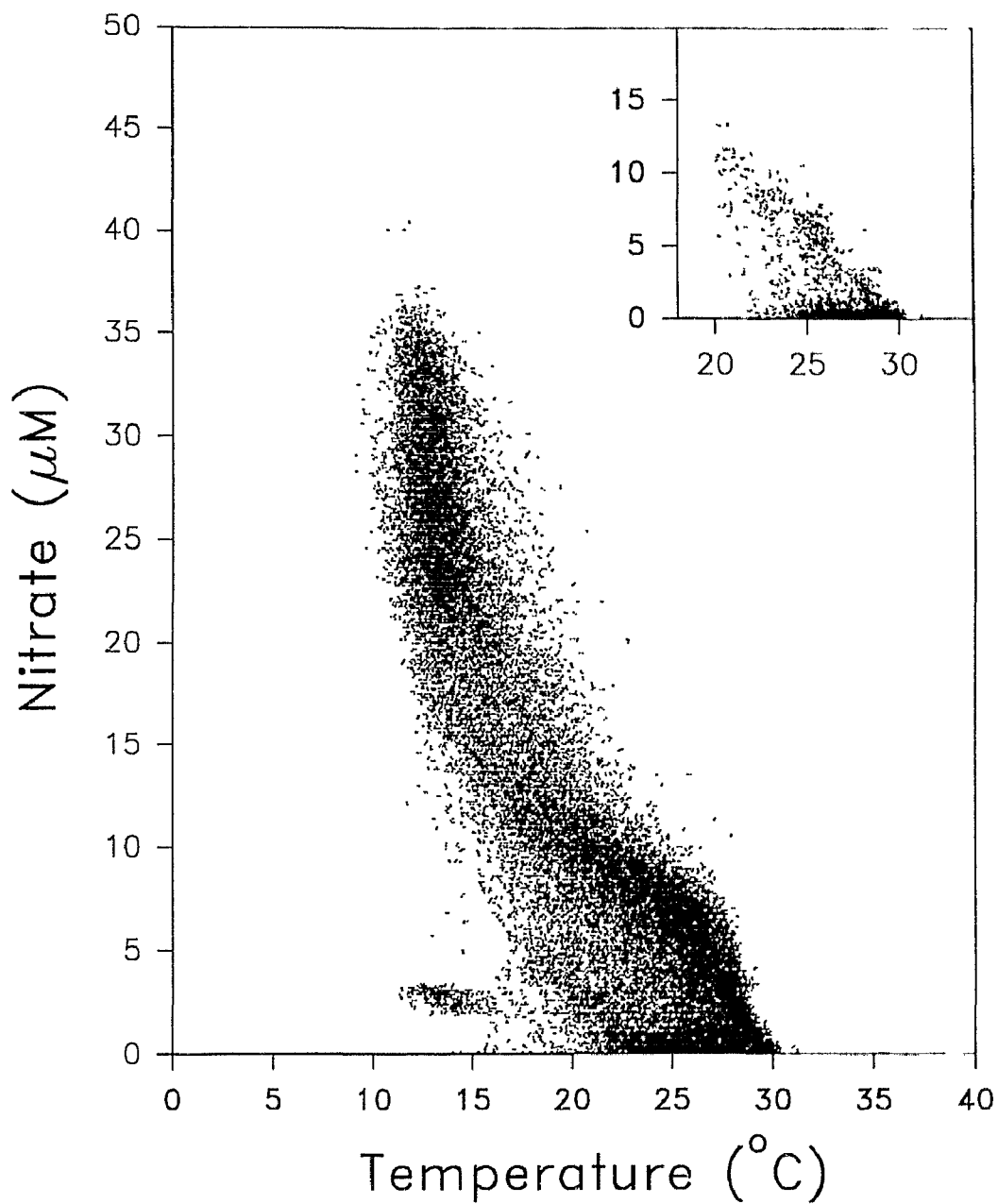


Figure 3.7: Scatter plot of temperature ( $^{\circ}\text{C}$ ) vs nitrate concentration ( $\mu\text{M}$ ) in the upper 250 m of the region enclosed by the 26  $^{\circ}\text{C}$  isotherm ( $n=48,100$ ). The same relationship is shown for the surface values in the insert ( $n=4,870$ ).

(Fig. 3.8a) showed longitudinal as well as latitudinal variations. Along the tropical Pacific, the slopes in the eastern sector ( $< -1.4 \mu\text{M } ^\circ\text{C}^{-1}$ ) were steeper than in the western sector ( $> -0.8 \mu\text{M } ^\circ\text{C}^{-1}$ ). Latitudinally, the values were less variable with the least steep slopes occurring in the western side poleward of  $10^\circ\text{N}$  and  $15^\circ\text{S}$  where the nutricline was deeper than the  $26^\circ\text{C}$  boundary. The variability in the slope (Fig. 3.8b) was higher near the equator between  $160^\circ$  to  $180^\circ\text{W}$  than elsewhere. These differences in slopes imply that a higher turbulent exchange of nitrate occurs in the eastern side, where the slopes are steeper, as compared to the western side for an equivalent turbulent flux of heat. Previous studies in this region have found a slope of  $-1.12$  and  $-2.04 \mu\text{M } ^\circ\text{C}^{-1}$  between  $180^\circ$  to  $93^\circ\text{W}$  and  $1.1^\circ\text{S}$  to  $1.1^\circ\text{N}$  [Halpern and Feldman, 1993] and eastward of  $130^\circ\text{W}$  between  $5^\circ\text{S}$  to  $20^\circ\text{N}$  [Fiedler *et al.*, 1991] respectively, which are consistent with the values estimated here. The average slope of the nitrate-temperature relationship was  $-0.89 \mu\text{M } ^\circ\text{C}^{-1}$  (95% confidence intervals  $-1.00$  to  $-0.78 \mu\text{M } ^\circ\text{C}^{-1}$ ) in the region enclosed by the  $26^\circ\text{C}$  isotherm.

### 3.4.3 Nitrate fluxes

The total surface area enclosed by the climatological  $26^\circ\text{C}$  isotherm and continental land masses, and the annual mean net surface heat flux into this region are shown in Table 3.1. Slight variations were obtained in the total surface area between the data sets mostly due to differences in the northern location of the  $26^\circ\text{C}$  isotherm. The net surface heat flux into the region obtained from climatologies ranged between  $8.3$  to  $11 \times 10^{14}$  W. Using the mean slope for the region given above, the new production resulting from turbulent input of nitrate into the Pacific warm water pool ranges from  $5.47$ - $7.26 \times 10^{12}$  mol N  $\text{y}^{-1}$  or an average of  $0.25$ - $0.31$  mmol N  $\text{m}^{-2} \text{d}^{-1}$  over the entire area. For comparison, this can be expressed in stoichiometrically equivalent carbon units using a Redfield ratio of 6.6; the new production rate is then  $4.37$ - $5.74 \times 10^{14}$  gC  $\text{y}^{-1}$  or  $19.9$ - $24.9$  mg C  $\text{m}^{-2} \text{d}^{-1}$ .

The net advective input of nitrate into the region enclosed by the  $26^\circ\text{C}$  isotherm (Table 3.2) is due to upwelling (26%) as well as horizontal transport (74%) of nitrate

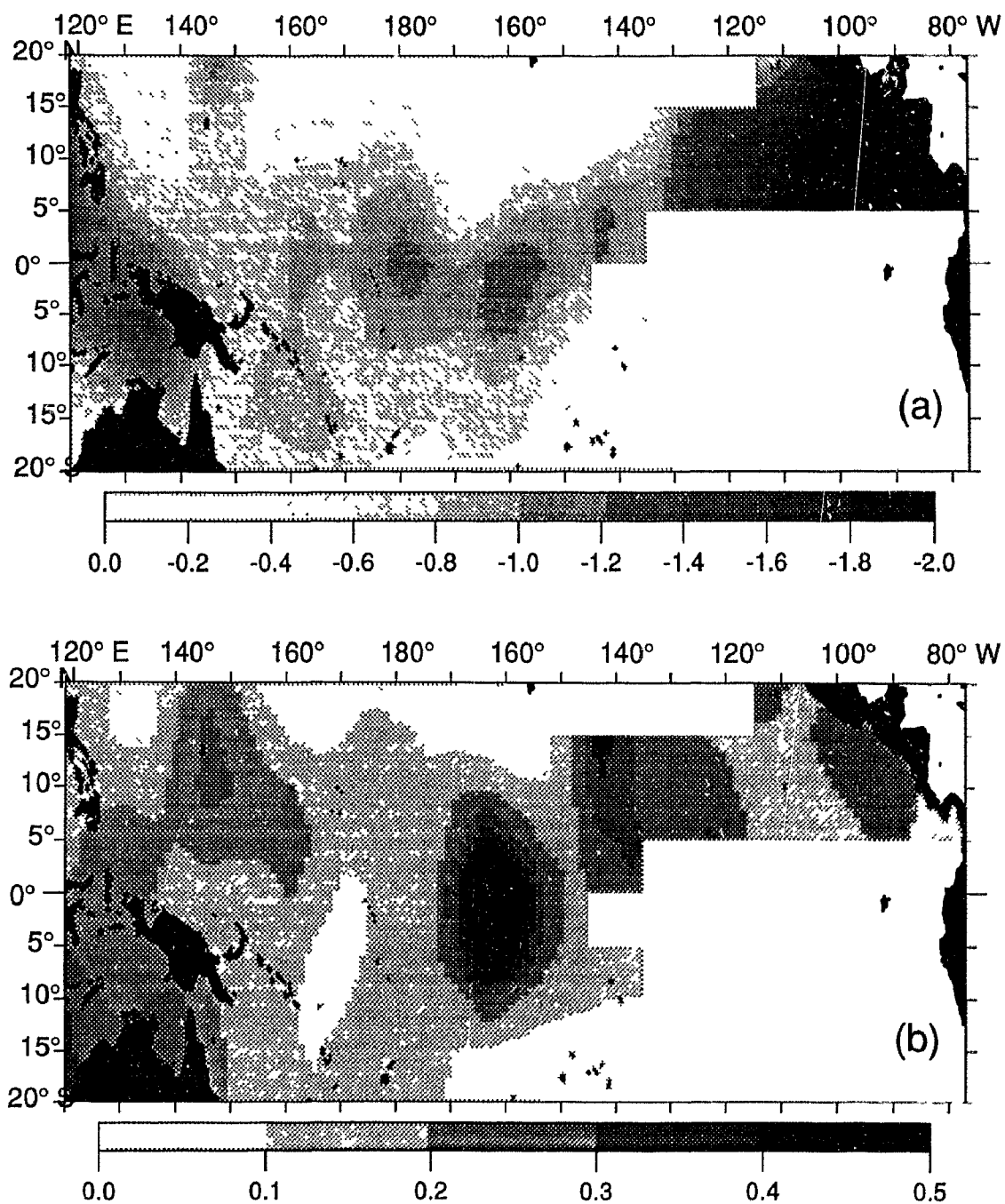


Figure 3.8: (a) The slope of the temperature-nitrate relationship ( $\mu\text{M } ^\circ\text{C}^{-1}$ ) at the base of the 26 °C and (b) the standard deviation of the slope at every 5° square in the region enclosed by the 26 °C isotherm.

Table 3.1: The net surface heat flux, mean turbulent nitrate transport and total surface area enclosed by the 26°C isotherm in the tropical Pacific and the corresponding mean new production using the Redfield ratio of C/N of 6.6 (at/at).

Heat flux (W x10 <sup>14</sup> )	Area (m <sup>2</sup> x10 <sup>13</sup> )	Nitrate transport (mol N y <sup>-1</sup> x10 <sup>12</sup> )	New production (mg C m <sup>-2</sup> d <sup>-1</sup> )	Source
11.0	6.31	7.26	24.9	Weare et al.[1981]
10.7	6.44	7.04	23.7	Oberhuber [1988]
8.3	5.98	5.47	19.9	Esbensen and Kushnir [1981]

Table 3.2: The mean advective nitrate balance of the region enclosed by the 26°C isotherm in the tropical Pacific and the corresponding mean new production using the Redfield ratio of C/N of 6.6 (at/at).

Mechanism	Nitrate Transport [mol N y <sup>-1</sup> ]	New production [mg C m <sup>-2</sup> d <sup>-1</sup> ]
<i>Vertical advection</i>		
Upwelling	2.0 x 10 <sup>12</sup>	7.0
Downwelling	-5.5 x 10 <sup>11</sup>	-1.9
Net input	1.5 x 10 <sup>12</sup>	5.1
<i>Horizontal advection</i>		
Meridional	2.6 x 10 <sup>12</sup>	9.1
Zonal	1.6 x 10 <sup>12</sup>	5.7
Net input	4.2 x 10 <sup>12</sup>	14.8
Net advective transport	5.7 x 10 <sup>12</sup>	19.9

into the region. At the 26°C surface, most (>60%) of the horizontal advection of nitrate occurs meridionally from the south, eastward of 110°W rather than zonally from the east between 2.5°N and 10°S. With the data available, the variability in the concentration of nitrate at the boundary is small (about  $\pm 1 \mu\text{M}$ ). Most of the vertical transport of nitrate was due to upwelling within 1° of the equator, whereas downwelling occurs north of the equator and represents <30% of the nitrate upwelled. Along the equator, the model of *Philander et al.* [1987] indicated maximum upwelling near 150° to 180°W with diminished upwelling eastward and westward of this region. In the vertical, their model shows that upwelling is constrained to the upper 100 m. The longitudinal pattern in upwelling velocities has been supported by other studies in this region [*Halpern et al.*, 1989; *Halpern and Freitag*, 1987]. Also, calculations of upwelling as a function of depth based on direct observations of divergence [*Halpern and Freitag*, 1987] and on a model of equatorial circulation [*Bryden and Brady*, 1985] show that vertical velocities fall sharply above 50 m and below 100 m. Although vertical nitrate input is constrained to within a degree of the equator [*Halpern and Freitag*, 1987], divergence of upwelled water produces a nutrient-rich area larger in meridional and zonal extent than the zone of upwelling.

### 3.5 Discussion

In the warm water of the tropical Pacific, we have estimated the mean annual rate of new production from a consideration of the large-scale nutrient balance based on the net surface heat flux, mean ocean circulation and nitrate and temperature correlation. Previously, new production has been inferred from nitrate-temperature correlation and experimental relationships between nitrate concentration and the uptake of nitrate [*Dugdale et al.*, 1989] or the *f*-ratio, i.e. the ratio of new production to total production [*Sathyendranath et al.*, 1991]. The approach used in this study is potentially more robust than previous ones because it does not require estimates of total production and it is independent of the relationship between *f*-ratio and nitrate

concentration, which have large uncertainties. However, our parameterization of new production only provides a large scale average, and can not provide detail on spatial or temporal variability in the rate of new production. Also, it does not allow a direct comparison to estimates of new production based on nitrate uptake ( $^{15}\text{N}$  experiments) [Dugdale *et al.*, 1992; Peña *et al.*, 1992] which, though more sensitive, are discrete and restricted to short time scales.

### 3.5.1 Potential sources of error

#### *Model assumptions*

In this study, new production has been defined as the production resulting from the net physical transport of nitrate into the volume bordered by the 26°C isotherm. This operational definition neglects other inputs of nitrogen to the region such as input from rain and from biological nitrogen fixation. In most of the ocean, fluxes of nitrate from below the nutricline are much more important than other sources [e.g. Eppley and Peterson, 1979]. In some locations, however, nitrogen fixation [Capone and Carpenter, 1982; Carpenter and Romans, 1991] can be significant. Although we are not aware of nitrogen fixation measurements in the tropical Pacific, this input is likely to be small since this process requires iron [Morel *et al.*, 1991], an element scarce in this region [Martin *et al.*, 1991]. Another consideration in the definition is that we assume that depth-integrated new production over the depth of the 26°C isotherm is equal to that of the euphotic zone. In the eastern tropical Pacific, the depth of the euphotic zone is around 60 to 70 m [Peña *et al.*, 1990; Fiedler *et al.*, 1991] which is close to that of the 26°C isotherm (Fig. 3.4). In the western equatorial Pacific, the euphotic zone depth as estimated from the average surface chlorophyll concentration within 10° latitude from the equator [ $0.11 \text{ mg m}^{-3}$ ; Dandonneau, 1992] and from Morel's [1988] model is about 95 m; almost 25 m shallower than the 26°C isotherm depth. However, several studies [Murray *et al.*, 1989; Barber and Chavez, 1991] in the tropical Pacific have shown phytoplankton production at the 0.1% light level which is several meters below the euphotic zone arbitrarily defined as the depth



at which light is reduced to 1% of surface irradiance. Therefore, our assumption regarding enclosure of the most significant productive layer is satisfied for the entire area considered.

To estimate turbulent fluxes of nitrate into the region we have assumed that there is no significant spatial covariance between the net heat flux across the 26°C isotherm and the slope of the nitrate-temperature relationship. Although there is not data available to estimate its value, the general trend in heat flux differs noticeably from the general trends in the slope of the temperature-nitrate relationship. Using the climatological net surface heat flux data from *Weare et al.* [1981] as a rough indicator of what occurs to the subsurface heat flux, and our slope of the nitrate temperature relationship, we found no significant covariance ( $r^2 = -0.16$ ) between these variables. On an annual scale, net surface heat fluxes in the tropical Pacific show mostly latitudinal variations, being higher near the equator and decreasing away from it [*Esbensen and Kushnir*, 1981; *Weare et al.*, 1981; *Oberhuber*, 1988]. Similarly, turbulent vertical fluxes are generally 3 to 5 times higher within 2 degrees of the equator than they are poleward [*Peters et al.*, 1989]. In comparison, we have found mainly longitudinal variations in the 5 degree-square slope of the temperature-nitrate relationship with higher values in the western tropical Pacific whereas heat fluxes vary latitudinally rather than longitudinally. Also, the slope of the nitrate-temperature relationship within 1° of the equator was not significantly different ( $p \ll 0.1$ ) from that poleward.

Finally, we have assumed that horizontal turbulent fluxes of nitrate into the region were small compared to those due to turbulent vertical fluxes. At the 26°C isotherm, the concentration of nitrate in the upper layer was detectable only in the southeastern boundary that surrounded the cold-nutrient rich waters of the eastern equatorial Pacific. In this region the maximum horizontal nitrate gradient was  $10^{-5}$  mmol  $m^{-4}$ . Considering an upper layer of 50 m and a lateral turbulent exchange coefficient of  $10^3$   $m^2$   $s^{-1}$  [*Bryden and Brady*, 1989], this will result in the transport of  $3.3 \times 10^{11}$  mmol N  $d^{-1}$  into the region which, though it may be significant locally, is two orders

of magnitude less than the estimated total turbulent vertical transport.

*Model parameter estimates*

Climatological temperature fields [Esbensen and Kushnir, 1981; Weare et al., 1981; Oberhuber, 1988] in the tropical Pacific shows that water warmer than 26°C reaches near 21-24°N and 20-21°S in the western region whereas our data set coverage is limited to 20° latitude from the equator. This discrepancy can be ignored with little consequence in our analysis where the horizontal grid boxes are as wide as 5° latitude and longitude. Also, despite the uneven temporal and spatial distribution of the data, they reproduce the main features present in the climatological temperature field.

With the data available, we have obtained a 95% confidence interval of about  $\pm 12\%$  in the estimation of the average slope of the nitrate-temperature relationship for the region. In comparison, the individual heat flux components have large uncertainties [Weare et al., 1981], so that the total heat flux has very large error bounds. In the tropical Pacific, the different estimates of net annual heat flux agree within a factor of two [Niiler and Stevenson, 1982]. Therefore, most of the uncertainty in the new production estimate due to turbulent input of nitrate is associated with errors in the magnitude of the net surface heat flux. The error in the estimation of the net advective transport of nitrate associated with changes of 1  $\mu\text{M}$  in the nitrate concentration of the source water is about 26% of the net advective transport. Although there is not data available to evaluate the errors in the mean water transport, the mean ocean circulation values given by Philander et al. [1987] agree well with field observations [Halpern and Freitag, 1987] and other model outputs [Bryden and Brady, 1985; Halpern et al., 1989]. We conclude that, the main quantifiable source of error in our estimation of new production is related to uncertainty in the value of the net surface heat flux used in the calculation.

For the western equatorial Pacific, annual mean surface heat fluxes reported in the literature range from 25 to 100  $\text{W m}^{-2}$  [Esbensen and Kushnir, 1981; Reed, 1985; Gordon, 1989]. In this region, the ocean circulation is too slow and the temperature gradient is too weak for either advection or mixing to carry any significant heat away

from the region [Niiler and Stevenson, 1982]. Thus, in order to maintain a steady annual mean temperature, the net heat flux through the sea surface must balance the vertical turbulent fluxes of heat. However, because the near-isothermal salt-stratified layer [Lukas and Lindstrom, 1991] found in the western equatorial Pacific seems to insulate the deep ocean from the surface layer much of the time [Godfrey and Lindstrom, 1989], either the net surface heat fluxes (18-22 W m<sup>-2</sup>) used by Niiler and Stevenson [1982] are too large, or the vertical fluxes of heat only occur episodically, for example, in association with wind bursts. For example, Godfrey and Lindstrom [1989] estimate a turbulent vertical heat flux of only 10-16 W m<sup>-2</sup> in the top 100 m of the western equatorial Pacific from data obtained in calm conditions, which is substantially smaller than that estimated by Niiler and Stevenson [1982]. However, they suggested that the strong westerly winds that occur intermittently in this region might produce strong mixing events. Field observations in the western Pacific between November 1989 and January 1990 have shown strong vertical shear down to 150 m in response to westerly wind events [McPhaden et al., 1992]. Although the mean wind speeds are weak in the western equatorial Pacific their variability is large. A climatology of westerly wind bursts in the western Pacific [Keen, 1988] shows that this area experiences such wind events more often than regions to the east, and that these events are far more frequent in the northern winter season.

Considerable progress has been made in the computation of the most important terms of surface heat fluxes (i.e. surface solar irradiance and latent heat flux) from satellite observations [Liu and Gautier, 1990]. Estimations of net surface heat flux in the tropical Pacific derived from meteorological reports from merchant ships and fishing vessels have uncertainties related to poor spatial and temporal coverage. Heat flux estimations based on satellite data, which can provide basin-wide coverage from days to years, may considerably improve the estimation of this parameter and thus reduce the error in our new production estimate.

### 3.5.2 Comparison with other new production estimates

Measurements to calculate the long term new production of the tropical Pacific are unavailable and are likely to be so for a considerable time. Thus, the only values available for a comparison of new production estimates at these scales is that obtained by *Bacastow and Maier-Reimer* [1990] from a three dimensional model of the carbon cycle in the ocean. They have estimated a new production rate of 18-20 gC m<sup>-2</sup> y<sup>-1</sup>, only slightly higher than the one we have obtained (14.5-16 gC m<sup>-2</sup> y<sup>-1</sup>) for approximately the same region. Given the uncertainties in both our and their estimates, and the approximations involved in these parameterizations, the agreement between the two estimates is remarkably good.

In the eastern equatorial Pacific region, a mean integrated annual new production of 1.3-1.9 x 10<sup>15</sup> gC y<sup>-1</sup> (or 320-470 mg C m<sup>-2</sup> d<sup>-1</sup>) has been reported within 5° of the equator and between 90° and 180°W [*Chavez and Barber*, 1987] based on estimation of nitrate upwelling. These values are approximately 30 to 90% higher than the total integrated new production estimated in this study. The area considered in the present analysis is approximately 6 times larger than that considered by *Chavez and Barber*, and includes large unproductive areas in the western Pacific not included by them. Several studies [e.g. *Thomas*, 1979] have shown the persistence of unused nitrate in surface waters of the eastern and central equatorial Pacific despite irradiance and stratification conditions favorable for complete nutrient uptake. This persistence results in the transport away from the upwelling zone of an important fraction of the nitrate upwelled [*Carr*, 1991; *Fiedler et al.*, 1991]. Because this loss of nitrate was not considered by *Chavez and Barber*, their estimation represents the upper limit of local new production. However, since downwelling of nitrate out of the euphotic zone (which represents a nutrient sink) was small in the region considered in this study, most of the upwelled nitrate is eventually consumed by phytoplankton but consumption may occur well away from the equator.

A net advective balance of nitrate into the euphotic zone of the eastern tropical Pacific [*Fiedler et al.*, 1991] gave an estimate of new production of 200 mgC m<sup>-2</sup> d<sup>-1</sup>

eastward of 130°W and within 5° from the equator, which was about 30% of total production. A similar value of new production ( $196 \text{ mgC m}^{-2} \text{ d}^{-1}$ ) was estimated from turbulent and advective fluxes of nitrate within 5° of the equator along a transect at 150°W [Carr, 1991]. In this region, turbulent diffusion of nitrate was about 30% of the advective transport of nitrate and the resulting new production was about 40% of the total production. These values are almost five times higher than our mean new production ( $44 \text{ mgC m}^{-2} \text{ d}^{-1}$ ). Considering a mean total production of  $312 \text{ mgC m}^{-2} \text{ d}^{-1}$ , as found between 160°W to 140°E and within 5° of the equator [Barber and Chavez, 1991], the new production estimated here is about 14% of the total production. This represents a lower-bound estimate, since we have considered regions away from the equator where total production is likely to be lower.

The productivity of the tropical Pacific region is very strongly affected by interannual events like El Niño Southern Oscillation (ENSO). Studies of both surface productivity and fluxes to the sediments [Dymond and Collier, 1988] suggest that the interannual variability associated with these events far exceeds the seasonal variability. It has been estimated [Chavez and Barber, 1985] that the total primary productivity within 5° of the equator and between 82° and 172°W was 2-3 times lower during El Niño than in normal oceanographic conditions. ENSO conditions also suppressed new production for a site close to the equator but enhanced it away from the equator [Dymond and Collier, 1988]. An important manifestation of El Niño is the increase in sea surface temperatures above their long term mean values by as much as 4°C in the central and eastern Pacific. This increase in the heat content of the upper ocean greatly exceeded (about 10 times) the estimated change in the surface heat flux [Reed, 1986]. This implies a decrease in the vertical transport of heat through the thermocline and therefore a decrease in the input of nitrate into the surface layer. Model analysis has shown that changes in the tropical Pacific sea surface temperature are associated mostly with anomalous zonal advection of warm water eastward and with variations in the depth of the thermocline [Wyrski, 1975; Seager, 1989; Halpern, 1987]. As a result of variations in the westerly winds, the thermocline is raised in the

west and is depressed in the east [Halpern, 1987]. Since the thermocline is depressed below the depth of entrainment in the eastern Pacific, the water upwelled towards the surface is warm and depleted of nutrients.

### 3.5.3 New production and the relationship to net air-sea exchange of carbon

Most of the new production in the ocean results from the supply of inorganic nitrogen from below the euphotic zone [e.g. *Eppley and Peterson, 1979*]. If the vertical transport of dissolved inorganic carbon and nitrate are in approximately the Redfield ratio, and are taken up in the euphotic zone and exported out of it in the same ratio, there would be no net biologically-mediated transport of carbon to the deep ocean [*Eppley and Peterson, 1979*]. Unlike nitrate, however, atmospheric CO<sub>2</sub> enters the ocean by sea-air gas exchange and is redistributed through the combined effects of advection, mixing, formation of particulate matter in the surface layer and subsequent remineralization in deep water. If there were sufficient data available in the tropical Pacific to determine the inorganic carbon concentration versus temperature relationship at the base of the subsurface boundary, the mean annual vertical flux of inorganic carbon could be estimated using the same computation as that for the turbulent nitrate fluxes. Then, the rate of new production could be compared with the rate of carbon fluxes, and an evaluation of the net air-sea exchange of carbon dioxide determined.

## 3.6 Conclusion

Our analysis gives an estimate of new production in the warm waters of the tropical Pacific from a consideration of the large scale nutrient balance. In this region, the new production resulting from vertical turbulent fluxes of nitrate was of the same magnitude as that due to advective nitrate transport. Most (about 75%) of the advective transport of nitrate was due to horizontal transport (zonal and meridional)

from the eastern equatorial Pacific rather than upwelling. Previous estimations of new production from nutrient budgets [*Chavez and Barber, 1987; Fiedler et al., 1991*] in the tropical Pacific region have ignored the input of nitrate due to vertical turbulent transport. The method employed here, which considers the input of nitrate due to turbulent diffusion as well as advection, yields more representative estimates of the large-scale average new production than those calculated from advection alone. We have estimated the new production resulting from vertical turbulent fluxes of nitrate based on fluxes of heat at the sea-surface. This approach can be applied to other regions of the world's ocean. The possibility therefore exists that there is a means to estimate new production from remotely-sensed observations which does not require the determination of physiological parameters of nitrate uptake from ship observations that are notoriously variable. Therefore, although our estimation of new production is based on several assumptions and is less sensitive than direct estimations, it provides an estimate over oceanographically-significant scales of time and space which are inaccessible to ship observations.

## Chapter 4

# The effect of fluctuations in the input of nitrate on phytoplankton biomass and new production

### 4.1 Introduction

The upper layer of the ocean is characterized by large temporal and spatial variations in physical, chemical and biological properties. In the marine environment, the availability of nutrients, particularly nitrogen, and light are limiting to phytoplankton. In most oceanic regions with sufficient insolation and stratification to allow plant growth, the input of nitrogen to the euphotic zone strongly influences phytoplankton production; where the flux of nutrients to the euphotic zone is high, phytoplankton biomass is enhanced compared to regions where the input of nitrogen is low [Yoder *et al.*, 1983; Hofmann and Ambler, 1988; Lewis *et al.*, 1988; Yoder *et al.*, 1993]. In coastal regions, fluctuations in the input of nitrate often result in an increase in the biological productivity of the system by up to several orders of magnitude. There is, however, considerable uncertainty regarding whether nutrients limit the rate of phytoplankton growth or its biomass [e.g. Cullen *et al.*, 1992; Falkowski *et al.*, 1992]. Laboratory



studies of nitrogen-limited cultures have shown an increase in the growth rate of phytoplankton when the availability of nitrogen is increased [Eppley and Renger, 1974; Goldman and McCarthy, 1978; Glover, 1980]. In contrast, it has been suggested [Goldman *et al.*, 1979] that in the ocean the specific growth rate of phytoplankton is independent of ambient nutrient concentration over time scales longer than the generation time and that only the steady-state total biomass of phytoplankton is controlled by nutrient supply.

Phytoplankton populations experience variability in the concentration of nitrate over a range of time-scales from seconds to the interannual [Glover *et al.*, 1988; Jenkins, 1988; Marra *et al.*, 1990; Barber, 1992]. Open ocean regions have, in general, lower physical and biological variability than coastal regions [Walsh, 1976]. The response of phytoplankton to variations in the availability of nitrate should vary according to the nitrogen status of the population. Under nitrogen-limited growth conditions, phytoplankton growth would be enhanced by even a small pulse of nitrate into the surface mixed layer and phytoplankton biomass could potentially increase [Glover *et al.*, 1988]. In contrast, if phytoplankton is growing at its maximum capacity, an increase in phytoplankton biomass is only possible by a reduction in the loss terms (i.e. grazing, sinking or transport). The main loss term in the open ocean appears to be grazing by zooplankton. In nitrogen-limited conditions, because the food web components react to perturbations at different rates, the frequency of response of the organisms is not necessarily the same as that of the nitrate perturbation. For example, since phytoplankton and zooplankton populations have a different response times (physiology and growth), the biomass of phytoplankton and the rate of nitrate utilization after a pulse of nitrate will differ [Price *et al.*, 1994]. High yields of phytoplankton biomass after an increase in the concentration of nitrate could arise from a poor coupling between phytoplankton and zooplankton populations. Therefore, in a fluctuating environment, the fluctuations themselves become a resource [e.g. Harris, 1986], and thus the characterization of the fluctuation is as important as is the measure of its average value.

The uptake of nitrate by phytoplankton depends on several factors in addition to the ambient nitrate concentration [*Harrison et al.*, 1987; *Garside*, 1981; *Glibert et al.*, 1982c; *Wheeler and Kokkinakis*, 1990]. These include the standing stock of phytoplankton, its specific uptake rate (which is a function of nutrient history), and the presence of other nitrogen sources (i.e. ammonia). In regions where the concentration of nitrate may be many times greater than that of ammonia, the rate of ammonia uptake can still be high because phytoplankton prefers ammonia rather than nitrate [*McCarthy et al.*, 1977; *Glibert et al.*, 1982b; but see *Dortch*, 1990]. Several studies have shown that the variability in the rate of new production (the primary production associated with newly available nitrogen, mainly nitrate; *Dugdale and Goering*, 1967) and the *f*-ratio (the ratio of new to total production; *Eppley and Peterson*, 1979) may be appreciable even in oceanic environments [e.g. *McCarthy et al.*, 1977]. It has been suggested that in the open ocean, local or transient fluctuations from oligotrophy associated with input of nitrate to the euphotic zone will account for a high proportion of the annual total production [*Platt and Harrison*, 1985] and that most of the production in these events will be new production. Moreover, *Walsh* [1976] has proposed that changes in the dominant frequencies of variability of the physical habitat may define the importance of grazing losses as a constraint on nutrient utilization in the sea. Bearing in mind the conceptual importance of new production to our understanding of sedimentation rates and yield to higher trophic levels [*Eppley and Peterson*, 1979; *Michaels and Silver*, 1988], it is important to consider the influence of environmental variability in the input of nitrate on the magnitude and variability of new production.

The objective of this study is to explore, by means of a mathematical model, the effect of variability on time scales of days to months in the input of nitrate on phytoplankton biomass and new production. For this purpose we used a simple plankton model of the mixed layer similar to other existing models [*Wroblewski et al.*, 1988; *Fasham et al.*, 1990; *Taylor and Joint*, 1990] which distinguish between nitrate and ammonia utilization. The next section describes the model, while the subsequent

section describes the steady-state properties of the model. Finally, the results of numerical simulations with a periodically variable nitrate input are presented and discussed.

## 4.2 Model Description

The model represents a plankton community homogeneously distributed within the surface mixed layer. An optimal light condition is assumed with only nitrogen limiting phytoplankton growth. The model (Fig. 4.1) has been kept as simple as possible to facilitate its interpretation; it consists of phytoplankton ( $P$ ), zooplankton ( $Z$ ) and nitrogen. The dissolved nitrogen pool is distinguished between new N (nitrate,  $N$ ) and regenerated N (ammonia,  $A$ ) pools. Other forms of regenerated nitrogen (i.e. urea) are not distinguished from ammonia in the model. All model components are expressed in terms of their nitrogen units ( $\mu\text{M}$ ). Variables and parameters are defined in Table 4.1.

The equations describing the system are:

$$\frac{dP}{dt} = \mu_m(\gamma_N + \gamma_A)P - \lambda Z - mP - F(t)P \quad (4.1)$$

$$\frac{dZ}{dt} = \lambda\beta Z - dZ - F(t)Z \quad (4.2)$$

$$\frac{dN}{dt} = F(t)(N_z - N) - \mu_m\gamma_N P \quad (4.3)$$

$$\frac{dA}{dt} = amP + cdZ + b\lambda(1 - \beta)Z - \mu_m\gamma_A P - F(t)A \quad (4.4)$$

The parameter  $F(t)$  represents the specific rate of water transport in and out of the mixed layer ( $\text{d}^{-1}$ ). It is assumed that phytoplankton and zooplankton behave as passive particles and are subject to dilution during nutrient input events, which

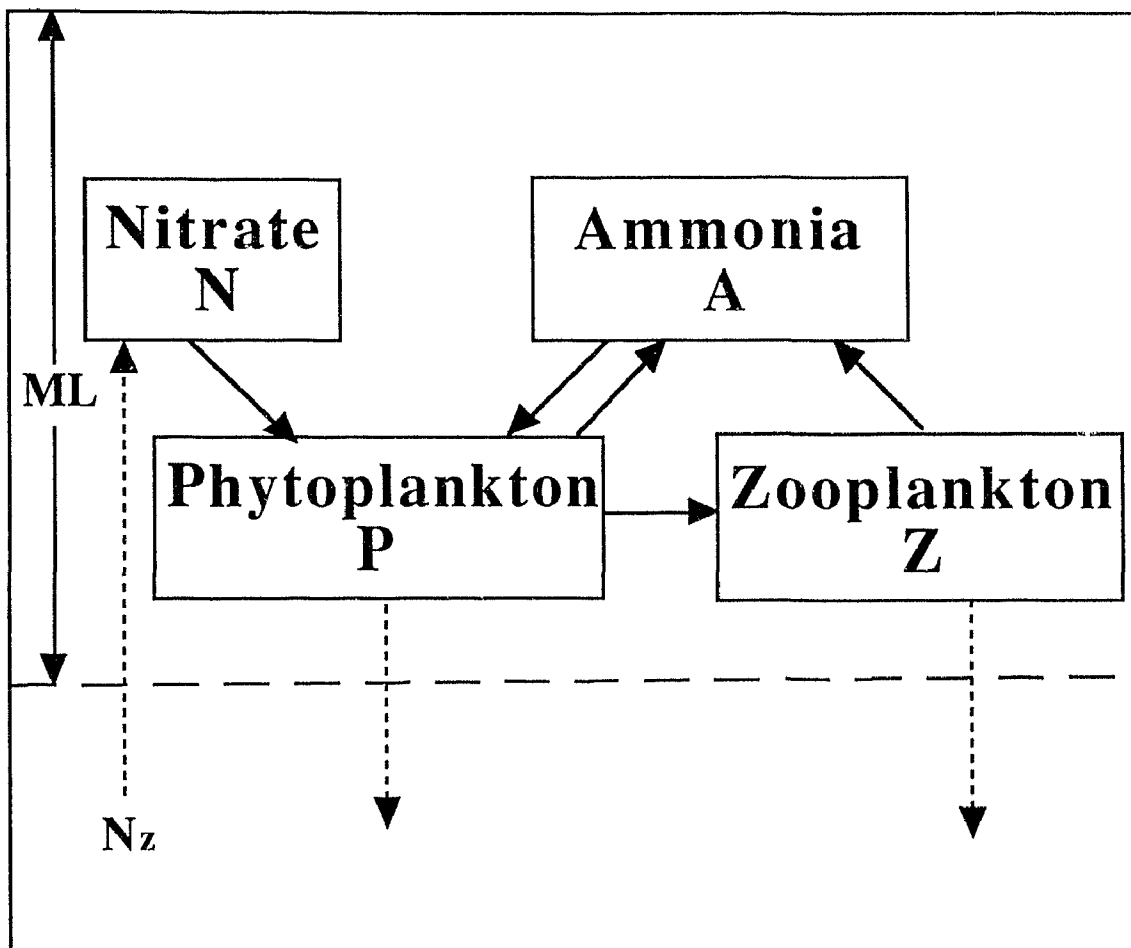


Figure 4.1: Diagrammatic representation of the simple plankton model.

Table 4.1: Model variables and parameters

Symbol	Definition	Values	Units
$P$	Phytoplankton biomass	—	$\mu\text{M}$
$Z$	Zooplankton biomass	—	$\mu\text{M}$
$N$	Nitrate concentration	—	$\mu\text{M}$
$A$	Ammonia concentration	—	$\mu\text{M}$
$\mu_m$	Phytoplankton maximum specific growth rate	1	$\text{d}^{-1}$
$\gamma_N$	Normalized nitrate uptake	—	—
$\gamma_A$	Normalized ammonia uptake	—	—
$\lambda$	Specific zooplankton grazing rate	—	$\text{d}^{-1}$
$m$	Phytoplankton specific mortality rate	0.1	$\text{d}^{-1}$
$F, F(t)$	Net water transport	—	$\text{d}^{-1}$
$\beta$	Zooplankton assimilation efficiency	0.4	—
$d$	Zooplankton specific mortality rate	—	$\text{d}^{-1}$
$a$	Regeneration efficiency of dead phytoplankton	0.5	—
$b$	Regeneration efficiency of zooplankton unassimilated food	0.5	—
$c$	Regeneration efficiency of dead zooplankton	0.8	—
$N_z$	Nitrate concentration below the mixed layer	10	$\mu\text{M}$
$k_N$	Half-saturation constant for nitrate uptake	0.1, 0.5	$\mu\text{M}$
$k_A$	Half-saturation constant for ammonia uptake	0.01	$\mu\text{M}$
$\Psi$	Ammonia inhibition parameter	1.5	$\mu\text{M}^{-1}$
$G_m$	Maximum specific ingestion rate	—	$\text{d}^{-1}$
$k_g$	Half-saturation constant of ingestion rate	—	$\mu\text{M}$
$F_0$	Minimum water transport	0.0002	$\text{d}^{-1}$
$w$	vertical velocity	1, 0.25	$\text{m d}^{-1}$
$H$	Mixed layer depth	50	m
$t$	Time	—	d
$\omega$	Frequency	—	$\text{d}^{-1}$

could be either upwelling or vertical mixing. It is also assumed that phytoplankton, zooplankton and ammonia are all absent below the mixed layer while nitrate there has a constant concentration  $N_z$  (equation 4.3).

The phytoplankton equation (4.1) considers rates of phytoplankton growth and loss due to grazing ( $\lambda$ ), which is a function of phytoplankton concentration, death ( $m$ ) and transport ( $F(t)$ ). Losses due to phytoplankton sinking are assumed to be negligible. Phytoplankton can utilize ammonia ( $A$ ) and nitrate ( $N$ ). Nitrogen limitation of phytoplankton growth is incorporated into  $\gamma_A$  and  $\gamma_N$ , which are normalized functions for ammonium and nitrate uptake respectively and can take values between 0 and 1. Under nitrogen-saturated conditions ( $\gamma_A + \gamma_N = 1$ ), phytoplankton specific growth rate is at its maximum value ( $\mu_m$ ). Zooplankton (equation 4.2) do not assimilate all they ingest. A constant fraction  $\beta$  of the ingested food is assumed to be assimilated. The remainder of the ingested phytoplankton ( $1 - \beta$ ) is partitioned between egested fecal material and excreted nitrogen (ammonia) according to a regeneration efficiency,  $b$ . Carnivores are not modeled explicitly; their effects are simulated by a constant mortality ( $d$ ) of herbivores. Nutrient regeneration (equation 4.4) is possible via excretion from the zooplankton and bacterial remineralization of dead phytoplankton and zooplankton ( $a$  and  $c$ , respectively). The bacteria component is also not explicitly modeled.

#### *Nitrogen uptake formulation*

Nitrogen limitation of phytoplankton growth (here represented as  $\gamma_A + \gamma_N < 1$ ) is usually formulated using the Michaelis-Menten hyperbola for nutrient uptake. Several modifications of this function has been used in models which distinguish between the utilization of nitrate and ammonia [*Wroblewski, 1977; Taylor and Joint, 1990; Frost and Frazer, 1994*]. The most common formulations are:

$$\gamma_1 = \frac{N e^{-A\Psi}}{(k_N + N)} + \frac{A}{(k_A + A)} \quad (4.5)$$

$$\gamma_2 = \frac{N}{(k_N + N)} \times \frac{1}{(1 + A\Psi)} + \frac{A}{(k_A + A)} \quad (4.6)$$

$$\gamma_3 = \frac{N/k_N}{\left(1 + \frac{N}{k_N} + \frac{A}{k_A}\right)} + \frac{A/k_A}{\left(1 + \frac{N}{k_N} + \frac{A}{k_A}\right)} \quad (4.7)$$

where  $\gamma_i = \gamma_N + \gamma_A$ . The first two formulations include, in addition to the half-saturation concentration of nitrate ( $k_N$ ) and ammonia ( $k_A$ ) uptake, a parameter ( $\Psi$ ) to simulate suppression of nitrate uptake by the presence of ammonia. The value of this parameter is rarely measured in the field; most models [Wroblewski, 1977; Fasham *et al.*, 1990; Sarmiento *et al.*, 1993] have used the value of  $1.5 \mu\text{M}^{-1}$  obtained from the data of Walsh and Dugdale [1972]. A serious problem with these two formulations is that they can reach values higher than the scaling factor of one depending on the value of the parameters used, and thus can artificially overestimate phytoplankton growth. In comparison, the nitrogen uptake formulation  $\gamma_3$  only predicts values between 0 and 1. For example, as Fig. 4.2 shows, for concentrations of nitrate and ammonia between 0 to 10 times their respective half-saturation constant, overestimation of the phytoplankton growth rate ( $\gamma_N + \gamma_A > 1$ ) occurs if the product  $k_A \Psi$  is lower than or equal to 0.6 for  $\gamma_1$  or 0.8 for  $\gamma_2$ . Thus, using the value of  $\Psi$  mentioned above, values of  $k_A < 0.5 \mu\text{M}$  could result in estimated phytoplankton growth rates greater than the assumed maximum.

Another difference among these formulations is that they predict a different value of the  $f$ -ratio (i.e.  $\gamma_N/(\gamma_N + \gamma_A)$ ) for a given concentration of nitrogen relative to their respective half-saturation constant (Fig. 4.3). This is particularly evident when the nitrate concentration is high relative to its half-saturation constant. When  $\gamma_1$  or  $\gamma_2$  are used to model phytoplankton nitrogen uptake, the  $f$ -ratios are almost entirely dependent on the concentration of ammonia except when the concentration of nitrate is lower than twice the  $k_N$ . Thus, when ambient nitrate concentrations are several times higher than the half-saturation constant of nitrate uptake, low  $f$ -ratios can still be obtained.

In contrast, when phytoplankton nitrogen uptake is represented by  $\gamma_3$  (equation 4.7), the  $f$ -ratio depend on the value of the ratio of the ambient nitrate (or ammonia)

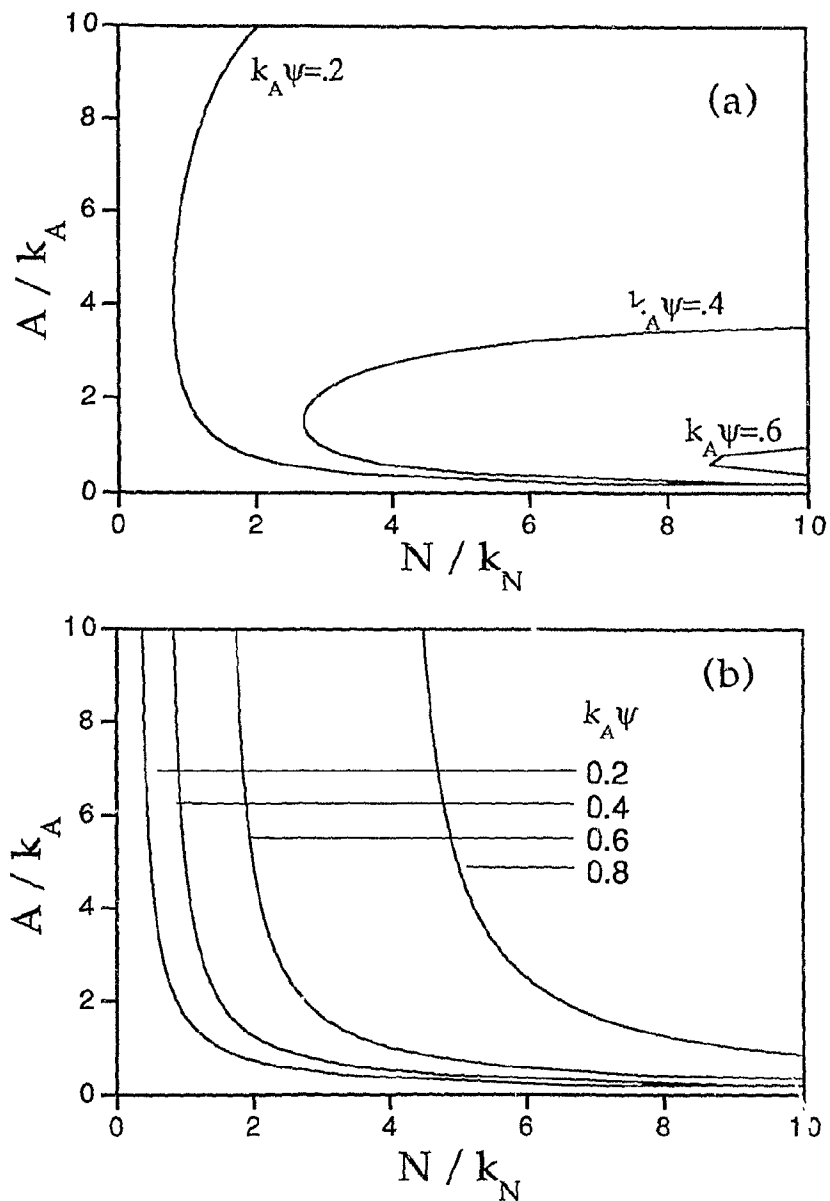


Figure 4.2: Combinations of nitrate and ammonium ( $N$  and  $A$ ;  $\mu\text{M}$ ), relative to their respective half-saturation constants ( $k_N$  and  $k_A$ ;  $\mu\text{M}$ ), for which growth is nitrogen-saturated ( $\gamma_A + \gamma_N = 1$ ). Solutions are presented for different values of the ammonia inhibition term ( $\Psi$ ;  $\mu\text{M}$ ) times the half-saturation constant of ammonium uptake ( $k_A$ ), calculated from equations 4.5 (a;  $\gamma_1$ ) and 4.6 (b;  $\gamma_2$ ). The space to the right of each line represents nutrient concentration exceeding saturation. In these formulations, growth rates greater than  $\mu_m$  are predicted.



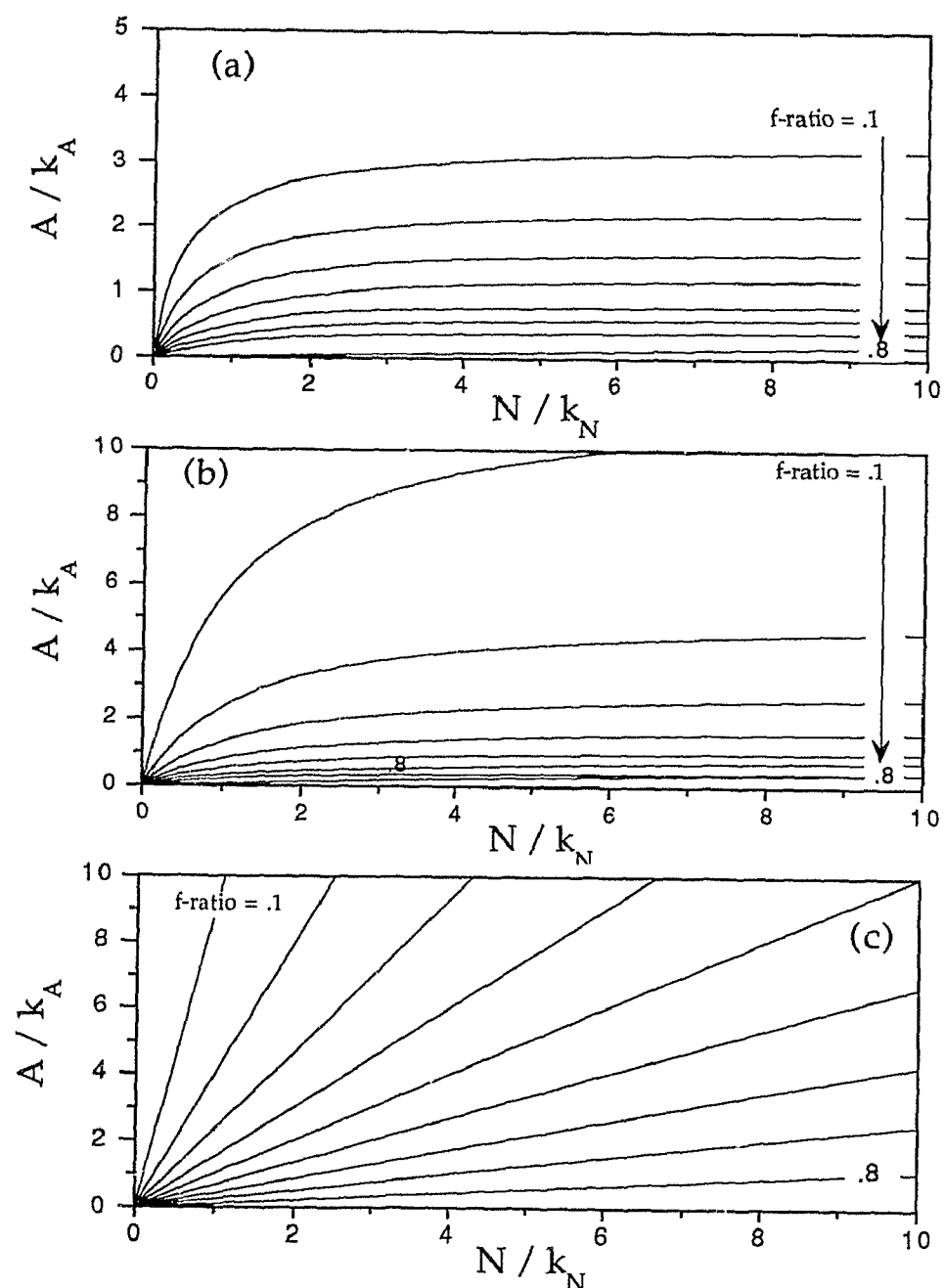


Figure 4.3: Contours of predicted  $f$ -ratios as a function of nitrate ( $N$ ) and ammonia ( $A$ ) concentrations ( $\mu\text{M}$ ) relative to their respective half-saturation constant ( $k_N$  and  $k_A$ ;  $\mu\text{M}$ ): a)  $\gamma_1$ ; equation 4.5, b)  $\gamma_2$ ; equation 4.6, and c)  $\gamma_3$ ; equation 4.7. The values of  $\gamma_1$  and  $\gamma_2$  were estimated using a fixed value of  $\Psi = 1.5 \mu\text{M}^{-1}$ . When  $N/k_N$  is  $>2$ , the  $f$ -ratio in a) and b) is mostly dependent on  $A/k_A$ , whereas in c) the  $f$ -ratio is directly proportional to the ratio of  $N/k_N$  to  $A/k_A$ .

concentration to its half-saturation constant when the other N species is held constant (Fig. 4.3c). Thus, to obtain a low  $f$ -ratio under high nitrate concentrations relative to its half-saturation constant, the concentration of ammonia relative to its half-saturation constant must be even higher than that for nitrate. This last formulation ( $\gamma_3$ ) is adequate to describe the nutrient dependence of growth rate when uptake of a limiting nutrient is catalyzed by a single transport mechanism [see *Cullen et al.*, 1993]. Although  $\gamma_3$  does not model the inhibition of nitrate uptake by the presence of ammonia explicitly, it can model the preference for ammonium uptake by selecting lower half-saturation constants for ammonia uptake than for nitrate uptake. A review of field studies have shown that the reduction of nitrate uptake in the presence of ammonia is rarely to the degree which is generally believed, and that it is a highly variable phenomenon [*Dortch*, 1990]. Due to uncertainties in the interaction between ammonia and nitrate uptake, no one of the formulations considered here is totally satisfactory to model nitrogen uptake accurately. However, we have chosen  $\gamma_3$  to model phytoplankton nitrogen utilization because it is the only formulation which does not predict growth rates greater than the maximum (i.e.  $\gamma_N + \gamma_A \leq 1$ ).

#### *Grazing formulation*

Several formulations have been used to model the grazing rate of zooplankton ( $\lambda$ ;  $\text{d}^{-1}$ ) as a function of food concentration based on two parameters: the maximum grazing rate ( $G_m$ ;  $\text{d}^{-1}$ ) and the concentration of phytoplankton at which grazing occurs at half the maximum value ( $k_g$ ;  $\mu\text{M}$ ), such as,

$$\lambda_1 = \frac{P^2 G_m}{k_g^2 + P^2} \quad (4.8)$$

$$\lambda_2 = G_m (1 - e^{-P(\ln 0.5)/k_g}) \quad (4.9)$$

$$\lambda_3 = G_m P(\ln 0.5)/k_g (1 - e^{-P(\ln 0.5)/k_g}) \quad (4.10)$$

These grazing formulations behave differently at low and high food concentrations. At low food concentrations, the grazing rate in  $\lambda_1$  [Hollings, 1965] and  $\lambda_3$  [Mayzaud and Poulet, 1978] is lower than that of  $\lambda_2$  [Ivlev, 1955] and increase nonlinearly with food concentration (Fig. 4.4). At high food concentrations, there is a saturation of the grazing rate in  $\lambda_1$  and  $\lambda_2$  whereas in  $\lambda_3$  the grazing rate increases without limitation as phytoplankton biomass increases. This last formulation (equation 4.10) is based on results of Mayzaud and Poulet [1978] which indicated that, over the naturally occurring range of food concentrations, copepods can adapt their digestion rate to food abundance, leading to a much steeper grazing function. These different grazing functions will be compared by examining their influence on the steady-state solution of the model in the next section.

### 4.3 Steady-state solution

In order to understand the basic behavior of the model and to explore the parameter space, the model equations (4.1 to 4.4) were solved for steady-state. Since the value of the transport term is at least an order of magnitude smaller than the biological parameters in oceanic regions (e.g.  $F(t) < 0.02$  even for the equatorial Pacific upwelling region; Wyrski, 1981), we have neglected it in the steady-state solution of the phytoplankton, zooplankton and ammonia equations. Transport must be included in the nitrate equation. The steady-state solution to the set of equations is,

$$\frac{Z}{P} = \frac{\beta(\mu_m(\gamma_N + \gamma_A) - m)}{d} \quad (4.11)$$

$$\lambda\beta = d \quad (4.12)$$

$$N = N_z - \frac{\mu_m\gamma_N P}{F(t)} \quad (4.13)$$

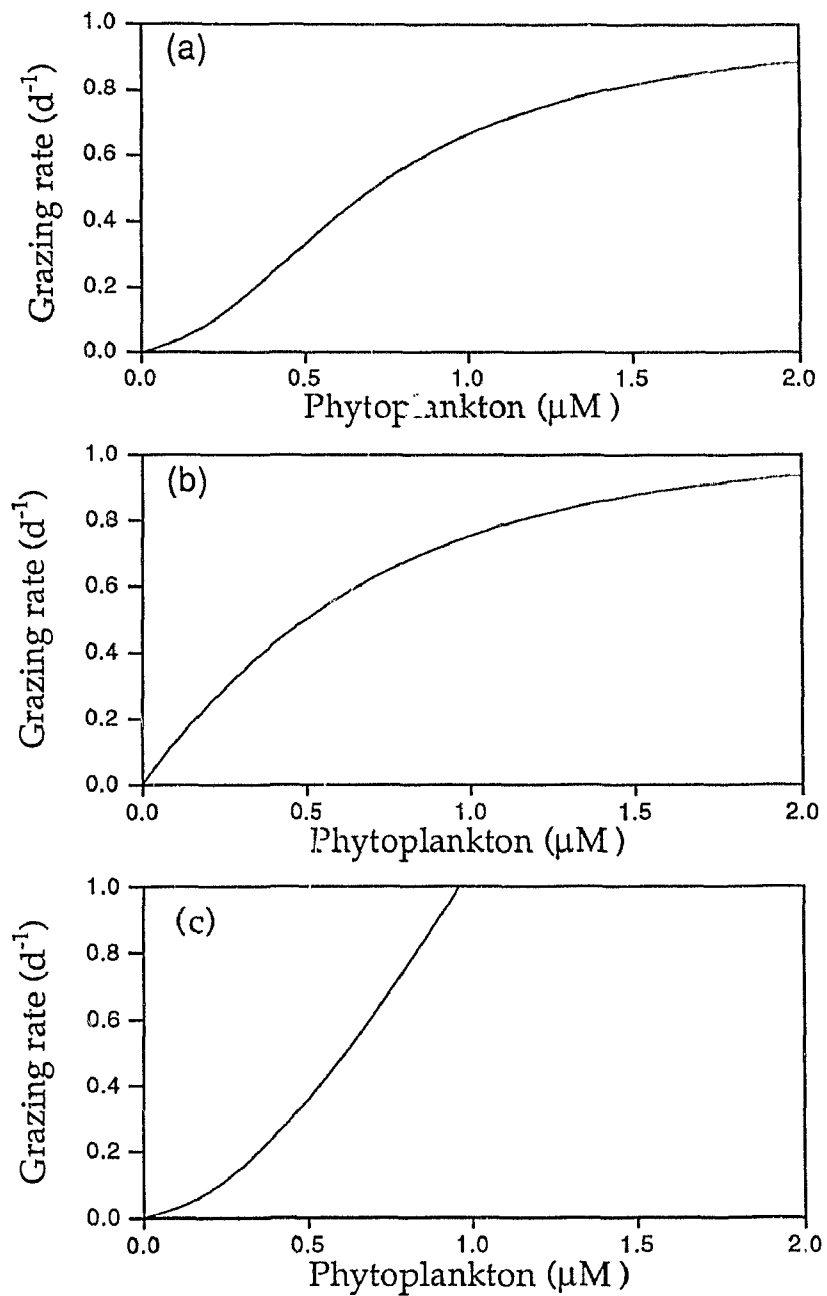


Figure 4.4: Zooplankton grazing rate as a function of phytoplankton biomass. a)  $\lambda_1$ , s-shaped grazing formulation [Hollings, 1965], b)  $\lambda_2$ , Ivlev formulation [Ivlev, 1955], and c)  $\lambda_3$ , Mayzaud and Poulet formulation [Mayzaud and Poulet, 1978].

$$\frac{\gamma_A}{(\gamma_A + \gamma_N)} = \left(1 - \frac{m}{\mu_m(\gamma_A + \gamma_N)}\right) \times (b - b\beta + c\beta) + \frac{am}{\mu_m(\gamma_A + \gamma_N)} \quad (4.14)$$

At steady-state, the ratio of zooplankton biomass to phytoplankton biomass (equation 4.11) is directly proportional to the net phytoplankton specific growth rate and the zooplankton assimilation efficiency and inversely proportional to the zooplankton specific mortality rate (or the zooplankton specific growth rate ( $\lambda\beta$ ), since it is equal to the zooplankton specific mortality rate ( $d$ ); equation 4.12). If the specific growth rate of phytoplankton increases relative to that of the zooplankton, the ratio of zooplankton biomass to phytoplankton biomass must also increase to achieve a steady-state (Fig. 4.5). This change in zooplankton biomass relative to phytoplankton biomass varies with the zooplankton assimilation efficiency and the phytoplankton specific mortality rate. When the zooplankton assimilation efficiency is high and the phytoplankton specific mortality rate is low, a change in the specific growth rate of phytoplankton relative to that of zooplankton causes the greatest increase in the ratio of zooplankton to phytoplankton biomass.

The influence of the grazing function on the model output is examined by replacing  $\lambda$  in equation 4.12 by the different grazing formulations (equations 4.8 to 4.10),

$$\lambda_1 = \frac{P^2 G_m}{k_g^2 + P^2} = \frac{d}{\beta} \quad (4.15)$$

$$\lambda_2 = G_m(1 - e^{-P(\ln 0.5)/k_g}) = \frac{d}{\beta} \quad (4.16)$$

$$\lambda_3 = G_m P(\ln 0.5)/k_g(1 - e^{-P(\ln 0.5)/k_g}) = \frac{d}{\beta} \quad (4.17)$$

For each of these equations, the magnitude of the ratio of phytoplankton biomass to the half-saturation constant of grazing ( $P/k_g$ ) was computed, and are shown in

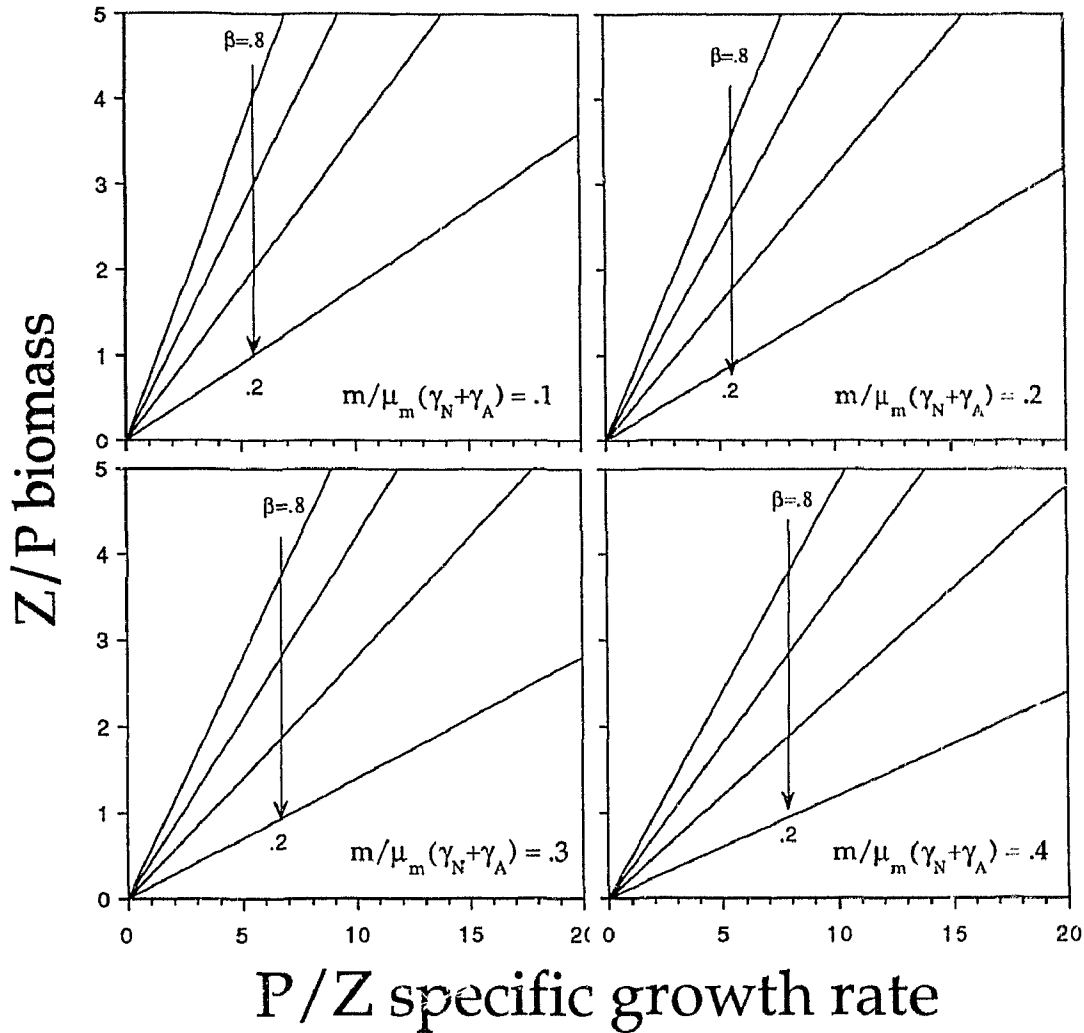


Figure 4.5: The ratio of zooplankton biomass ( $\mu\text{M}$ ) to phytoplankton biomass ( $\mu\text{M}$ ) at steady-state as a function of the phytoplankton specific growth rate ( $\text{d}^{-1}$ ) relative to the zooplankton specific growth rate ( $\text{d}^{-1}$ ) for different values of the zooplankton assimilation efficiency ( $\beta$ ) and the ratio of phytoplankton specific mortality rate to phytoplankton specific growth rate ( $m/\mu_m(\gamma_N + \gamma_A)$ ; dimensionless). Efficiency in assimilation and growth translates into greater accumulation of zooplankton.

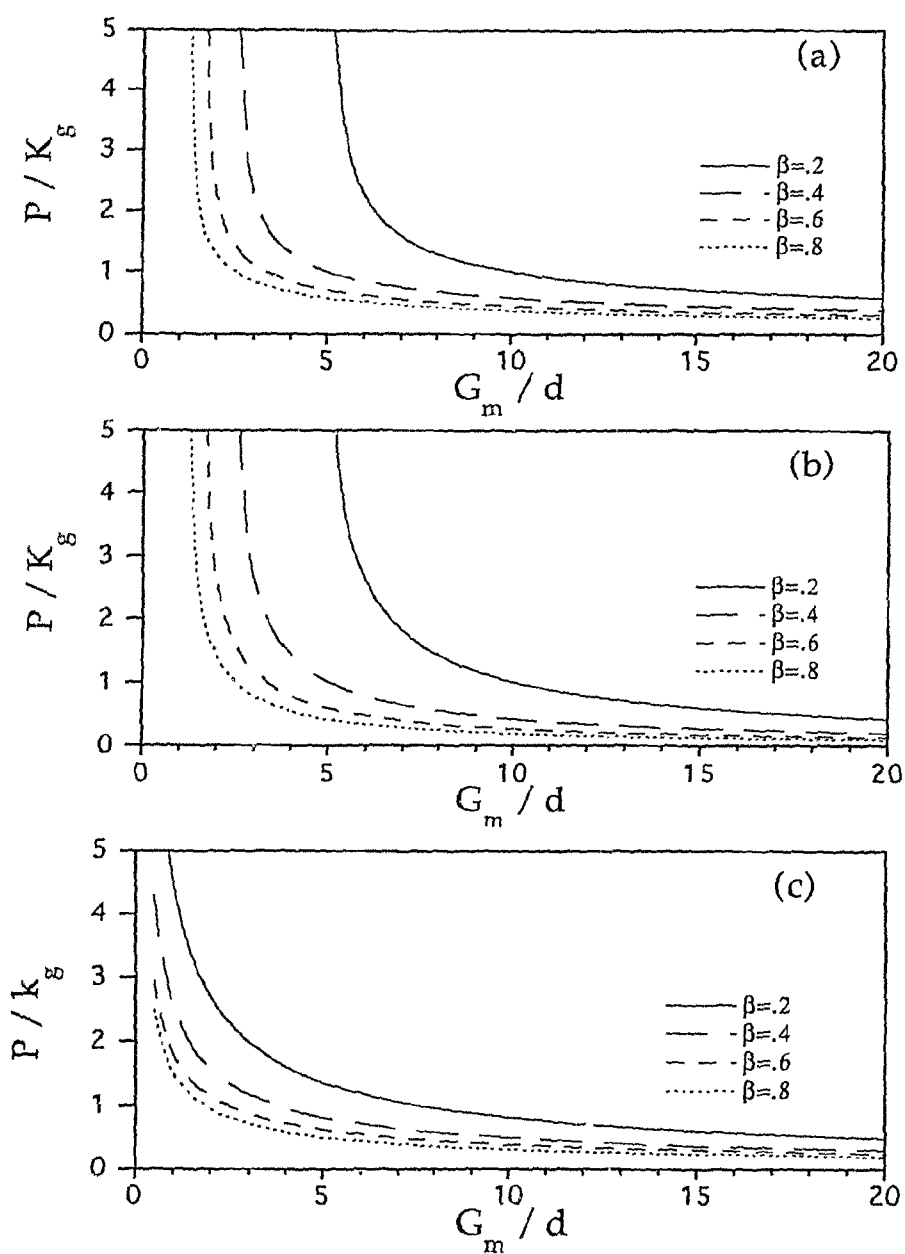


Figure 4.6: Non-dimensional steady-state solution of phytoplankton biomass ( $P$ ;  $\mu\text{M}$ ) relative to the half-saturation concentration of grazing ( $k_g$ ;  $\mu\text{M}$ ) as a function of the ratio of zooplankton maximum specific grazing rate ( $G_m$ ;  $\text{d}^{-1}$ ) to zooplankton specific mortality rate ( $d$ ;  $\text{d}^{-1}$ ). Solutions are presented for different grazing formulations: a)  $\lambda_1$ ; equation 4.15, b)  $\lambda_2$ ; equation 4.16, and c)  $\lambda_3$ ; equation 4.17.

Fig. 4.6 for a range of parameter values. In each of the grazing formulations, the ratio of phytoplankton biomass to the half-saturation constant of grazing ( $P/k_g$ ) decreases non-linearly with the increase in the ratio of the zooplankton maximum grazing rate to its mortality rate ( $G_m/d$ ). At higher values of the ratio  $G_m/d$ , phytoplankton biomass is under grazing control and approaches zero. There is a minimum value of  $G_m/d$  above which steady-state can be reached. Just above this minimum value, phytoplankton biomass is high since it is not grazing controlled. Below this value, zooplankton are unable to support themselves against their mortality rate. At lower zooplankton assimilation efficiencies, this minimum value increases and phytoplankton biomass approach zero more slowly. The main difference among these formulations is in the minimum value of the ratio of zooplankton grazing rate to the zooplankton specific mortality rate which is required to obtain a steady-state. The value is similar for the grazing formulation  $\lambda_1$  and  $\lambda_2$  while it is lower for  $\lambda_3$  (Fig. 4.6). Because of that, a steady-state solution can be obtained in the widest range of parameters values using  $\lambda_3$  (i.e. Mayzaud and Poulet formulation). However, in this formulation, the grazing rate never reaches a saturation level, so the maximum grazing rate parameter,  $G_m$ , is not physiologically meaningful.

Another difference among these formulations is that at higher values of the grazing rate compared to the mortality rate ( $G_m/d$ ; i.e. phytoplankton biomass is grazing controlled) for any given zooplankton assimilation efficiency ( $\beta$ ), the steady-state ratio of phytoplankton biomass to the half-saturation constant of grazing ( $P/k_g$ ) is higher for  $\lambda_1$  and  $\lambda_3$  than for  $\lambda_2$ . *Franks et al.* [1986] compare the responses of  $\lambda_2$  and  $\lambda_3$  grazing formulations at a value of  $G_m/d$  of 7.5 and  $\beta$  of 0.7, which correspond to a steady-state values of  $P/k_g$  of about 0.3 and 0.45 respectively, and concluded that  $\lambda_3$  leads to more stable and robust models. Thus, at values of  $P/k_g < 0.5$  (i.e. low food concentration), where the grazing formulations  $\lambda_1$  and  $\lambda_3$  have similar behavior, we can infer that the grazing formulation  $\lambda_1$  is also more stable than  $\lambda_2$ . Because of that, in this model we have chosen  $\lambda_1$  (s-shaped formulation) rather than  $\lambda_2$  (Ivlev formulation) to represent zooplankton grazing. Since the zooplankton assimilation



efficiency is constant in this model, the use of  $\lambda_3$  grazing formulation would imply that the zooplankton growth rate is limitless which is not realistic. Thus, by replacing  $\lambda$  by  $\lambda_1$ , equation 4.12 can be written as,

$$P = \sqrt{\frac{1}{\frac{G_m \beta}{d} - 1}} \times k_g \quad (4.18)$$

Equation 4.18 (=equation 4.12) determines the phytoplankton abundance at steady-state which is given solely by the zooplankton parameters and is independent of the nitrate input. Phytoplankton biomass is directly proportional to the half-saturation constant of grazing ( $k_g$ ) and decreases nonlinearly with the increase in the maximum grazing rate ( $G_m$ ) and the zooplankton assimilation efficiency ( $\beta$ ), and with the decrease in the zooplankton specific mortality rate ( $d$ ).

Equation 4.13 determines the concentration of nitrate at steady-state which is given by the difference between the nitrate concentration below the mixed layer ( $N_z$ ) and the ratio of phytoplankton nitrate uptake ( $P\mu_m\gamma_N$ ) to water transport ( $F$ ). Note that the solutions for  $N < 0$  are invalid since a concentration can not be negative. As shown in Fig. 4.7 the nitrate concentration in the mixed layer relative to that below this layer decreases linearly with the increase in the ratio of phytoplankton growth to nitrate input. The nitrate concentration in the mixed layer decreases faster at higher values of the normalized nitrate uptake ( $\gamma_N$ ). For example, for typical values of these parameters in the eastern equatorial Pacific ( $P=0.3 \mu\text{M}$ ,  $\mu=0.7 \text{ d}^{-1}$ ,  $F(t)=1.7 \times 10^{-2}$  and  $N_z=10 \mu\text{M}$ ) a steady-state nitrate concentration in the mixed layer of  $5 \mu\text{M}$  as observed in this region is obtained when  $\gamma_N$  is 0.4. Considering that nitrogen is not limiting phytoplankton growth ( $\gamma_N + \gamma_A=1$ ) since it is abundant, then, a low  $f$ -ratio (0.4) is required to keep high residual nitrate in this region.

Combining equation 4.13 and 4.18 for  $P$ , we have,

$$\frac{N}{N_z} = 1 - \sqrt{\frac{1}{\frac{G_m \beta}{d} - 1}} \times \frac{k_g \mu_m \gamma_N}{F N_z} \quad (4.19)$$

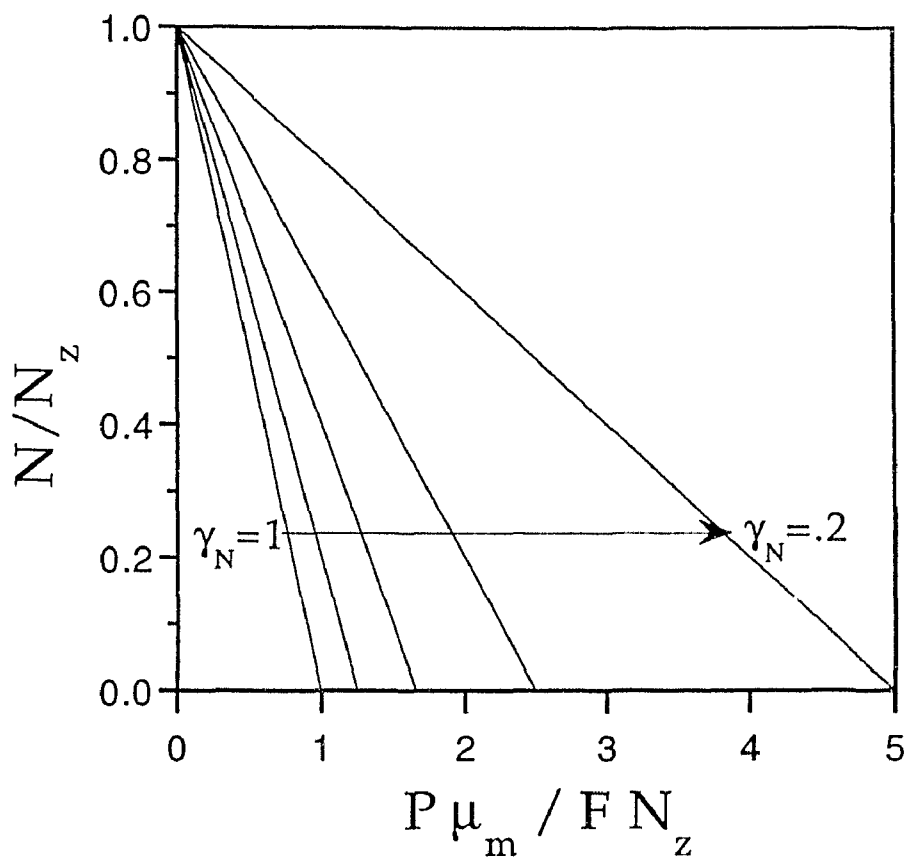
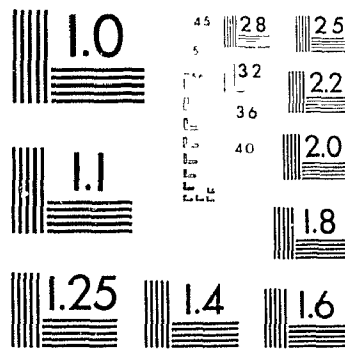


Figure 4.7: Non-dimensionalized representation of the isolines of normalized nitrate uptake ( $\gamma_N$ ) as a function of the ratio of nitrate concentration in the mixed layer ( $N$ ;  $\mu\text{M}$ ) to that below this layer ( $N_z$ ;  $\mu\text{M}$ ) and the ratio of phytoplankton growth rate ( $P\mu_m$ ;  $\mu\text{M d}^{-1}$ ) to nitrate input ( $F(t)N_z$ ;  $\mu\text{M d}^{-1}$ ).

# 2 OF 2

PM-1 3½"x4" PHOTOGRAPHIC MICROCOPY TARGET  
NBS 1010a ANSI/ISO #2 EQUIVALENT



PRECISION<sup>SM</sup> RESOLUTION TARGETS

As mentioned previously, the ratio of maximum grazing rate to zooplankton specific mortality rate must be higher than a minimum value to reach a steady-state (i.e.  $G_m\beta/d > 1$ ). Below this value (i.e. when the zooplankton are unable to support themselves against their death rate), the system does not arrive to steady-state but phytoplankton biomass increases until  $N$  is consumed. Above this minimum value, the normalized nitrate uptake  $\gamma_N$  increases with the increase in the ratio of the maximum grazing rate to zooplankton specific mortality rate ( $G_m/d$ ) and the nitrate input ( $FN_z$ ; see Fig. 4.8). When  $G_m/d$  is just above its minimum possible value to reach steady-state, a high input of nitrate (low  $k_g\mu_m/FN_z$ ) is necessary even when the nitrate uptake ( $\gamma_N$ ) is low. At high nitrate inputs ( $k_g\mu_m/FN_z \leq 1$ ) the biomass of phytoplankton cannot be controlled by grazing (that is,  $G_m/d$  must be low) if it is to consume all the available nitrogen, since  $\gamma_N$  must be  $\leq 1$ . As noted above, the steady-state solution of the model predicts that for a given nitrate input, the concentration of nitrate in the mixed layer is higher when the uptake of nitrate is lower. Therefore, at steady-state, lower  $f$ -ratios would be found at higher ambient nitrate concentration. This is the opposite of expectation based on empirical models [Harrison *et al.*, 1987; Platt and Harrison, 1985].

Equation 4.14 determines the utilization of ammonia. A significant property of the solution is that at steady-state the  $f$ -ratio ( $= 1 - \gamma_A/(\gamma_A + \gamma_N)$ ) is directly influenced by the production of ammonia (efficiency of recycling) and it is independent of the nitrate concentration. Most of the variations in the  $f$ -ratio are due to changes in the zooplankton excretion rate, the zooplankton assimilation efficiency and the regeneration efficiency of dead zooplankton (Fig. 4.9). The effect of changes in the regeneration efficiency of dead phytoplankton ( $a$ ) is small since in most of the ocean, the phytoplankton mortality is low ( $< 30\%$  of the growth rate). Note that high efficiencies of nitrogen regeneration ( $f$ -ratio  $< 0.1$ ) as those reported in the oligotrophic ocean are only obtained at very high rates of the regeneration efficiency parameters ( $b$  and  $c > 0.9$ ).

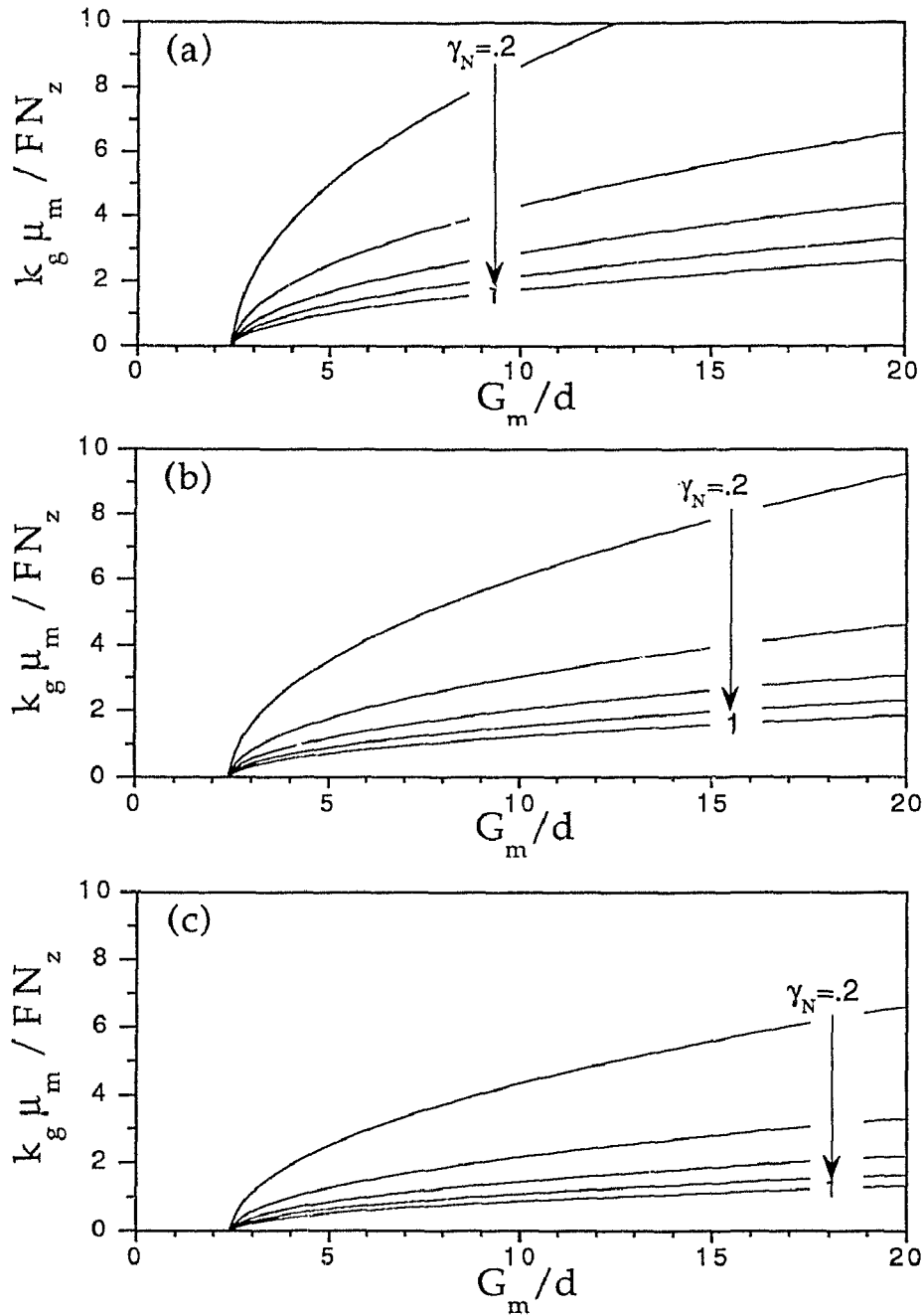


Figure 4.8: Contours of normalized nitrate uptake ( $\gamma_N$ ) at steady-state as a function of the dimensionless ratio of  $k_g \mu_m$  to nitrate transport ( $FN_z$ ) and the ratio of zooplankton maximum specific grazing rate ( $G_m$ ;  $d^{-1}$ ) to zooplankton specific mortality rate ( $d$ ;  $d^{-1}$ ) for a fixed value of  $\beta = 0.4$ , computed for different levels of residual nitrate: a) all nitrate is consumed;  $N/N_z=0$ , b) 70% of the nitrate input is consumed;  $N/N_z=0.3$ , and c) 50% is consumed;  $N/N_z=0.5$ .

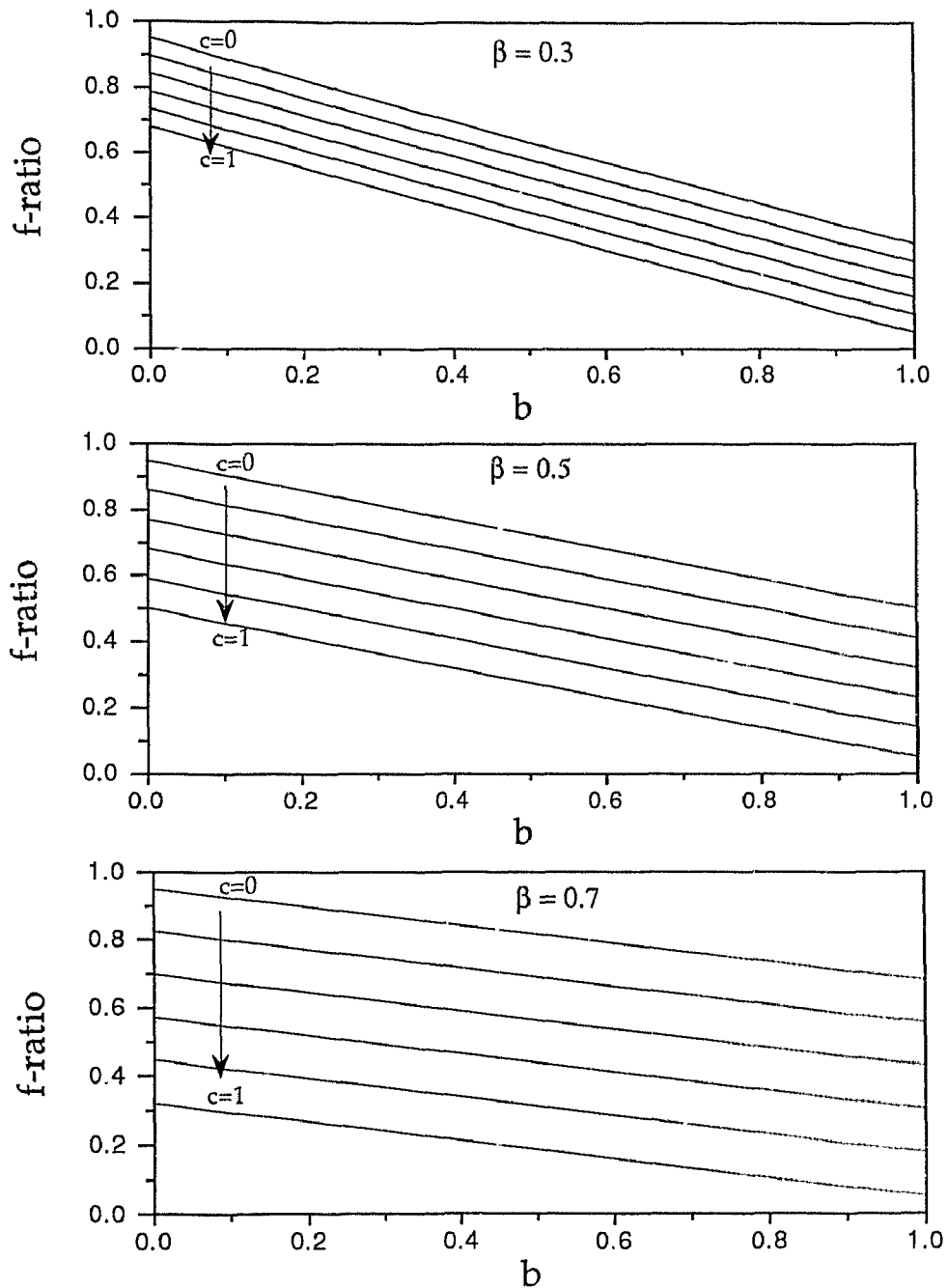


Figure 4.9:  $f$ -ratios at steady-state as a function of zooplankton excretion rate ( $b$ ), regeneration efficiency of dead zooplankton ( $c$ ) and zooplankton assimilation efficiency ( $\beta$ ) for a fixed value of the regeneration efficiency of dead phytoplankton  $a = 0.5$  and the ratio of phytoplankton specific mortality rate to phytoplankton specific growth rate  $m/\mu_m(\gamma_N + \gamma_A) = 0.1$  (dimensionless).

To summarize, at steady-state: 1) phytoplankton biomass is set only by the zooplankton parameters ( $\beta$ ,  $G_m$ ,  $k_g$  and  $d$ ), 2) the  $f$ -ratio is determined only by the regeneration efficiency parameters and is independent of nitrate concentration, 3) higher nitrate concentrations in the mixed layer are obtained at lower  $f$ -ratios, and 4) the value of the ratio of maximum grazing rate to zooplankton specific mortality rate alters the steady-state nitrate and phytoplankton concentration and determines if the system arrives to steady-state. It is useful to remember that steady-state solutions contain no information on causality, so it is not legitimate to conclude too much about food web interactions.

## 4.4 Variability in the input of nitrate

Model simulations with periodic variations in the nitrate supply from the lower layer were used to explore the effect of variability in the input of nitrate on phytoplankton biomass and new production. The supply of nitrate ( $F(t)N$ ) to the mixed layer was simulated as a small constant transport ( $F_0$ ) and a temporally variable flux represented as a cosine function,

$$F(t) = F_0 + \frac{w}{H}(1 + \cos(2\pi\omega t)) \quad (4.20)$$

where  $w$  is the vertical velocity,  $H$  is the depth of the mixed layer,  $\omega$  is a given frequency and  $t$  is time. The value of  $F_0$  used in the simulation is similar to the turbulent nitrate transport reported by *Lewis et al.* (1986) in the North Atlantic. Two different amplitudes of the nitrate input were obtained by changing the vertical velocity. The two values were  $1 \text{ m d}^{-1}$ , corresponding to the mean upwelling velocity of the equatorial Pacific upwelling region [*Brady and Bryden, 1987; Halpern et al., 1989*] and  $0.25 \text{ m d}^{-1}$ , which is more appropriate to generate the input of nitrate typical elsewhere in the open ocean. The input of nitrate was supplied as a series of pulses with periods of 2, 4, 7, 14, 30 or 90 days in an attempt to mimic nutrient

enrichments that may be associated with weather events. The set of differential equations comprising the model were solved numerically by the Runge-Kutta fourth-order method. Time steps of 3 hours were used to solve the equations to minimize errors in numerical integration; diurnal variations in processes were not represented in the model. The simulations were run until the same cycle was achieved.

The parameter values used in the simulations are within the range of measured values and are summarized in Tables 4.1, 4.2 and 4.3. Given the importance of the value of the zooplankton parameters ( $G_m$ ,  $k_g$  and  $d$ ) to the model output, and because there is very little experimental or observational basis for choosing specific values, we ran the model with different values of the grazing parameters (Tables 4.2 and 4.3). The values of the parameters were chosen such that, under the same amount of nitrogen input but at a constant rate, the steady-state zooplankton biomass ( $Z$ ) was lower, similar to, and higher than, the phytoplankton biomass ( $P$ ). Likewise, the biomass of phytoplankton was lower, close to, and higher than, the value of the half-saturation constant of grazing  $k_g$ . The value of the half-saturation constant of nitrate uptake was set higher ( $k_N=0.5 \mu\text{M}$ ) in simulations using a relatively high nitrate input ( $w=1 \text{ m d}^{-1}$ ) than in the low input case ( $k_N=0.1 \mu\text{M}$ ,  $w=0.25 \text{ m d}^{-1}$ ). The initial values of  $N$ ,  $A$ ,  $P$  and  $Z$  for each simulation were set at the steady-state values for the set of parameters used and are given in Tables 4.2 and 4.3. In the analysis of the simulation outputs, variations in the concentrations of  $N$ ,  $A$ ,  $P$  and  $Z$  lower than  $0.05 (\mu\text{mol-N/l})$  were considered not significant.

Examples of the time response of nitrate, phytoplankton and zooplankton concentrations at two different frequencies of nitrate input (periods of 4 and 14 days) are shown in Fig. 4.10 and Fig. 4.11 for simulations with a high and a low input of nitrate, respectively. With the higher input of nitrate ( $w=1 \text{ m d}^{-1}$ ), simulations of the model were only possible using  $P/k_g \leq 1$ , since a non steady-state solution was found otherwise. Simulations with  $P/k_g > 1$  produce large limit cycle oscillations of phytoplankton and zooplankton which have not been observed on field studies in the equatorial Pacific region. In all the simulations where the model variables responded



Table 4.2: Zooplankton parameters used in simulation with  $w=1$  (m d<sup>-1</sup>) and the steady-state values of the model variables.

Parameters	I	II	III	IV	V	VI
$Z/P$	<1	<1	~1	~1	>1	>1
$P/k_g$	<1	~1	<1	~1	<1	~1
$G_m$	9.00	3.50	5.00	1.90	2.25	0.90
$k_g$	0.60	0.30	0.60	0.29	0.60	0.30
$d$	0.70	0.70	0.35	0.35	0.15	0.15
$P$	0.30	0.31	0.29	0.28	0.29	0.28
$Z$	0.14	0.14	0.26	0.25	0.56	0.55
$N$	4.10	3.90	4.26	4.29	4.00	4.05
$A$	0.11	0.11	0.11	0.11	0.10	0.10
$\gamma_N$	0.40	0.41	0.41	0.43	0.41	0.43
$\gamma_A$	0.55	0.55	0.55	0.54	0.52	0.54

Table 4.3: Zooplankton parameters used in simulation with  $w=0.25$  ( $\text{m d}^{-1}$ ) and the steady-state values of the model variables.

Parameters	VII	VIII	IX	X	XI	XII	XIII	XIV	XV
$Z/P$	<1	<1	<1	$\sim 1$	$\sim 1$	$\sim 1$	>1	>1	>1
$P/k_g$	<1	$\sim 1$	>1	<1	$\sim 1$	>1	<1	$\sim 1$	>1
$G_m$	5.00	3.10	1.70	4.50	1.80	1.00	2.50	0.90	0.45
$k_g$	0.20	0.20	0.10	0.30	0.15	0.11	0.32	0.15	0.09
$d$	0.60	0.60	0.60	0.35	0.35	0.29	0.16	0.16	0.14
$P$	0.13	0.19	0.28	0.15	0.15	0.18	0.14	0.14	0.18
$Z$	0.07	0.07	0.06	0.12	0.12	0.15	0.26	0.26	0.29
$N$	0.50	0.08	0.04	0.23	0.24	0.09	0.28	0.35	0.08
$A$	0.07	0.01	0.01	0.03	0.03	0.01	0.04	0.05	0.01
$\gamma_N$	0.38	0.26	0.18	0.33	0.33	0.28	0.36	0.36	0.28
$\gamma_A$	0.56	0.42	0.25	0.53	0.53	0.44	0.50	0.50	0.39

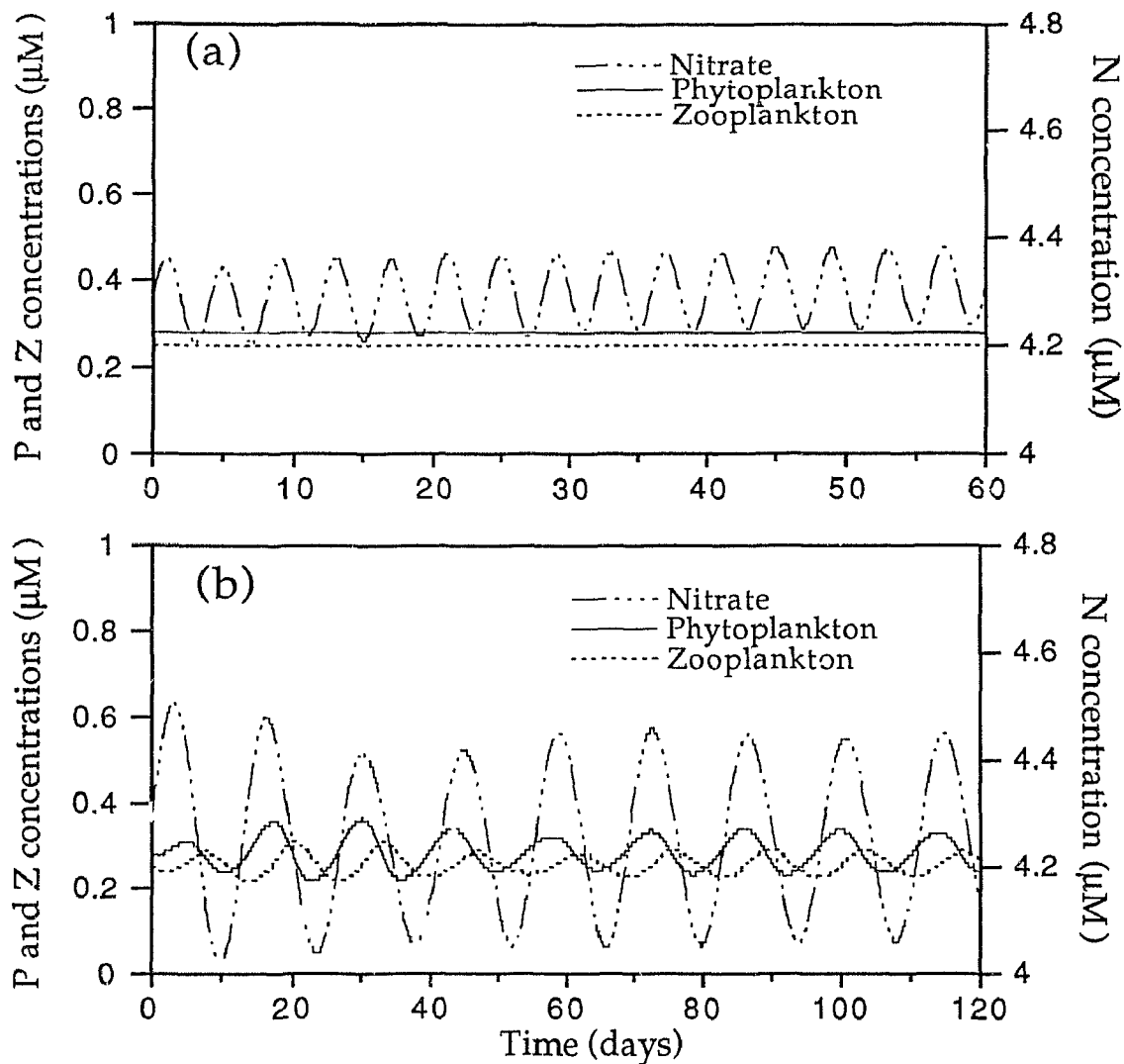


Figure 4.10: Model output of nitrate, phytoplankton and zooplankton concentrations for a simulation with a high amplitude ( $w = 1 \text{ m d}^{-1}$ ) of nitrate inputs of: a) 4 days periods, and b) 14 days. Parameters values correspond to simulation IV ( $Z/P \sim 1$  and  $P/k_g \sim 1$ ) and are shown in Table 4.2.

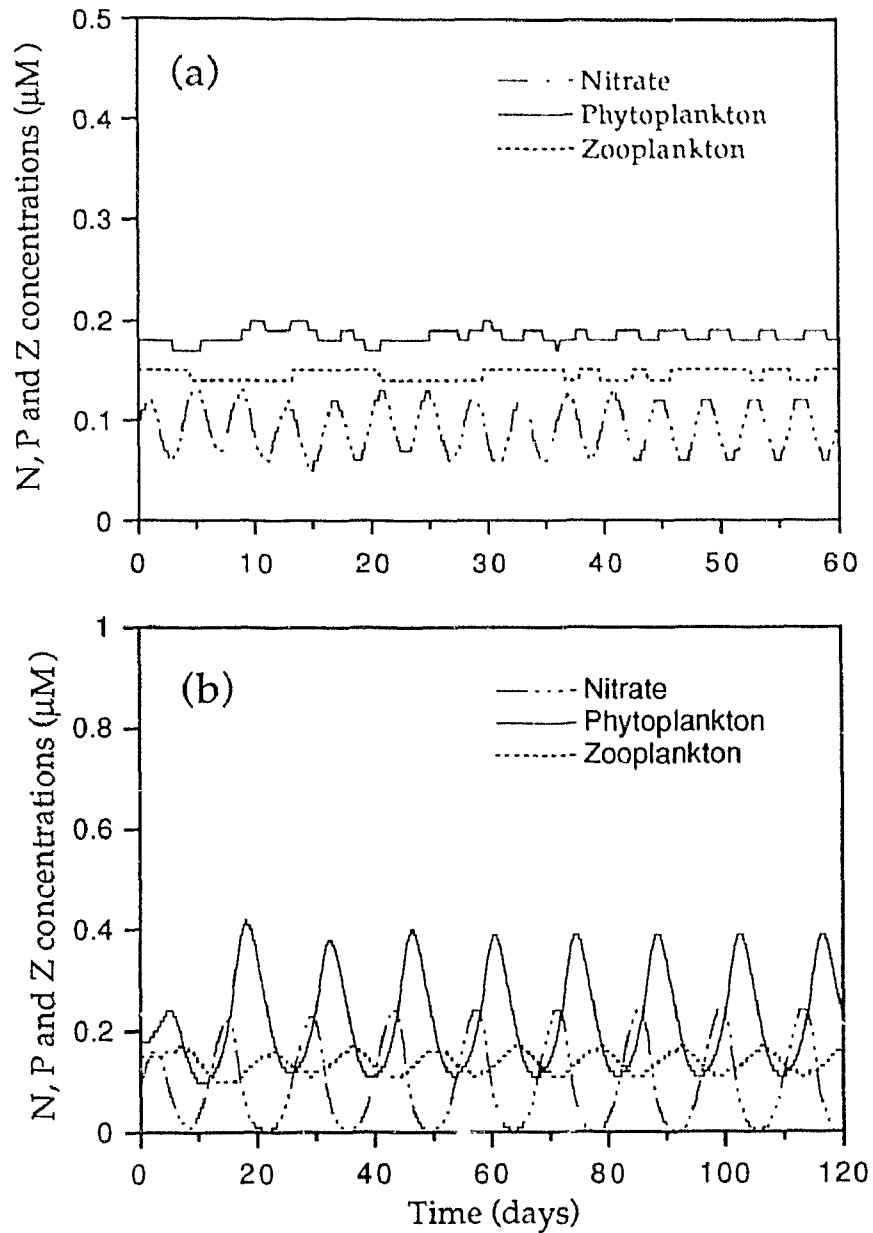


Figure 4.11: Model output of nitrate, phytoplankton and zooplankton concentrations for a simulation with a low amplitude ( $w = 0.25 \text{ m d}^{-1}$ ) of nitrate inputs of: a) 4 days periods, and b) 14 days. Parameters values correspond to simulation XII ( $Z/P \approx 1$  and  $P/k_g > 1$ ) and are shown in Table 4.3.

to fluctuations in the input of nitrate, the frequency of response was the same as that of the nitrate input. Results from these simulations show that only the concentration of nitrate in the mixed layer changes significantly with variations in the nitrate input at all frequencies (Fig. 4.12). The range of nitrogen concentration increases at lower frequencies and was independent of variations in the zooplankton parameters. In all simulations (I to VI) there was a similar time delay between the maximum input of nitrate and the maximum concentration of nitrate in the mixed layer that was longer at lowest frequencies (Fig. 4.13).

In comparison, phytoplankton and zooplankton biomasses did not show responses to variations in the input of nitrate at periods shorter than 7 and 14 days respectively. Also, at these frequencies, phytoplankton biomass only responded in simulations (II, IV and VI) where the value of  $P/k_g$  was close to 1 (i.e. grazing control was weak) and its increase was small ( $<0.2 \mu\text{mol-N/l}$ ). In comparison, zooplankton biomass responded mainly in simulations where the ratio of zooplankton to phytoplankton biomass was higher than 1 (simulations V and VI). The time delay between the maximum input of nitrate and the maximum increase in zooplankton biomass was shorter in the simulation where phytoplankton biomass was similar to the half-saturation constant of grazing (simulation VI). New production responded to the same frequencies as phytoplankton biomass. Also, the variations in the biomass of phytoplankton and that of new production were highly correlated (Table 4.4a). The small effect of variations in the input of nitrate on phytoplankton biomass and new production in these simulations (I to VI) is not surprising considering that the phytoplankton is growing at rates close to its maximum ( $\sim 95\%$ , see  $\gamma_1 + \gamma_2$  in Table 4.2).

In model simulations with the lower input of nitrate ( $w=0.25 \text{ m d}^{-1}$ ), the response of phytoplankton to variations in the input of nitrate increases with the increase in the ratio of phytoplankton biomass to the half-saturation of grazing ( $P/k_g$ ) and the decrease in the zooplankton to phytoplankton biomass ratio (Fig. 4.14). At low values of  $P/k_g$  ( $<1$ , i.e. when phytoplankton is grazing controlled), of the frequencies

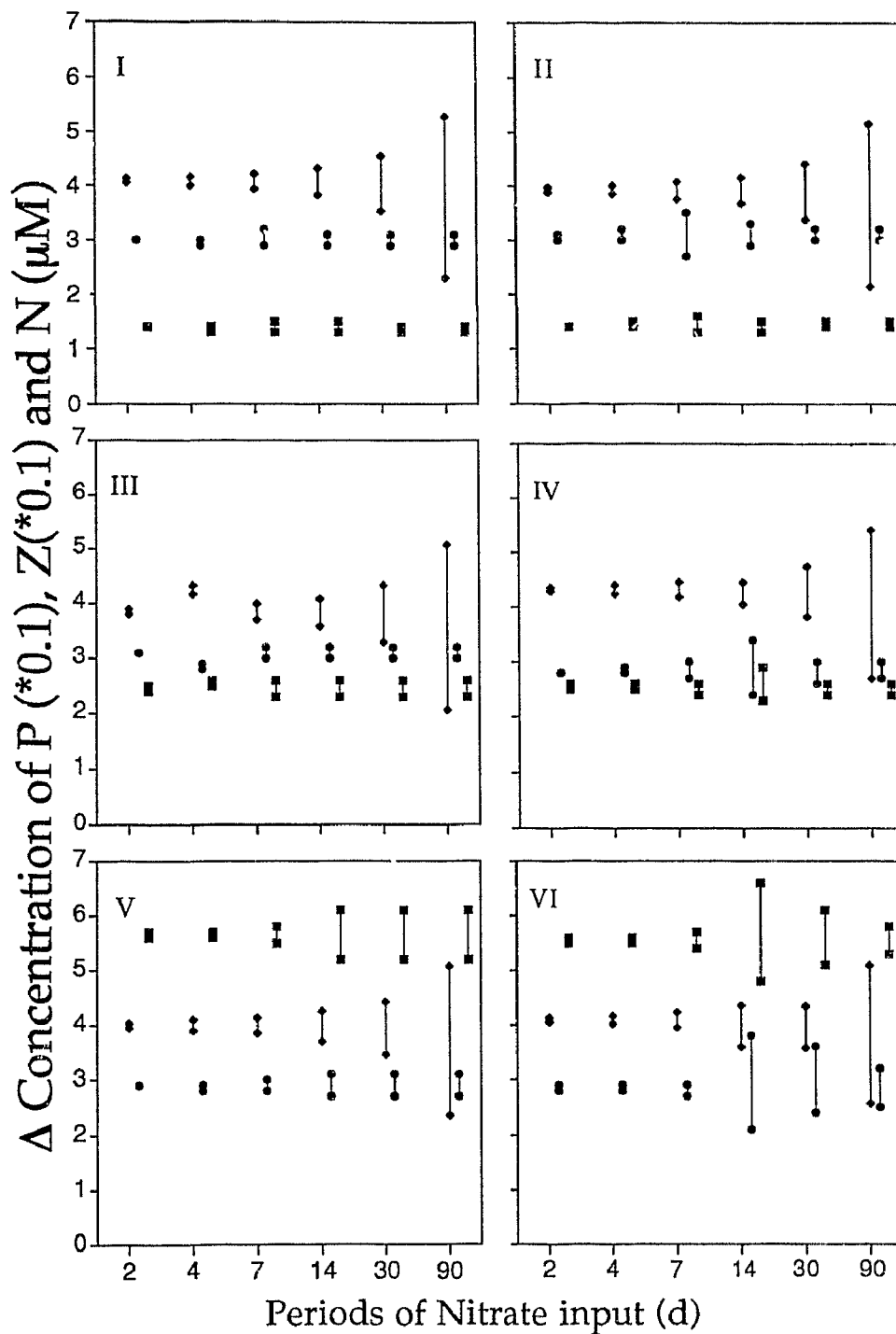


Figure 4.12: Amplitude of variations in the concentration of phytoplankton (circles;  $10^{-1} \mu\text{M}$ ), zooplankton (squares;  $10^{-1} \mu\text{M}$ ), and nitrate (diamonds;  $\mu\text{M}$ ) at different frequencies of the nitrate fluctuations for simulations with high input of nitrate ( $w = 1 \text{ m d}^{-1}$ ). Parameter values used in each simulation are given in Table 4.2.

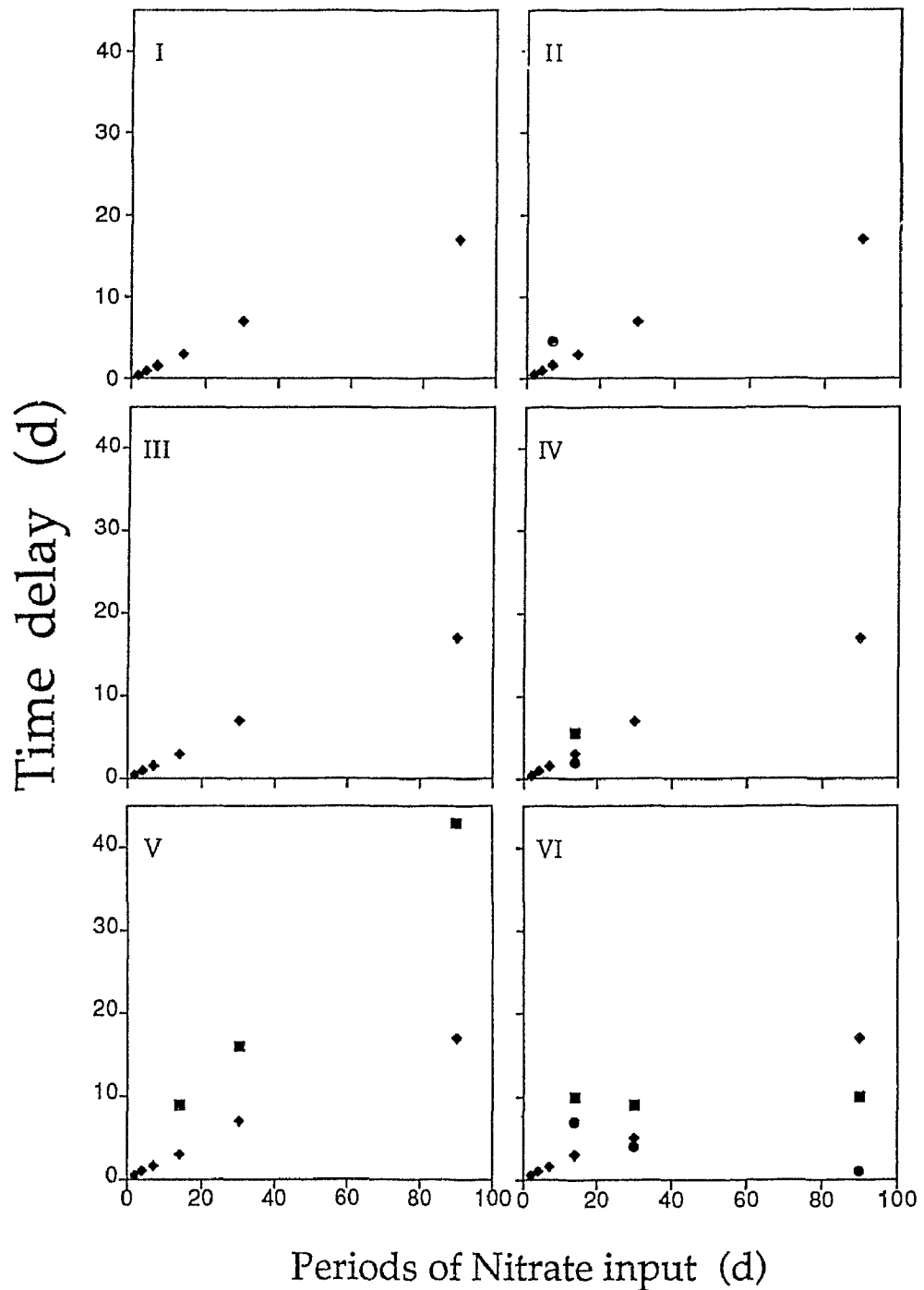


Figure 4.13: Time delay between the maximum input of nitrate to the mixed layer and maximum concentration of phytoplankton (circles), zooplankton (squares) and nitrate (diamonds) in simulations where a significant variation in concentrations was obtained. Results are presented for different frequencies of the nitrate fluctuations for simulations with a high input of nitrate ( $w = 1 \text{ m d}^{-1}$ ). Parameters values as in Fig 4.10.

Table 4.4: Matrix of correlation between the variation of ammonia ( $A$ ), nitrate ( $N$ ), phytoplankton ( $P$ ), zooplankton ( $Z$ ), new production ( $P\gamma_N$ ) and regenerated production ( $P\gamma_A$ ) for different nitrate input, all simulations combined

	$\Delta A$	$\Delta N$	$\Delta P$	$\Delta Z$	$\Delta P\gamma_N$
a) high nitrate input					
$\Delta A$	1.00				
$\Delta N$	0.75	1.00			
$\Delta P$	0.31	0.05	1.00		
$\Delta Z$	0.22	0.05	0.72	1.00	
$\Delta P\gamma_N$	0.54	0.16	0.84	0.69	1.00
$\Delta P\gamma_R$	0.26	0.08	0.62	0.55	0.53
b) low nitrate input					
$\Delta A$	1.00				
$\Delta N$	0.78	1.00			
$\Delta P$	0.12	0.00	1.00		
$\Delta Z$	0.43	0.15	0.62	1.00	
$\Delta P\gamma_N$	0.15	0.03	0.61	0.55	1.00
$\Delta P\gamma_R$	0.36	0.09	0.67	0.69	0.58



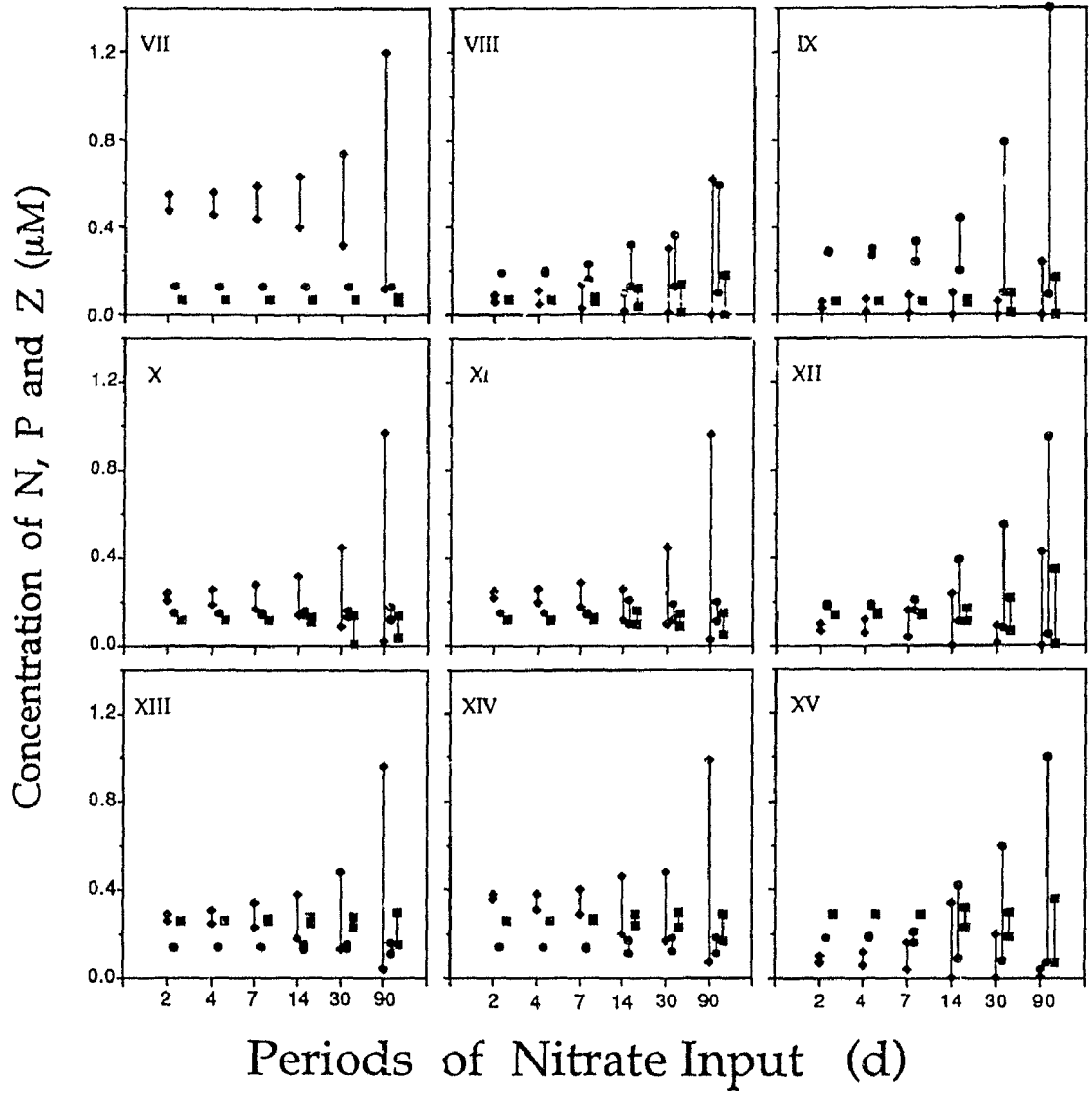


Figure 4.14: Amplitude of variations in the concentration of phytoplankton (circles), zooplankton (squares) and, nitrate (diamonds) at different frequencies of the nitrate fluctuations for simulations with low input of nitrate ( $w= 0.25 \text{ m d}^{-1}$ ). See Table 4.3 for values of the parameters used in each simulation.

used, phytoplankton respond only at the lowest frequency (90 days). Thus, an increase in the input of nitrate causes a rise in the phytoplankton standing-stock only when it can not be grazed sufficiently rapidly by zooplankton. Similarly, the rate of new production only changes with variations in the input of nitrate when the values of  $P/k_g$  are close to or higher than 1 and, thus, variations in phytoplankton biomass are significant correlated to variations in the new production rate (Table 4.4b). In contrast, variations in the concentration of nitrate in the mixed layer are not correlated to variations in phytoplankton biomass or new production. The response of zooplankton biomass is not marked in any of the simulations. The concentrations of nitrate in the mixed layer respond to higher frequencies of nitrate input (periods  $\geq 4$  days) than phytoplankton biomass (periods  $\geq 7$  days) and zooplankton biomass (periods  $\geq 14$  days). As periods of nutrient disturbance become shorter than 7 days, the variations of phytoplankton and zooplankton do not follow the fluctuations of nutrients in any of the simulations.

To summarize, the results from model simulations with periodic variations in the input of nitrate indicate that: 1) phytoplankton biomass and new production do not respond to variations in the nitrate input when phytoplankton is growing at its maximum capacity, or when it is limited by grazing, even when the input of nitrate to the euphotic zone is high, 2) nitrate fluctuations at periods of less than or equal to 4 days do not influence phytoplankton biomass and new production. This lack of response at high frequencies is likely due to the similar phytoplankton and zooplankton growth rates used in the model runs, 3) the response of phytoplankton to variations in the input of nitrate is greater when phytoplankton biomass is higher than the half-saturation constant of grazing and when the ratio of zooplankton to phytoplankton biomass is low (i.e. grazing control is low), and 4) variations in the phytoplankton biomass are correlated with variations in the rate of new production.

## 4.5 Discussion

In this study, a plankton model with four compartments has been used to explore the effect of periodic variations in the input of nitrate on phytoplankton biomass and new production. The model has been kept as simple as possible in order to understand its fundamental interactions and to evaluate its dependencies on critical parameters. However, the response of the model is ultimately limited by the uncertainties in the model's structure and parameter values. Even simple biological models, like the one used here, contain a large number of parameters which are difficult to measure, and only represent the typical value of the mixed populations of phytoplankton and zooplankton present. Therefore, rather than focusing on modeling a particular region, we have tried to simulate a wide range of oceanic conditions. By modifying the model's structure and analyzing the steady-state solutions over a wide range of parameter values, we have tried to determine the sensitivity of the model to individual processes. In the following, we discuss specific points of interest that result from these analyses.

### 4.5.1 The role of predation on surface nitrate concentration

In most planktonic models, the predation term is parameterized to avoid developing an equation for the next higher trophic level. This is either done through density-dependent or constant mortality of the prey. *Steele* and others [*Steele*, 1976; *Steele and Henderson*, 1981] have found that the functional form of the zooplankton mortality and the values given to this parameter have a marked effect on the stability of the model. *Steele and Henderson* [1992] have shown that models with a constant mortality rate, as the one used in this study, can produce limit cycle oscillations of zooplankton and phytoplankton when the nitrate flux to the mixed layer is very high. Thus, they conclude that in systems with constant zooplankton mortality, nutrient limitation may be necessary to prevent limit-cycle behavior. In comparison, in models with zooplankton density-dependent mortality rates, large values of the steady-state nutrient concentration relative to the half-saturation concentration of nutrient uptake

can be obtained with an appropriate choice of coefficients [Frost, 1987; Hofmann and Ambler, 1988]. In this study, we have been able to obtain a steady-state solution at a high input of nitrate even though a constant zooplankton mortality was used. To do this, phytoplankton must be grazing controlled and must be using mostly regenerated forms of nitrogen. This is in agreement with field observations in oceanic regions having high concentrations of surface nitrate such as the eastern equatorial Pacific and the northeast Pacific where  $f$ -ratios lower than 0.4 have been found [Murray *et al.*, 1989; Dugdale *et al.*, 1992]. Thus, the different ratios of nitrate concentration to the half-saturation constant of nitrate uptake found in those previous models seem to be the result of the formulation and parameters used in modeling the nitrogen uptake, rather than due to the use of a constant predation rate. In most studies, the significance of the nitrogen uptake formulation in determining the model output is not investigated. Results from this study stress the need to improve the formulation of nitrate uptake in a way that realistically reflects the natural environment particularly when new production is the variable of interest.

Model simulations with a high input of nitrate, similar to that found in the eastern equatorial Pacific region, indicate that grazing control of phytoplankton biomass is necessary to achieve a steady-state. If grazing control is less important ( $P/k_g > 1$ ; i.e. zooplankton grazing approach saturation level as shown Fig. 4.4) large fluctuations in phytoplankton and zooplankton biomasses were obtained. In the equatorial Pacific region, Walsh [1976] suggested that herbivory by grazers was the process responsible for the high nutrient and low chlorophyll concentration found in this region. He suggested that this grazing control results because, in contrast to continental shelf regions, there is a lack of physical variability on time scales of days to weeks. This facilitates a close coupling between the growth of phytoplankton cells and zooplankton grazing. It has recently been recognized, however, that the protozoan consumers of small phytoplankton are capable of extremely fast specific growth rates, exceeding those of their prey. This allows rapid development of tight coupling between herbivores and small phytoplankton [Banse, 1982; Goldman *et al.*, 1985]. In the equatorial

Pacific region where phytoplankton biomass is dominated by small cells [*Chavez*, 1989; *Peña et al.*, 1990] a lack of physical variability is not necessary for grazing control of small cells. Thus, the physical disruption hypothesis will only apply to larger phytoplankton and to the slowly responding metazoan herbivores. Alternatively, iron could be limiting phytoplankton growth and nitrate utilization in this region [e.g. *Martin et al.*, 1991]. Results from this model suggest that even if there were variability in the input of nitrogen, phytoplankton biomass would not significantly increase without a release from grazing control. Only the concentration of nitrate in the mixed layer would show variations. This is supported by the field observation of *Carr* [1991] where a significant change in nutrient concentration over a 6 day study was observed at the equator at 150° W. However, during this period, vertical profiles of important biological properties (i.e. in situ fluorescence and beam attenuation) showed very little day-to-day variability.

Examining the Peruvian upwelling region, *Minas et al.* [1986] suggested that the existence of grazing pressure at the beginning of the phytoplankton bloom (i.e. in the upwelled source water) appears to be of major importance in determining the utilization of nitrate. In the same region, *Dortch and Packard* [1989] found that the chlorophyll to protein ratio of particulate matter, a relative index of phytoplankton to total biomass, was low and similar to the value found in oligotrophic waters. This led them to suggest that most of the biomass in this region consists of bacteria and zooplankton, but at much higher levels of phytoplankton biomass than in oligotrophic regions. This is in agreement with model results that show lower response when zooplankton to phytoplankton biomass is high. Thus, in different regions of the ocean, even though the biomass of phytoplankton may be different, the proportion of zooplankton to phytoplankton may be similar and therefore the response to variations in the input of nitrate is independent of the biomass of phytoplankton.

#### 4.5.2 Control of phytoplankton biomass in oligotrophic ocean

There is often considerable uncertainty as to whether nutrients limit the specific rate of phytoplankton growth or its biomass. *Goldman et al.* [1979] showed that phytoplankton cells growing in cultures had constant elemental ratios approximating the Redfield ratio only when growing at rates close to their maximum. Since several studies have found that in the ocean, the C/N ratio of particulate matter is usually in the Redfield ratio, it has been suggested [*Goldman et al.*, 1979] that phytoplankton cells are growing at maximum rates. They have also suggested that the specific growth rate of phytoplankton is independent of the concentration of ambient nutrient, and only the abundance of phytoplankton would be a function of nutrient supply. In this study, the steady-state solution of the model indicates that zooplankton parameters are of critical importance in determining phytoplankton biomass and nitrate concentration. Whether the phytoplankton biomass is grazing controlled or nitrogen limited depends on the grazing parameters. When phytoplankton is controlled by grazing, its biomass can be kept low; high specific growth rates can be achieved even at low nitrate concentrations. Thus, if phytoplankton growth is tightly coupled to zooplankton grazing and nutrient regeneration, high growth rates of phytoplankton need not be exclusively found in environments of high new nitrogen availability. However, if phytoplankton cells are growing at a rate close to maximum as suggested by *Goldman et al.* [1979], the possibility of them taking advantage of enhanced pulses of nitrogen is marginal.

In offshore oligotrophic areas, where the nutrient depleted zone is isolated from deeper waters rich in nutrients by a seasonal or permanent thermocline, the nutrient input in the upper layer occur on scales that range from a small, more or less continuous flux through the nutricline to larger episodic fluxes associated with destabilization of the mixed layer, as upwelling or deepening of the mixed layer [*Klein and Coste*, 1984; *Jenkins*, 1988]. For example, in the Sargasso Sea, physical variability at time scales of 2-4 days has been found [*Glover et al.*, 1988; *Dickey et al.*, 1990]. Results

from simulations of periodic variation in nitrate inputs show different responses if the system is nitrogen limited or grazing limited. Our model suggests that the response of phytoplankton to variations in the input of nitrate is low if phytoplankton are under grazing control or if they are nitrogen saturated. In this case, only the concentration of nitrate increases. In contrast, if phytoplankton cells are nutrient limited they can respond to an input of nitrate by increasing their biomass. In the Sargasso Sea during winter conditions, for example, when disturbances in the mixed layer occur more often, elevated values of nutrients ( $>0.6 \mu\text{M}$ ; *Dickey et al.*, 1992) have been found. Also, *Eppley and Renger* [1986] have reported nanomolar increases in surface layer nitrate concentration following a small wind event in stratified California waters. Thus, these increases in nitrate concentration, without corresponding increases in phytoplankton biomass, suggest grazing control in these regions.

The response to variations in the input of nitrate by the planktonic community will likely vary depending upon whether the herbivore stock consists predominantly of macrozooplankton or microzooplankton. *Strom and Welschmeyer* [1991] found that zooplankton grazing rates were most closely matched with growth rates for small ( $<10 \mu\text{m}$ ) phytoplankton species. In the Sargasso Sea, elevated nanomolar increases in surface nitrate concentration were accompanied by high rates of primary production and were followed 48 hours later by a 50% net increase in *Synechococcus* cell numbers [*Glover et al.*, 1988]. However, the increase in *Synechococcus* numbers was only about 27% of what could be supported by the nitrate increase. They suggested that this resulted from close coupling between production and grazing during the transient bloom based on their observation that the number of heterotrophic flagellates doubled. In southern Kattegat (Denmark), *Nielsen and Kiorboe* [1991] found that primary production increased and the size distribution of the phytoplankton changed toward larger cells subsequent to a storm. A change in the size distribution of phytoplankton after an input of nitrate could occur if the dominant small phytoplankton were growing at, or near maximum growth rates and subsequently large phytoplankton cells, that were nitrogen limited, increased.

### 4.5.3 Role of variations in the nitrate input on new production

The importance of episodic injections of nutrients [Cullen *et al.*, 1984; Eppley and Renger, 1988; Jenkins, 1988; Marra *et al.*, 1990] in fueling new production has become apparent only recently. Along the outer U.S. southern shelf, Hoffman and Ambler [1988] found that episodic upwelling resulting from frontal eddies and bottom intrusions at a frequency of four to six weeks brings nutrients to the upper layer and produces productive but short-lived phytoplankton blooms [Yoder *et al.*, 1983; Yoder *et al.*, 1985]. During these events, Yoder *et al.* [1983] estimated that approximately 75% of the production was new production. Results from our model indicate that variations in new production rates were associated with variations in phytoplankton biomass. Thus, the control of phytoplankton biomass by zooplankton grazing may play an important role in setting the upper limit of the photosynthetic nitrate uptake rate. In contrast, it has been suggested [e.g. Martin *et al.*, 1989; Barber and Chavez, 1991] that iron could be controlling phytoplankton biomass and new production. The concept that new production may be primarily correlated with algal standing stock may be of general importance on a global scale. For example, since small phytoplankton cells are more likely to be grazing controlled than large ones, the growth rate of large phytoplankton could be very important to new production [Goldman, 1988; Michaels and Silver, 1988; Legendre and Le Fevre, 1989], and factors that keep large phytoplankton in check may be the principal control of nutrient utilization. In the Sargasso Sea, it has been estimated [Goldman, 1993] that to attain the level of annual new production of  $5 \text{ mol O}_2 \text{ m}^{-2} \text{ y}^{-1}$  [Jenkins and Goldman, 1985] one 18-day bloom per year or five 10-day blooms per year are required.

### 4.5.4 Control of $f$ -ratio

Results from our model show that  $f$ -ratios are determined by the recycling efficiency of the individual components of the system. The recycling efficiency is a function of



the excretion-to-ingestion ratios of organisms at each trophic level as well as the complexity of the food web. Thus, the  $f$ -ratio depends on the structure and dynamics of the local food web. In oligotrophic waters, it has been found [Eppley *et al.*, 1973] that ammonia may supply more than 90% of the nitrogen necessary for primary production. The regeneration efficiency of the system is mostly determined by the excretion rates of zooplankton and the efficiency at which the dead zooplankton is remineralized. High regeneration efficiencies are only obtained when these values are very high. Similarly, King [1987] reported that the values of the ratio of excretion to ingestion necessary to achieve a recycling efficiency of 0.9 are greater than the average reported physiological ratios reported in the literature. Some studies [Gaudy, 1974; Valiela, 1984] have found that the zooplankton assimilation efficiency tends to decrease with ingestion rate, suggesting that in oligotrophic regions the recycling efficiency is low. In contrast, Dagg and Walsen [1987] noted that in low food concentrations, the fecal pellets produced are smaller, less dense and more fragile than those produced at higher food concentrations. Thus, they could be more easily recycled to ammonia. In the transfer of phytoplankton nitrogen to higher trophic levels, nitrogen can be lost by the sinking of fecal pellets and detritus from the euphotic zone and by being changed to forms not used by phytoplankton (e.g. some form of dissolved organic nitrogen). Many zooplankton migrate vertically, remaining below the thermocline during the day and any nitrogen excreted or defecated during this time will be lost from the euphotic zone [Longhurst and Harrison, 1988]. An additional loss of nitrogen not available for phytoplankton consumption which has been neglected in the model is the uptake of ammonia by bacteria. Heterotrophic utilization of ammonia could lead to an overestimate of phytoplankton ammonia uptake. Up to now, little has been done to determine the potential significance of nitrate fluctuations for phytoplankton growth, and biomass accumulation, and it is not clear over which scales these fluctuations are most important. In this study, we have tried to address these questions through model simulations with different frequencies of variability in the input of

nitrate. Results indicate that if phytoplankton growth is tightly coupled to zooplankton grazing and nutrient regeneration, high growth rates of phytoplankton need not be found exclusively in environments of high new nitrogen availability. However, if phytoplankton is growing at its maximum capacity, phytoplankton biomass and new production will not be enhanced by a pulse of nitrate into the surface layer. It was also found that the response of phytoplankton and new production to variations in the input of nitrate are strongly affected by the grazing parameters and by the ratio of zooplankton to phytoplankton biomass. It is also dependent on the frequency of nutrient fluctuations being higher the response at low frequencies. Therefore, the availability of nitrate seems to be less directly important to phytoplankton growth and biomass than previously suggested.

# Chapter 5

## Conclusions

This thesis has focused on the rates of new production in the tropical Pacific region and on the factors that influence this rate. Determination of new production rates on a transect across the equatorial Pacific permitted the comparison of these rates over a region of varying nitrate availability. The observed vertical and horizontal distributions of new production were then discussed in terms of current hypotheses to account for persistence of nitrate in this region. An analysis of the nitrate balance in the warm waters of the tropical Pacific, where upwelling of nitrate is considerably less important than in the cooler, east waters, reveals that a significant fraction of the new production is due to the horizontal advection of nitrate from the eastern equatorial Pacific. Therefore, although most of the nitrate upwelled in the eastern equatorial Pacific is not utilized locally, it is used by phytoplankton cells away from this region. In addition to examining spatial variations of nitrate input, the influence of temporal fluctuations in the nitrate input on phytoplankton biomass and new production was investigated. The analysis reveals that temporal fluctuations in the input of nitrate cause an increase in phytoplankton biomass and new production only when phytoplankton is not growing at its maximum capacity or when phytoplankton is not strongly grazing controlled.

The results from Chapter 2 indicate that:

- Latitudinally, higher rates of new production were observed near the equator

coinciding with higher concentrations of chlorophyll *a* and nitrate.

- Despite significant variation in nitrate concentration, variability of phytoplankton biomass and production was low along the transect.
- Most of the production in the nutrient rich equatorial region was fueled by nitrogen regenerated in the euphotic zone rather than nitrate.

The low utilization of available nitrate in the equatorial region was likely the consequence of grazing. A high grazing pressure in the equatorial Pacific region would reduce the absolute nitrogen consumption by reducing phytoplankton biomass, and also would increase the availability of regenerated nitrogen (i.e. ammonia). Since ammonia is generally the preferred form of N used by phytoplankton, its availability may be an important regulator of new production in this nitrate-rich environment.

In Chapter 3, a nitrate budget over the warm waters of the tropical Pacific is presented. The main conclusion are:

- The average depth-integrated rate of new production resulting from vertical turbulent fluxes of nitrate was found to be similar in magnitude to that due to advective transport.
- Most (about 75%) of the advective transport of nitrate was due to horizontal transport (zonal and meridional) of nutrient-rich water from the eastern equatorial Pacific rather than from equatorial upwelling.

The determination of new production resulting from the vertical turbulent transport of nitrate was based on fluxes of heat at the sea-surface and the nitrate-temperature relationship at subsurface depths. This approach can be applied to other regions of the world's ocean. The possibility therefore exists to estimate new production from remotely-sensed observations, not requiring the determination of physiological parameters of nitrate uptake from ship observations that are notoriously variable.

In Chapter 4, a simple biological model of the mixed layer was used to study the effects of fluctuations in the input of nitrate on phytoplankton biomass and new production. The most significant results from this model suggest that:

- The steady-state  $f$ -ratio is determined only by the regeneration efficiency of the planktonic system and is independent of nitrate concentration.
- Phytoplankton biomass does not respond to variations in the nitrate input if it is growing at its maximum capacity or if it is grazing-limited, even when the nitrate input to the euphotic zone is high.
- Phytoplankton biomass at steady-state is set only by the zooplankton parameters (i.e. zooplankton assimilation efficiency, specific mortality rate, maximum grazing rate and the half-saturation constant of grazing).
- The value of the maximum zooplankton grazing rate relative to the zooplankton mortality rate was critical to achieve a steady-state solution.
- From the frequency response, it was found that periods less than or equal to 4 days did not influence phytoplankton biomass and new production. On longer time scales, the magnitude of the increase depends on the frequency and magnitude of the fluctuations, as well as on the zooplankton parameters used.

The general results of this thesis indicate that zooplankton grazing may play a crucial role in determining the magnitude of new production. Additional work is needed to elucidate the effect of iron availability on nitrate utilization and on the size structure of phytoplankton populations. However, even though iron could increase the specific growth rate of phytoplankton and change the size composition of phytoplankton towards larger cells, an increase in nitrate consumption may only be possible if phytoplankton are released from grazing control. This seems unlikely in the equatorial Pacific where the quasi-stationary nature of the equatorial divergence seems to permit a close coupling between phytoplankton and zooplankton populations. Thus, although nitrate is necessary for new production, in the equatorial Pacific grazing, rather than nitrate input, seems to be the dominant regulator of new production.

# Bibliography

- BACASTOW, R. AND MAIER-REIMER, E. (1990). Ocean-circulation model of the carbon cycle, *Climate Dynamics*, 4: 95-125.
- BANSE, K. (1982). Cell volumes, maximal growth rates of unicellular algae and ciliates, and the role of ciliates in the marine pelagial, *Limnol. Oceanogr.*, 27: 1059-1071.
- BANSE, K. (1991). Rates of phytoplankton cell division in the field and iron enrichment experiments, *Limnol. Oceanogr.*, 36: 1879-1885.
- BARBER, R.T. AND CHAVEZ, F.P. (1991). Regulation of primary productivity rate in the equatorial Pacific, *Limnol. Oceanogr.*, 36: 1,803-1,815.
- BARBER, R.T. (1992). Geological and climatic time scales of nutrient variability. In: Falkowski, P.G. and A.D. Woodhead (eds), *Primary Productivity and Biogeochemical Cycles in the Sea*, Plenum Press, New York, p 89-106.
- BETZER, P. R., SHOWERS, W.J., LAWS, E.A., WINN, C.D., DITULLIO, G.R., AND KROOPNOCK, P.M. (1984). Primary productivity and particle fluxes on a transect of the equator at 153° W in the Pacific Ocean, *Deep Sea Res.*, 31: 1-11.
- BIENFANG, P.K. AND HARRISON, P.J. (1984). Sinking-rate response of natural assemblage of temperate and subtropical phytoplankton to nutrient depletion, *Mar. Biol.*, 83: 293-300.
- BRADY, E.C. AND BRYDEN, H.L. (1987). Estimating vertical velocity at the equator. In: *Oceanol. Acta, Proceedings International Symposium on Equatorial Vertical Motion, Paris, 6-10 May, 1985*, pages 33-37.

- BRZEZINSKI, M.A. (1988). Vertical distribution of ammonium in stratified oligotrophic waters, *Limnol. Oceanogr.*, 33: 1176-1182.
- BRYDEN, H.L. AND BRADY, E.C. (1985). Diagnostic model of the three-dimensional circulation in the upper equatorial Pacific ocean, *J. Phys. Oceanogr.*, 15: 1,255-1,273.
- BRYDEN, H. L. AND BRADY, E.C. (1989). Eddy momentum and heat fluxes and their effects on the circulation of the equatorial Pacific, *J. Mar. Res.*, 47: 55-79.
- BUMA, A.G.J., DE BAAR, H.J.W., NOLTING, R.F., AND VAN BENNEKON, A.J. (1991). Metal enrichment experiments in the Weddell-Scotia Seas: effects of Fe and Mn on various plankton communities, *Limnol. Oceanogr.*, 36: 1865- 1878.
- CAMPBELL, J. W. AND AARUP, T. (1992). New production in the North Atlantic derived from seasonal patterns of surface chlorophyll, *Deep Sea Res.*, 39: 1,669-1,694.
- CAPONE, D.G. AND CARPENTER, E.J. (1982). Nitrogen fixation in the marine environment, *Science*, 217: 1,140-1,142.
- CARPENTER, E.J. AND ROMANS, K. (1991). Major Role of the Cyanobacterium *Trichodesmium* in Nutrient Cycling in the North Atlantic Ocean, *Science*, 254: 1,356-1,358.
- CARR, M.E. (1991). Interactions between physical and biological processes in the equatorial Pacific, Ph.D. thesis, Dalhousie University.
- CARR, M.E., N.S. OAKEY, B. JONES, AND M.R. LEWIS. (1992). Hydrographic patterns and vertical mixing in the equatorial Pacific along 150° W, *J. Geophys. Res.*, 97: 611-626.
- CHAVEZ, F. P. AND BARBER, R.T. (1985). Plankton production during El Niño, *WCRP Publications series*, 4: 23-31.
- CHAVEZ, F.P. AND BARBER, R.T. (1987). An estimate of new production in the

equatorial Pacific, *Deep Sea Res.*, 34: 1,229-1,243.

CHAVEZ, F.P. (1989). Size distribution of phytoplankton in the central and eastern tropical Pacific, *Global Biogeochem. Cycles*, 3: 27-35.

COALE, K.H. (1991). The effects of iron, manganese, copper and zinc enrichments on productivity and biomass in the subarctic Pacific, *Limnol. Oceanogr.*, 36: 1851-1864.

COCHLAN, W.P., PRICE, N.M., AND HARRISON, P.J. (1991). Effects of irradiance on nitrogen uptake by phytoplankton: comparison of frontal and stratified communities, *Mar. Ecol. Prog. Ser.*, 69: 103-116.

CONWAY, H.L. (1977). Interactions of inorganic nitrogen in the uptake and assimilation by marine phytoplankton, *Mar. Biol.*, 39: 221-232.

CONWAY, H.L. AND WHITLEDGE, T.E. (1979). Distribution, fluxes and biological utilization of inorganic nitrogen during a spring bloom in the New York Bight, *J. Mar. Res.*, 37: 657-668.

CRAIG, H., BROECKER, W.S., AND SPENCER, D.W. (1982). GEOSECS Pacific Expedition: Sections and Profiles, U.S. Government Printing Office, Washington, D.C., Vol. 4, 251 pp.

CROMWELL, T. (1953). Circulation in a meridional plane in the central equatorial Pacific, *J. Mar. Res.*, 12: 196-213.

CULLEN, J.J., STEWART, E., RENGER, E., EPPLEY, R.W. AND WINANT, C.D. (1983). Vertical motion of the thermocline, nitracline and chlorophyll maximum layers in relation to currents on the Southern California Shelf, *J. Mar. Res.*, 41: 239-262.

CULLEN, J.J. (1991). Hypothesis to explain high-nutrient conditions in the open sea, *Limnol. Oceanogr.*, 36: 1578-1599.



- CULLEN, J.J., LEWIS, M.R., DAVIS, C.O., AND BARBER, R.T. (1992). Photosynthetic characteristics and estimated growth rates indicate grazing is the proximate control of primary production in the equatorial Pacific, *J. Geophys. Res.*, 97: 639-654.
- CULLEN, J.J., YANG, X., AND MACINTYRE, H.L. (1992). Nutrient limitation of marine photosynthesis. In: Falkowski, P.G. and A.D. Woodhead (eds), *Primary Productivity and Biogeochemical Cycles in the Sea*, Plenum Press, New York, p 69-88.
- CULLEN, J.J., GEIDER, R.J., ISHIZAKA, J., KIEFER, D.A., MARRA, J., SAKSHAUG, E., AND RAVEN, J.A. (1993). Towards a general description of phytoplankton growth for biogeochemical models. In: Evans, G.T and M.J.R. Fasham (eds), *Towards a Model of Ocean Biogeochemical Processes*, NATO ASI Series, Vol I 10, Springer-Verlag, Berlin Heidelberg, p 153-176.
- DAGG, M.J. AND WALSER, W.E. (1987). Ingestion, gut passage, and egestion by the copepod *Neocalanus plumchrus* in the laboratory and in the subarctic Pacific Ocean, *Limnol. Oceanogr.*, 25: 597-609.
- DANDONNEAU, Y. (1992). Surface chlorophyll concentration in the tropical Pacific ocean: an analysis of data collected by merchant ships from 1978 to 1989, *J. Geophys. Res.*, 97: 3,581-3,591.
- DICKEY, T., GRANATA, T., HAMILTON, M, WIGGERT, J., MARRA, J., LANGDON, C., AND SIEGEL, D.A. (1990). Time series observations of bio-optical properties in the upper layer of the Sargasso Sea, *Ocean Opt.*, 10: 202-214.
- DORTCH, Q. AND PACKARD, T.T. (1989). Differences in biomass structure between oligotrophic and eutrophic marine ecosystems, *Deep Sea Res.*, 36: 223- 240.
- DORTCH, Q. (1990). The interaction between ammonium and nitrate uptake in phytoplankton, *Mar. Ecol. Prog. Ser.*, 61: 183-201.
- DUGDALE, R.C. (1967). Nutrient limitation in the sea: dynamics, identification,

and significance, *Limnol. Oceanogr.*, 12: 685-695.

DUGDALE, R.C. AND GOERING, J.J. (1967). Uptake of new and regenerated forms of nitrogen in primary production, *Limnol. Oceanogr.*, 12: 196-206.

DUGDALE, R.C. AND WILKERSON, F.P. (1986). The use of  $^{15}\text{N}$  to measure nitrogen uptake in eutrophic oceans: experimental considerations, *Limnol. Oceanogr.*, 31: 673-689.

DUGDALE, R.C., MOREL, A., BRICAUD, A., AND WILKERSON, F.P. (1989). Modeling new production in upwelling centers: A case study of modeling new production from remotely sensed temperature and color, *J. Geophys. Res.*, 94: 18,119-18,132.

DUGDALE, R.C., WILKERSON, F.P., BARBER, R.T., AND CHAVEZ, F.P. (1992). Estimating new production in the equatorial Pacific Ocean at 150° W, *J. Geophys. Res.*, 97: 681-686, 1992.

DYMOND, J. AND COLLIER, R. (1988). Biogenic particle fluxes in the equatorial Pacific: evidence for both high and low productivity during the 1982-1983 El Niño, *Global Biogeochem. Cycles*, 2: 129-137.

EPPLEY, R.W., RENGER, E.H., VENRICK, E.L., AND MULLIN, M.M. (1973). A study of plankton dynamics and nutrient cycling in the central gyre of the North Pacific Ocean, *Limnol. Oceanogr.*, 18: 534-551.

EPPLEY, R.W. AND RENGER, E.H. (1974). Nitrogen assimilation of an oceanic diatom in nitrogen- limited continuous culture, *J. Phycol.*, 10: 15-23.

EPPLEY, R.W. AND PETERSON, B.J. (1979). Particulate organic matter flux and planktonic new production in the deep ocean, *Nature*, 282: 677-680.

EPPLEY, R.W. AND RENGER, E.H. (1986). Nitrate-based primary production in nutrient-depleted surface waters off California, *Oceanogr. Trop.*, 21: 229-238.

- EPPLEY, R.W. AND RENGER, E.H. (1988). Nanomolar increase in surface layer nitrate concentration following a small wind event, *Deep Sea Res.*, 35: 1119- 1125.
- EPPLEY, R.W. AND RENGER, E.H. (1991). Nitrate utilization by plankton in the equatorial Pacific, March 1988 along 150° W., *J. Geophys. Res.*, 97: 663-668.
- EPPLEY, R.W., CHAVEZ, F.P., AND BARBER, R.T. (1991). Standing stocks of particulate carbon and nitrogen in the equatorial Pacific at 150° W, *J. Geophys. Res.*, 97: 655-661.
- ESBENSEN, S.K. AND KUSHNIR, Y. (1981). The heat budget of the global ocean: An atlas based on estimates from marine observations. Climate Research Institute, Oregon State University, Corvallis, Report No. 29.
- FALKOWSKI, P.G. (1992). Molecular ecology of phytoplankton photosynthesis, pp. 47-88. In: P.G. Falkowski and A.D. Woodhead (eds.), *Primary productivity and Biogeochemical Cycles in the Sea*, Plenum Press, New York.
- FASHAM, M.J.R., DUCKLOW, H.W., AND MCKELVIE, S.M. (1990). A nitrogen-based model of plankton dynamics in the ocean mixed layer, *J. Mar. Res.*, 48: 591-639.
- FIELDER, R. AND PROKSCH, G. (1975). The determination of nitrogen-15 by emission and mass spectrometry in biochemical analysis: a review, *Anal. Chimica Acta*, 78: 1-62.
- FIEDLER, P.C., PHILBRICK, V. AND CHAVEZ, F.P. (1991). Oceanic upwelling and productivity in the eastern tropical Pacific, *Limnol. Oceanogr.*, 36: 1,834-1,850.
- FRANKS, P.J.S., WROBLEWSKI, J.S. AND FLIERL, G.R. (1986). Behavior of a simple plankton model with food-level acclimatation by herbivores, *Mar. Biol.*, 91: 121-129.
- FROST, B.W. (1987). Grazing control of phytoplankton stock in open sub-Arctic

Pacific Ocean, *Mar. Ecol. Prog. Ser.*, 39: 49-68.

FROST, B.W. AND FRANZEN, N.C. (1994). Grazing and iron limitation in the control of phytoplankton stock and nutrient concentration: a chemostat analogue of the Pacific equatorial upwelling zone, *Mar. Ecol. Prog. Ser.*, (in press).

GARSDIE, C. (1981). Nitrate and ammonia uptake in the apex of the New York Bight, *Limnol. Oceanogr.*, 26: 731-739.

GARSDIE, C. (1991). Shift-up and the nitrate kinetics of phytoplankton in upwelling systems, *Limnol. Oceanogr.*, 36: 1239-1244.

GAUDY, R. (1974). Feeding four species of pelagic copepods under experimental conditions, *Mar. Biol.*, 25: 124-141.

GLIBERT, P.M., LIPSCHULTZ, F., MCCARTHY, J.J., AND ALTABET, M.A. (1982a). Isotope dilution models of uptake and remineralization of ammonium by marine plankton, *Limnol. Oceanogr.*, 27: 639-650.

GLIBERT, P.M., BIGGS, D.C., AND MCCARTHY, J.J. (1982b). Utilization of ammonium and nitrate during austral summer in the Scotia Sea, *Deep Sea Res.*, 29: 837-850.

GLIBERT, P.M., GOLDMAN, J.C., AND CARPENTER, E.J. (1982c). Seasonal variations in the utilization of ammonium and nitrate by phytoplankton in Vineyard Sound, Massachusetts, USA, *Mar. Biol.*, 70: 237-249.

GLOVER, H.E. (1980). Assimilation numbers in cultures of marine phytoplankton, *J. Plankton Res.*, 2: 69-75.

GLOVER, H.E., PREZELIN, B.B., CAMPBELL, L., WYMAN, M., AND GARSDIE, C. (1988). A nitrate-dependent *Synechococcus* bloom in surface Sargasso Sea water, *Nature*, 331: 161-163.

- GODFREY, J.S. AND LINDSTROM, E.J. (1989). The heat budget of the equatorial Western Pacific surface mixed layer, *J. Geophys. Res.*, 94: 8,007-8,017.
- GOLDMAN, J.C. AND MCCARTHY, J.J. (1978). Steady state growth and ammonium uptake of a fast-growing marine diatom, *Limnol. Oceanogr.*, 23: 695-730.
- GOLDMAN, J.C., MCCARTHY, J.J., AND PEAVEY, D.G. (1979). Growth rate influence on the chemical composition of phytoplankton in oceanic waters, *Nature*, 279: 210-215.
- GOLDMAN, J.C., CARON, D.A., ANDERSEN, O.K., AND DENNETT, M.R. (1985). Nutrient recycling in a microflagellate food chain: 1. Nitrogen dynamics, *Mar. Ecol. Prog. Ser.*, 24: 231-242.
- GOLDMAN, J.C. (1988). Spatial and temporal discontinuities of biological processes in pelagic surface waters, p. 273-296. In: B.J. Rothschild (ed.), *Towards a theory on biological-physical interactions in the world ocean*. Kluwer.
- GOLDMAN, J.C. (1993). Potential role of large oceanic diatoms in new primary production, *Deep Sea Res.*, 40: 159-168.
- GORDON, C. (1989). Comparison of the surface fluxes in the tropical Pacific Ocean derived from a general atmospheric circulation model and from climatology, *Tropical Ocean-Atmosphere Newsletter*, 51: 1-4.
- HALPERN, D. (1987). Observations of annual and El Niño thermal and flow variations at 0°, 110° W and 0°, 95° W during 1980-1985, *J. Geophys. Res.*, 92: 8,197-8,212.
- HALPERN, D. AND FREITAG, P.H. (1987). Vertical motion in the upper ocean of the equatorial eastern Pacific, *Oceanol. Acta*, 6: 19-26.
- HALPERN, D., KNOX, R.A., LUTHIER, D.S., AND PHILANDER, S.G.H. (1989). Estimates of equatorial upwelling between 140° and 110° W during 1984, *J. Geophys. Res.*, 94: 8,018-8,020.

- HALPERN, D. AND FELDMAN, G.C. (1994). Annual and interannual variations of phytoplankton pigment concentration and upwelling along the Pacific equator, *J. Geophys. Res.*, 99: 7347-7365.
- HARRIS, G.P. (1986). Phytoplankton ecology: structure, function and fluctuation. Chapman and Hall, New York, 384 p.
- HARRISON, W.G. (1983). Nitrogen in the marine environment IV.2 Use of isotopes. In: E.J. Carpenter and D.G. Capone (eds.), *Nitrogen in the marine environment*, Academic Press. pp. 763-807.
- HARRISON, W.G., PLATT, T., AND LEWIS, M.R. (1987). f-Ratio and its relationship to ambient nitrate concentration in coastal waters, *J. Plank. Res.*, 9: 235-248.
- HARRISON, W.G. AND WOOD, L.J.E. (1988). Inorganic nitrogen uptake by marine picoplankton: evidence for size partitioning, *Limnol. Oceanogr.*, 33: 468-475.
- HARRISON, W.G., HARRIS, L.R., KARL, D.M., KNAUER, G.A., AND REDALJE, D.G. (1992). Nitrogen dynamics at the VERTEX time-series site, *Deep-Sea Res.*, (in press).
- HOFMANN, E.E. AND AMBLER, J.W. (1988). Plankton dynamics on the outer southeastern U.S. continental shelf. Part II: A time-dependent biological model, *J. Mar. Res.*, 46: 883-917.
- HOLLING, C.S. (1965). The functional response of predators to prey density and its role in mimicry and population regulation, *Mem. Entomol. Soc. Can.*, 45: 1-60.
- HOLM-HANSEN, O., LORENZEN, C.J., HOLMES, R.W., AND STRICKLAND, J.D.H. (1965). Fluorometric determination of chlorophyll, *Int. Council Expl. Sea.*, 30: 3-15.
- HUDSON, R.J.M. AND MOREL, F.M.M. (1990). Iron transport in marine phytoplankton: Kinetics of cellular and medium coordination reactions, *Limnol. Oceanogr.*,

35: 1002-1020.

IVLEV, V.S. (1955). Experimental ecology of the feeding of fishes. Pischepromizdat, Moscow, 302 pp. (transl. from Russian by D. Scott) New Haven: Yale University Press 1961.

JENKINS, W.J. AND GOLDMAN, J.C. (1985). Seasonal oxygen cycling and primary production in the Sargasso Sea, *J. Mar. Res.*, 43: 465-491.

JENKINS, W.J. (1988). Nitrate flux into the euphotic zone near Bermuda, *Nature*, 331: 521-523.

KANDA, J., LAWS, E., SAINO, T., AND HATTORI, A. (1987). An evaluation of isotope dilution effects from conventional data sets of  $^{15}\text{N}$  uptake experiments, *J. Plank. Res.*, 9: 79-90.

KAMYKOWSKI, D. AND ZENTARA, S.-J. (1986). Predicting plant nutrient concentration from temperature and sigma-t in the world ocean, *Deep Sea Res.*, 33: 89-105.

KAMYKOWSKI, D. (1987). A preliminary biophysical model of the relationship between temperature and plant nutrients in the upper ocean, *Deep Sea Res.*, 34: 1,067-1,079.

KEEN, R. (1988). Equatorial westerlies and Southern Oscillation, 121-140. In: R. Lukas and P. Webster, *Proceeding of the U.S. TOGA Western Pacific Air-sea Interaction Workshop*.

KING, F.D. (1987). Nitrogen recycling efficiency in steady-state oceanic environments, *Deep Sea Res.*, 34: 843-856.

KIRCHMAN, D.L., KEIL, R.G., AND WHEELER, P.A. (1988). The effect of amino acids on ammonium utilization and regeneration by heterotrophic bacteria in the subarctic Pacific, *Deep-Sea Res.*, 36: 1763-1776.

- KLEIN, P. AND COSTE, B. (1984). Effects of wind-stress variability on nutrient transport into the mixed layer, *Deep Sea Res.*, 31: 21-37.
- KNAUSS, J.A. (1963). Equatorial current systems. In: *The Sea*, Vol. 2, Inters. Publ., London, pp. 235-252.
- LEGENDRE, L. AND LE FEVRE, J. (1989). Hydrodynamical singularities as controls of recycled versus export production in oceans, p. 49-63. In: W.H. Berger et al. (eds.), *Productivity of the ocean: Present and past*. Wiley.
- LEWIS, M.R., HARRISON, W.G., OAKEY, N.S., HEBERT, D., AND PLATT, T. (1986). Vertical nitrate fluxes in the oligotrophic ocean, *Science*, 234: 870-873.
- LEWIS, M.R., KURING, N., AND YENTSCH, C. (1988). Global patterns of ocean transparency: implications for the new production of the open ocean, *J. Geophys. Res.*, 93: 6,847-6,856.
- LEWIS, M.R., CARR, M.E., FELDMAN, G.C., ESAIAS, W. AND MCCLAIN, C. (1990). Influence of penetrating solar radiation on the heat budget of the equatorial Pacific Ocean, *Nature*, 347: 543-545.
- LEWIS, M.R. (1992). Satellite ocean color observations of global biogeochemical cycles, pp.139-156. In: P. G. Falkowski and A. D. Woodhead (eds.), *Primary productivity and Biogeochemical Cycles in the Sea*, Plenum Press, New York.
- LIU, T.W. (1988). Moisture and latent heat flux variabilities in the tropical Pacific derived from satellite data, *J. Geophys. Res.*, 93: 6,749-6,760.
- LIU, T.W. AND GAUTIER, C. (1990). Thermal forcing on the tropical Pacific from satellite data, *J. Geophys. Res.*, 95: 13,209-13,217.
- LONGHURST, A.R. AND HARRISON, W.G. (1988). Vertical nitrogen flux from the oceanic photic zone by diel migrant zooplankton and nekton, *Deep Sea Res.*, 35: 881-889.



- LUKAS, R. AND LINDSTROM, E. (1991). The mixed layer of the western equatorial Pacific Ocean, *J. Geophys. Res.*, 96: 3,343-3,357.
- MACISAAC, J.J. AND DUGDALE, R.C. (1969). The kinetics of nitrate and ammonia uptake by natural populations of marine phytoplankton, *Deep Sea Res.*, 16: 45-57.
- MACISAAC, J.J. AND DUGDALE, R.C. (1972). Interactions of light and inorganic nitrogen in controlling nitrogen uptake in the sea, *Deep Sea Res.*, 19: 209- 232.
- MACISAAC, J.J., DUGADALE, R.C., BARBER, R.T., BLASCO, D., AND PACKARD, T.T. (1985). Primary production cycle in an upwelling center, *Deep Sea Res.*, 32: 503- 522.
- MALONE, T.C. (1980). Algal size, p. 433-464. In: Morris, I. (ed), *The physiological ecology of phytoplankton*, Blackwell, London,
- MARRA, J., BIDIGARE, R.R., AND DICKEY, T.T. (1990). Nutrient and mixing, chlorophyll and phytoplankton growth, *Deep Sea Res.*, 37: 127-143.
- MARTIN, J.H., GORDON, R.M., FITZWATER, S., AND BROENKOW, W.W. (1989). VERTEX: phytoplankton/iron studies in the Gulf of Alaska, *Deep Sea Res.*, 36: 649-680.
- MARTIN, J.H., GORDON, R.M., AND FITZWATER, S.E. (1991). The case for iron, *Limnol. Oceanogr.*, 36: 1,793-1,802.
- MAYZAUD, P. AND POULET, S.A. (1978). The importance of the time factor in the response of zooplankton to varying concentrations of naturally occurring particulate matter, *Limnol. Oceanogr.*, 23: 1144-1154.
- MCCARTHY, J.J., TAYLOR, W.R., AND TAFT, J.L. (1977). Nitrogenous nutrition of the plankton in the Chesapeake Bay. I. Nutrient availability and phytoplankton preferences, *Limnol. Oceanogr.*, 22: 996-1011.

- MCCARTHY, J.J. (1981). The kinetics of nutrient utilization. In: Physiological bases of phytoplankton ecology, *Can. Bull. Fish. Aquat. Sci.*, 210: 211-233.
- MCCARTHY, J.J. AND NEVINS, J.L. (1986). Sources of nitrogen for primary production in warm-core rings 79-E and 81-D, *Limnol. Oceanogr.*, 31: 690-700.
- MCPHADEN, M.J. AND TAFT, B.A. (1988). Dynamics of seasonal and interseasonal variability in the eastern equatorial Pacific, *J. Phys. Oceanogr.*, 18: 1713-1732.
- MCPHADEN, M.J., BAHR, F., DU PENHOAT, Y., FIRING, E., HAYES, S.P., NIILER, P.P., RICHARDSON, P.L., AND TOOLE, J.M. (1992). The response of the western equatorial Pacific Ocean to westerly wind bursts during November 1989 to January 1990, *J. Geophys. Res.*, 97: 14,289-14,303.
- MICHAELS, A.F. AND SILVER, M.W. (1988). Primary production, sinking fluxes and the microbial food web, *Deep Sea Res.*, 35: 473-490.
- MINAS, H.J., MINAS, M., AND PACKARD, T.T. (1986). Productivity in upwelling areas deduced from hydrographic and chemical fields, *Limnol. Oceanogr.*, 31: 1182-1206.
- MINAS, H.J. AND MINAS, M. (1992). Net community production in "High Nutrient-Low Chlorophyll" waters of the tropical and Antarctic Oceans: grazing vs iron hypothesis, *Oceanol. Acta*, 15: 145-162.
- MOREL, A. (1988). Optical modelling of the upper ocean in relation to its biogenous matter content (case I waters), *J. Geophys. Res.*, 93: 10,749-10,768.
- MOREL, F.M.M., RUETER, J.G., AND PRICE, N.M. (1991). Iron nutrition of phytoplankton and its possible importance in the ecology of ocean regions with high nutrient and low biomass, *Oceanography*, 4: 56-61.
- MOUM, J.N., CALDWELL, D.R., AND PAULSON, C.A. (1989). Mixing in the equatorial surface layer and thermocline, *J. Geophys. Res.*, 94: 2005-2021.

MURRAY, J.W., DOWNS, J.N., STROM, S., WEI, C.-L., AND JANNASCH, H.W. (1989). Nutrient assimilation, export production and  $^{234}\text{Th}$  scavenging in the eastern equatorial Pacific, *Deep Sea Res.*, 36: 1471-1489.

NALEWAJKO, C. AND GARSIDE, C. (1983). Methodological problems in the simultaneous assessment of photosynthesis and nutrient uptake in phytoplankton as functions of light intensity and cell size, *Limnol. Oceanogr.*, 28: 591-597.

NELSON, D.M. AND CONWAY, H.L. (1979). Effects of the light regime on nutrient assimilation by phytoplankton in the Baja California and northwest Africa upwelling systems, *J. Mar. Res.*, 37: 301-318.

NIELSEN, T.G. AND KIORBOE, T. (1991). Effects of a storm event on the structure of the pelagic food web with special emphasis on planktonic ciliates, *J. Plank. Res.*, 13: 35-51.

NIILER, P. AND STEVENSON, J. (1982). The heat budget of tropical ocean warm-water pools, *J. Mar. Res.*, 40 (supplement): 465-480.

OBERHUBER, J.M. (1988). An atlas based on the 'COADS' data set: the budgets of heat, buoyancy and turbulent kinetic energy at the surface of the global ocean. Max-Planck-Institute for Meteorology. Report # 15.

OSBORNE, J., SWIFT, J., AND FLINCHEM, E.P. (1992). Ocean Atlas for Macintosh: A microcomputer application for examining oceanographic data, version 2.0. S.I.O. Reference #92-29.

PARSONS, T.R. AND LALLI, C.M. (1988). Comparative oceanic ecology of the plankton communities of the subarctic Atlantic and Pacific oceans, *Oceanogr. Mar. Biol. Annu. Rev.*, 26: 317-359.

PEÑA, M.A., LEWIS, M.R., AND HARRISON, W.G. (1990). Phytoplankton productivity and size structure of phytoplankton biomass on a transect of the equator

at 135° W in the Pacific Ocean, *Deep Sea Res.*, 37: 295-315.

PEÑA, M.A., LEWIS, M.R., AND HARRISON, W.G. (1991). Particulate organic matter and chlorophyll in the surface layer of the equatorial Pacific Ocean along 135° W, *Mar. Ecol. Prog. Ser.*, 72: 179-188.

PEÑA, M.A., HARRISON, W.G., AND LEWIS, M.R. (1992). New production in the central equatorial Pacific, *Mar. Ecol. Prog. Ser.*, 80: 265-274.

PETERS, H., GREGG, M.C. AND TOOLE, J.M. (1989). Meridional variability of turbulence through the equatorial undercurrent, *J. Geophys. Res.*, 94: 18,003-18,009.

PHILANDER, S.G.H., HURLIN, W.J., AND SEIGEL, A.D. (1987). Simulation of the seasonal cycle of the tropical Pacific Ocean, *J. Phys. Oceanogr.*, 17: 1,986-2,002.

PHILANDER, G. (1989). El Niño and La Niña, *Am. Sci.*, 77: 451-459.

PLATT, T. AND HARRISON, W.G. (1985). Biogenic fluxes of carbon and oxygen in the ocean, *Nature*, 318: 55-58.

PLATT, T., HARRISON, W.G., LEWIS, M.R., LI, W.K.W., SATHYENDRANATH, S., SMITH, R.E., AND VEZINA, A.F. (1989). Biological production of the oceans: the case for a consensus, *Mar. Ecol. Prog. Ser.*, 52: 77-88.

PRICE, N.M., HARRISON, P.J., LANDRY, M.R., AZAM, F., AND HALL, K.J.F. (1986). Toxic effects of latex and Tygon tubing on marine phytoplankton, zooplankton and bacteria, *Mar. Ecol. Prog. Ser.*, 34: 41-49.

PRICE, N.M., ANDERSEN, L.F., AND MOREL, F.M.M. (1991). Iron and nitrogen nutrition of equatorial Pacific plankton, *Deep Sea Res.*, 38: 1361-1378.

PRICE, N.M., AHNER, B.A. AND MOREL, F.M.M. (1994). The equatorial Pacific Ocean: Grazer-controlled phytoplankton populations in an iron-limited ecosystem, *Limnol. Oceanogr.*, 39: 520-534.

- PRISCU, J.C. (1984). A comparison of nitrogen and carbon assimilation in the shallow and deep- water phytoplankton populations of a subalpine lake: response to photosynthetic photon flux density, *J. Plank. Res.*, 6: 733-749.
- PROBYN, T.A. (1985). Nitrogen uptake by size-fractionated phytoplankton populations in the southern Benguela upwelling system, *Mar. Ecol. Prog. Ser.*, 22: 249-258.
- PROBYN, T.A., WALDRON, H.N., AND JAMES, A.G. (1990). Size-fractionated measurements of nitrogen uptake in aged upwelled waters: Implications for pelagic food webs, *Limnol. Oceanogr.*, 35: 202-210.
- REED, R.K. (1985). An estimate of the climatological fluxes over the tropical Pacific Ocean, *J. Climate Appl. Meteor.*, 24: 833-840.
- REED, R.K. (1986). Effects of surface heat flux during the 1972 and 1982 El Niño episodes, *Nature*, 322: 449-450.
- SARMIENTO, J.L., SLATER, R.D., FASHAM, M.J.R., DUCKLOW, H.W., TOGGWEILER, J.R., AND EVANS, G.T. (1993). A seasonal three-dimensional ecosystem model of nitrogen cycling in the North Atlantic euphotic zone, *Global Biogeochem. Cycles*, 7: 417-450.
- SATHYENDRANATH, S., PLATT, T., HORNE, E.P.W., HARRISON, W.G., ULLOA, O., OUTERBRIDGE, R., AND HOEPFFNER, N. (1991). Estimation of new production in the ocean by compound remote sensing, *Nature*, 353: 129-133.
- SEAGER, R. (1989). Modeling tropical Pacific sea surface temperature: 1970-87, *J. Phys. Oceanogr.*, 19: 419-434.
- STEELE, J.H. (1976). The role of predation in ecosystem models, *Mar. Biol.*, 35: 9-11.
- STEELE, J.H. AND HENDERSON, E.W. (1981). A simple plankton model, *Am. Nat.*, 117: 676-691.

- STEELE, J.H. AND HENDERSON, E.W. (1992). The role of predation in plankton models, *J. Plank. Res.*, 14: 157-172.
- STEEMANN NIELSEN, E. (1952). The use of radioactive carbon ( $^{14}\text{C}$ ) for measuring organic production in the sea, *Int. Council Expl. Sea*, 18: 117-140.
- STEEMANN NIELSEN, E. AND HANSEN, V.K. (1959). Measurements with the  $^{14}\text{C}$  technique of the respiration rates in natural populations of phytoplankton, *Deep Sea Res.*, 5: 222-232.
- STRICKLAND, J.D.H. AND PARSONS, T.R. (1972). A practical handbook of sea water analysis, *Bull. Fish. Res. brd. Can.*, 167: 311 pp.
- STROM, S.L. AND WELSCHMEYER, N.A. (1991). Pigment-specific rates of phytoplankton growth and microzooplankton grazing in the open subarctic Pacific Ocean, *Limnol. Oceanogr.*, 36: 50-63.
- SYRETT, P.J. (1981). Nitrogen metabolism of microalgae. In: Physiological bases of phytoplankton ecology, *Can. Bull. Fish. Aquat. Sci.*, 210: 182-210.
- TAYLOR, A.H. AND JOINT, I. (1990). A steady-state analysis of the 'microbial loop' in stratified systems, *Mar. Ecol. Prog. Ser.*, 59: 1-17.
- THOMAS, W.H. (1979). Anomalous nutrient chlorophyll interrelationships in the offshore eastern tropical Pacific Ocean., *J. Mar. Res.*, 37: 327-335.
- THOMPSON, P.A., LEVASSEUR, M.E., AND HARRISON, P.J. (1989). Light-limited growth on ammonium vs. nitrate: What is the advantage for marine phytoplankton?, *Limnol. Oceanogr.*, 34: 1014-1024.
- VALIELA, I. (1984). Marine ecological processes. Springer.
- WALSH, J.J. AND DUGDALE, R.C. (1972). Nutrient submodels and simulation models of phytoplankton production in the sea, pp. 171-191. In: Kramer, J. and

Allen, H., *Nutrients in Natural Waters*, Wiley.

WALSH, J.J. (1976). Herbivory as a factor in patterns of nutrient utilization in the sea, *Limnol. Oceanogr.*, 21: 1-13.

WEARE, C., STRUB, P.T., AND SAMUEL, M.D. (1981). Annual mean surface heat fluxes in the tropical Pacific Ocean, *J. Phys. Oceanogr.*, 11: 705-717.

WELLS, M.L. (1994). Pumping iron in the Pacific, *Nature*, 368: 295-296.

WHEELER, P.A. AND KOKKINAKIS, S.A. (1990). Ammonium recycling limits nitrate use in the oceanic subarctic Pacific, *Limnol. Oceanogr.*, 35: 1267-1278.

WILKERSON, F.P. AND DUGDALE, R.C. (1987). The use of large shipboard barrels and drifters to study the effects of coastal upwelling on phytoplankton nutrient dynamics, *Limnol. Oceanogr.*, 32: 368-382.

WILKERSON, F.P. AND DUGDALE, R.C. (1992). Measurements of nitrogen productivity in the equatorial Pacific, *J. Geophys. Res.*, 97: 669-679.

WROBLEWSKI, J.S. (1977). A model of phytoplankton plume formation during variable Oregon upwelling, *J. Mar. Res.*, 35: 257-394.

WROBLEWSKI, J.S., SARMIENTO, J.L., AND GLENN, R.F. (1988). An ocean basin scale model of plankton dynamics in the North Atlantic 1. Solutions for the climatological oceanographic conditions in May, *Global Biogeochem. Cycles*, 2: 199-218.

WYRTKI, K. (1974). Sea level and the seasonal fluctuations of the equatorial currents in the western Pacific Ocean, *J. Phys. Oceanogr.*, 5: 91-103.

WYRTKI, K. (1975). El Niño- The dynamic response of the equatorial currents in the western Pacific Ocean to atmospheric forcing, *J. Phys. Oceanogr.*, 5: 572-584.

WYRTKI, K. (1981). An estimate of equatorial upwelling in the Pacific, *J. Phys. Oceanogr.*, 11: 1205-1214.

YODER, J.A., ATKINSON, L.P., BISHOP, S.S., HOFMANN, E.E. AND LEE, T.N. (1983). Effect of upwelling on phytoplankton productivity of the outer southeastern United States continental shelf, *Cont. Shelf Res.*, 1: 385- 404.

YODER, J.A., ATKINSON, L.P., BISHOP, S.S., BLANTON, J.O., LEE, T.N., AND PIETRAFESA, L.J. (1985). Phytoplankton dynamics within Gulf Stream intrusions on the southeastern United States continental shelf during summer 1981, *Cont. Shelf Res.*, 4: 611-635.

YODER, J.A., MCCLAIN, C.R., FELDMAN, G.C., AND ESAIAS, W.E. (1993). Annual cycles of phytoplankton chlorophyll concentrations in the ocean: a satellite view, *Global Biogeochem. Cycles*, 7: 181-193.

ZENTARA, S.J. AND KAMYKOWSKI, D. (1977). Latitudinal relationships among temperature and selected plant nutrients along the west coast of North and South America, *J. Mar. Res.*, 35: 321-337.